Supporting Information

Electronic spectroscopy of homo- and heterometallic binuclear coinage metal phosphine complexes in isolation

Marcel J. P. Schmitt[a], Sebastian V. Kruppa[a], Simon P. Walg[a], Werner R. Thiel[a], Wim Klopper[b]*, Christoph Riehn[a,c]*

[a] M. J. P. Schmitt, Dr. S. V. Kruppa, Dr. S. P. Walg, Prof. Dr. W. R. Thiel, Dr. C. Riehn
Department of Chemistry
Rheinland-Pfälzische Technische Universität (RPTU)
Erwin-Schrödinger Str. 52, 67663 Kaiserslautern (Germany)
E-mail: riehn@chemie.uni-kl.de

[b] Prof. Dr. W. Klopper
Institute of Physical Chemistry
Karlsruhe Institute of Technology (KIT)
Fritz-Haber-Weg 2, 76131 Karlsruhe (Germany)
E-Mail: klopper@kit.edu

[c] Dr. C. Riehn
Research Center OPTIMAS
Erwin-Schrödinger Str. 46, 67663 Kaiserslautern (Germany)

* Corresponding authors.

Table of contents

1. Mass spectrometric results

1.1 ESI-MS overview spectrum

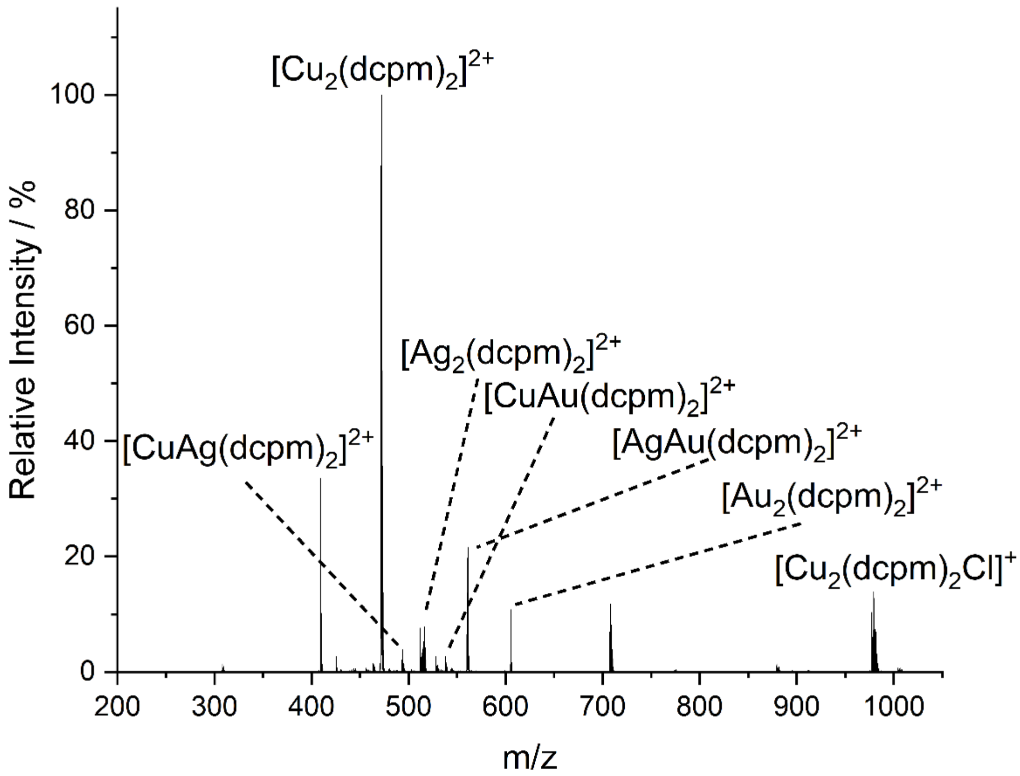

Fig. S1 Overview ESI-MS of $[Cu_2(\textit{dcpm})_2][PF_6]_2$, $[Ag_2(\textit{dcpm})_2][PF_6]_2$, and $[Au_2(\textit{dcpm})_2][PF_6]_2$ mixture (MeCN, c = 10^{-6} M, respectively).

1.2 Collision induced dissociation (CID) and photodissociation (PD)

1.2.1 Isolated, CID and PD mass spectra

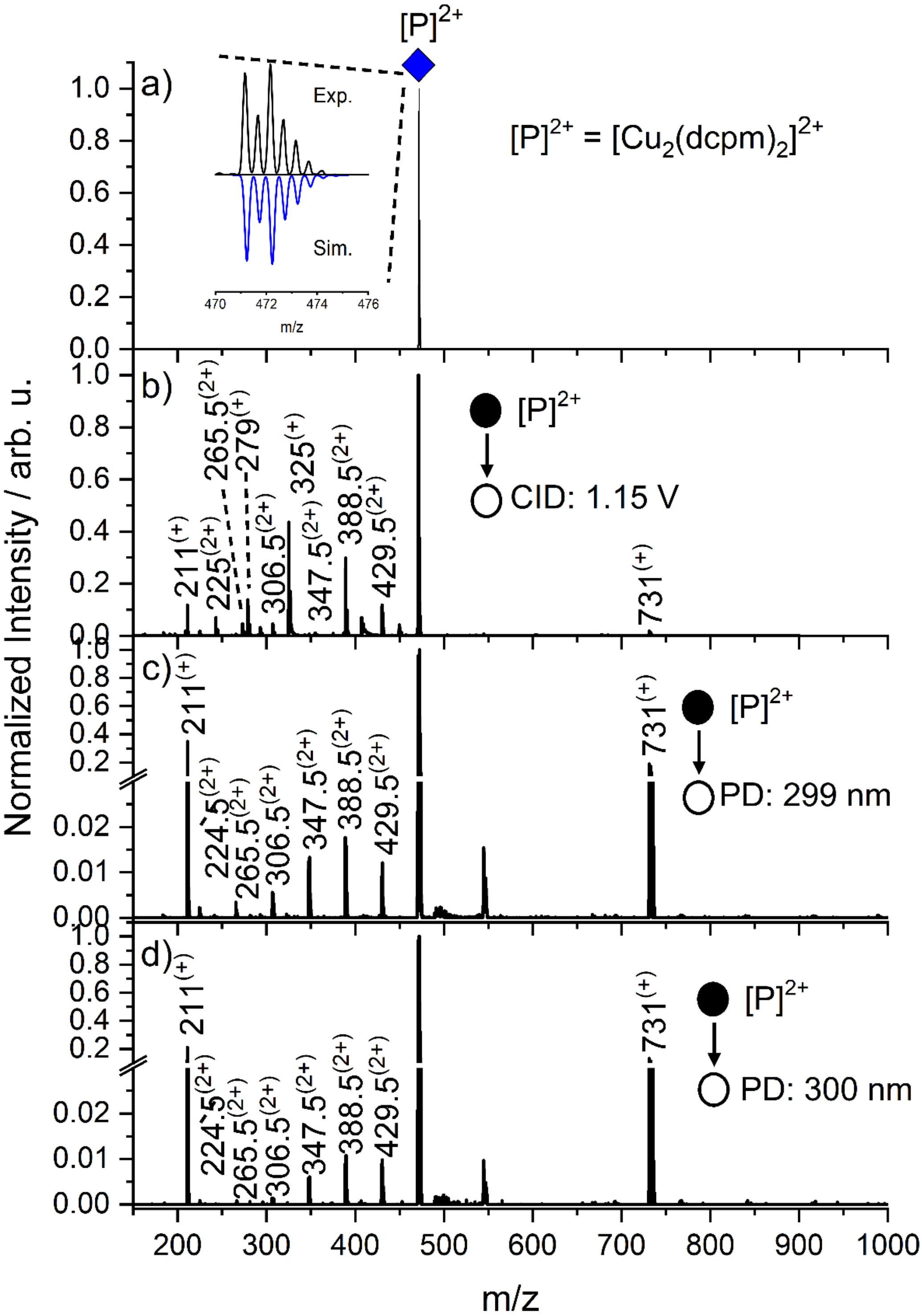

Fig. S2 a) Isolation, b) CID (excitation amplitude = 1.15 V), and UV PD mass spectra of $[Cu_2(dcpm)_2]^{2+}$ precursor ions (*m/z* 471) with corresponding fragmentation products recorded by c) femto- (299 nm, 2 µJ, ca. 118 pulses), or d) nanosecond laser system (300 nm, 2 µJ, ca. 118 pulses), respectively. Integer nominal masses are indicated. Isolated experimental (black) and simulated (blue) isotope patterns are displayed in inset.

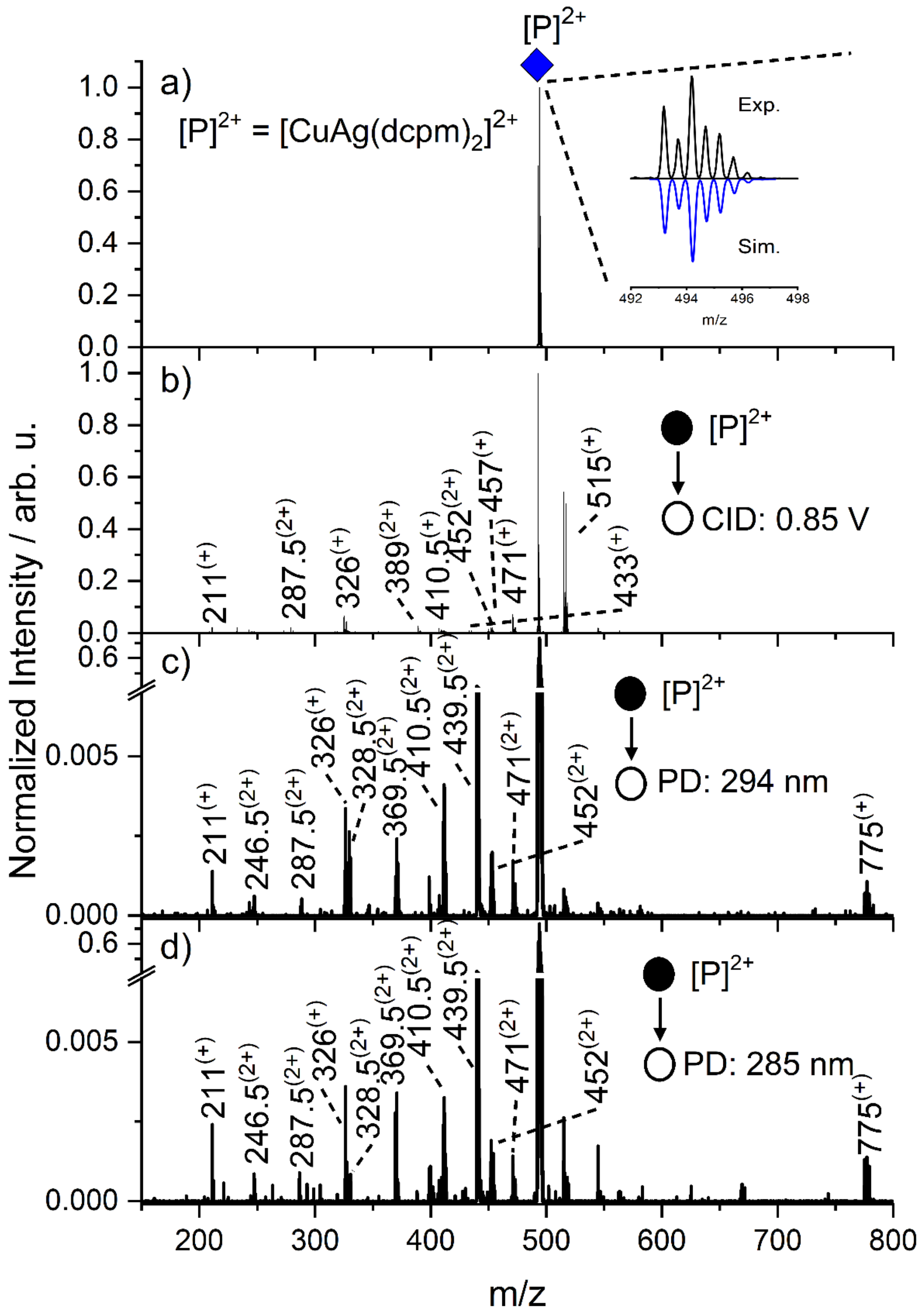

Fig. S3 a) Isolation, b) CID (excitation amplitude = 0.85 V), and UV PD mass spectra of $[CuAg(dcpm)_2]^{2+}$ precursor ions (*m/z* 494) with corresponding fragmentation products recorded by c) femto- (294 nm, 2 µJ, ca. 118 pulses), or d) nanosecond laser system (285 nm, 2 µJ, ca. 118 pulses), respectively. Integer nominal masses are indicated. Isolated experimental (black) and simulated (blue) isotope patterns are displayed in inset.

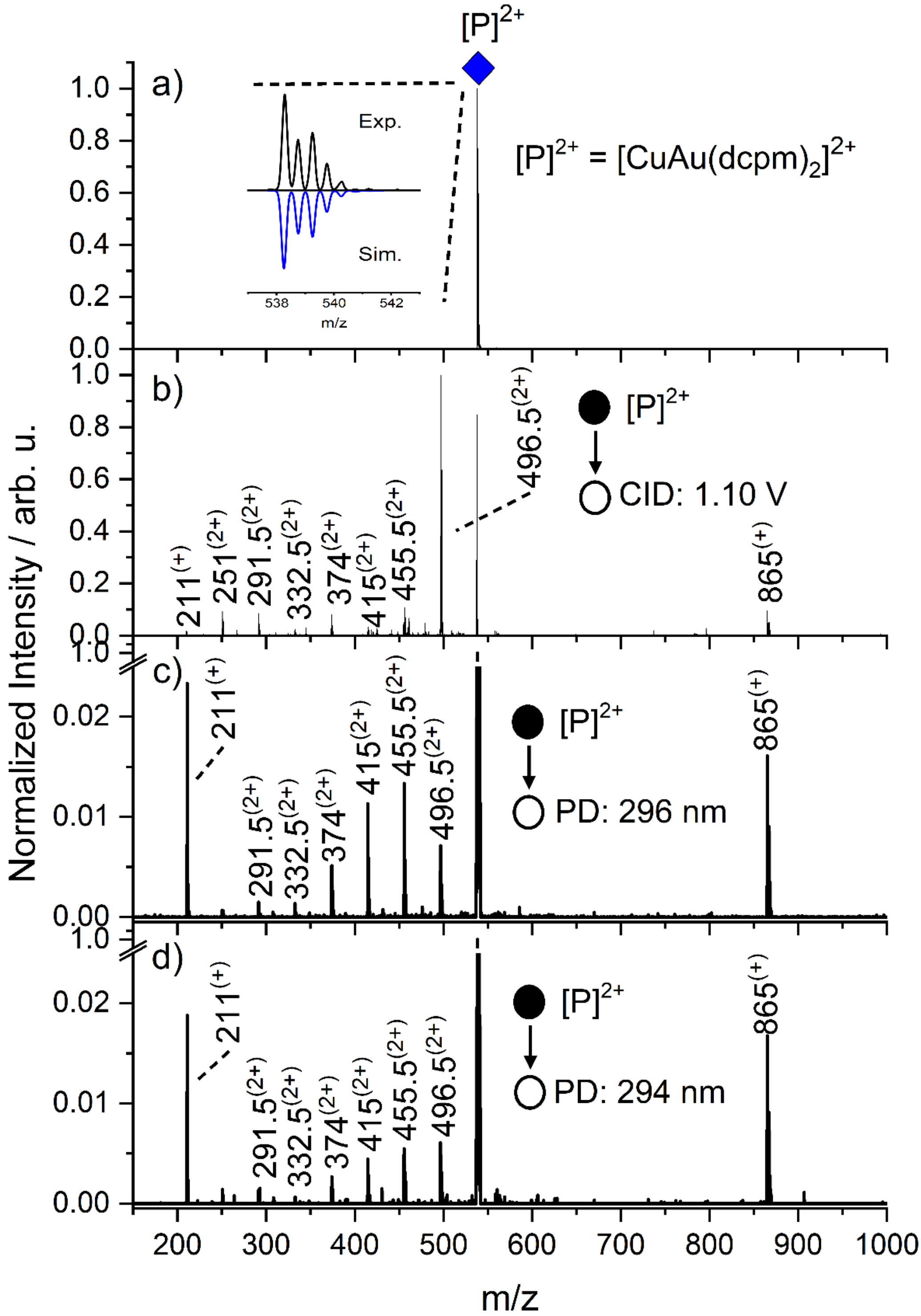

Fig. S4 a) Isolation, b) CID (excitation amplitude = 1.1 V), and UV PD mass spectra of $[CuAu(dcpm)_2]^{2+}$ precursor ions (*m/z* 538) with corresponding fragmentation products recorded by c) femto- (296 nm, 2 µJ, ca. 118 pulses), or d) nanosecond laser system (294 nm, 2 µJ, ca. 118 pulses), respectively. Integer nominal masses are indicated. Isolated experimental (black) and simulated (blue) isotope patterns are displayed in inset.

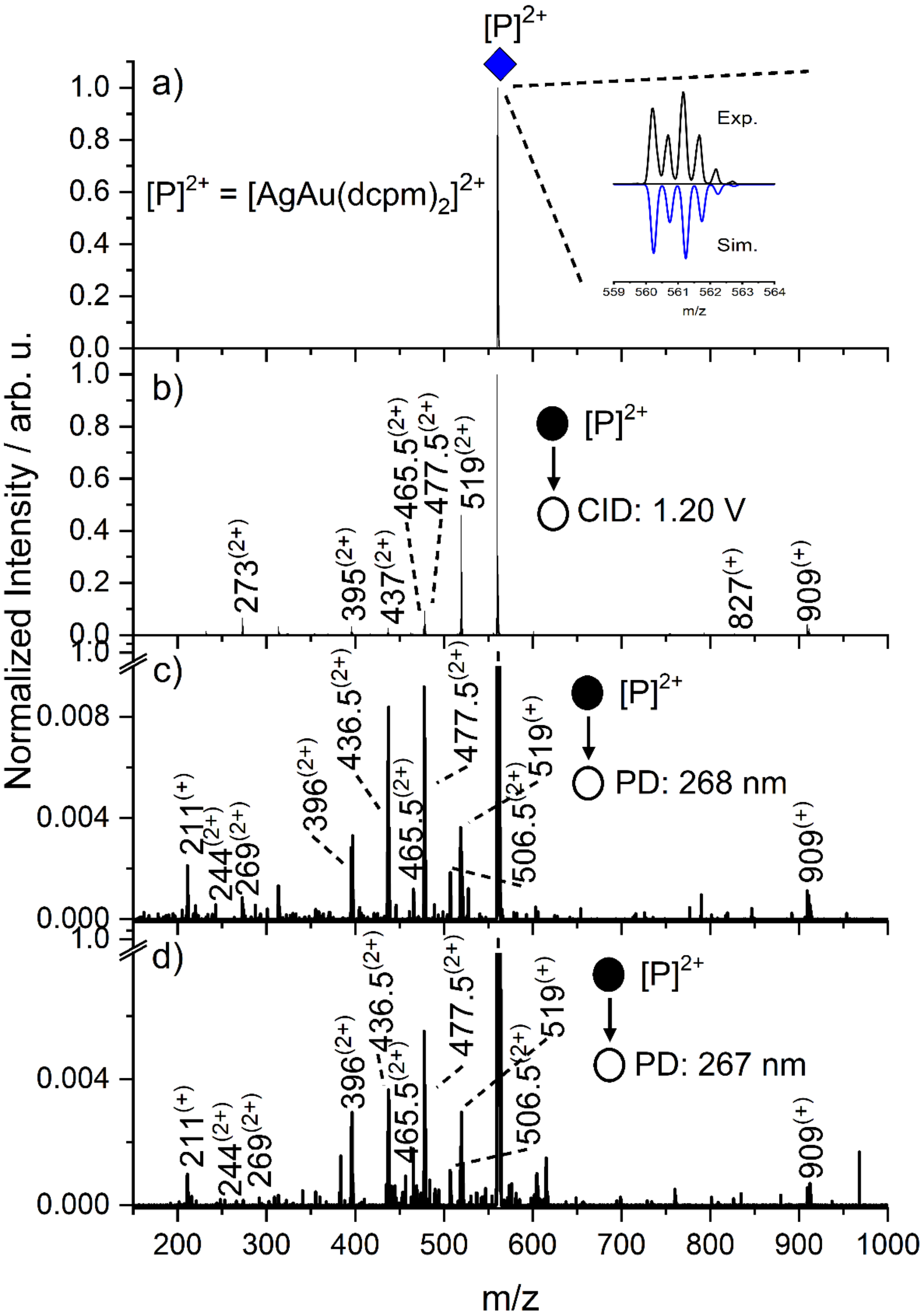

Fig. S5 a) Isolation, b) CID (excitation amplitude = 1.2 V), and UV PD mass spectra of $[AgAu(\mathit{dcpm})_2]^{2+}$ precursor ions (*m/z* 560) with corresponding fragmentation products recorded by c) femto- (268 nm, 2 µJ, ca. 118 pulses), or d) nanosecond laser system (267 nm, 2 µJ, ca. 118 pulses), respectively. Integer nominal masses are indicated. Isolated experimental (black) and simulated (blue) isotope patterns are displayed in inset.

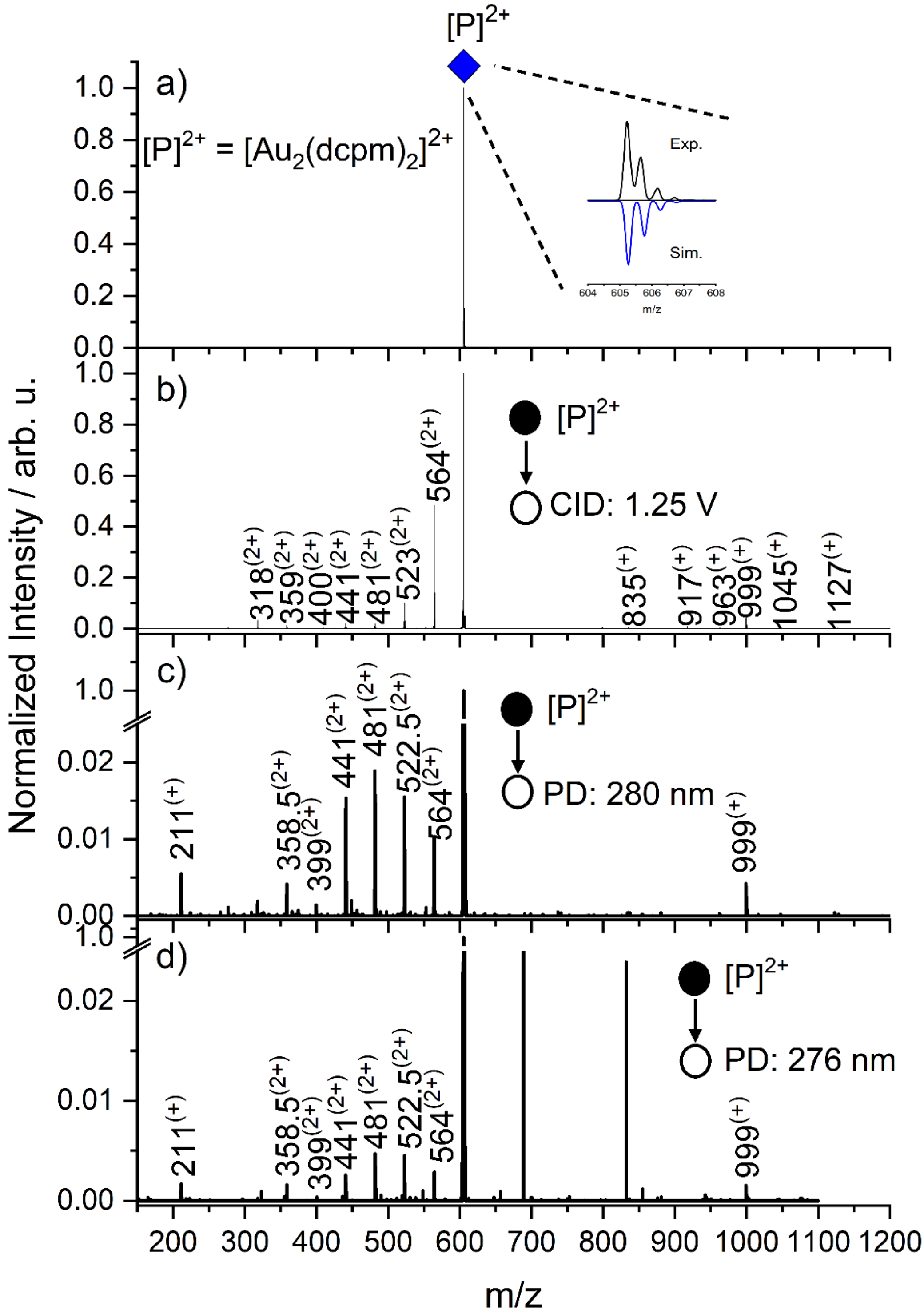

Fig. S6 a) Isolation, b) CID (excitation amplitude = 1.25 V), and UV PD mass spectra of $[Au_2(dcpm)_2]^{2+}$ precursor ions (*m/z* 605) with corresponding fragmentation products recorded by c) femto- (280 nm, 2 µJ, ca. 118 pulses), or d) nanosecond laser system (276 nm, 2 µJ, ca. 118 pulses), respectively. Integer nominal masses are indicated. Isolated experimental (black) and simulated (blue) isotope patterns are displayed in inset.

1.2.2 Fragment assignment

Tab. S1 Mass spectrometric PD and CID fragment assignments of $[Cu_2(dcpm)_2]^{2+}$ dication. Nominal masses of isolated precursor P and fragment ions F_i are indicated. Charge states, fragment formula and losses are shown. Fragments are categorized into ionic and neutral losses. Percentages of total fragment yields were displayed for CID (excitation amplitude = 1.1 V) and UV PD (λex = 297.5 nm, 2 µJ), respectively.

Label	Isolation	*m/z*	z	Loss	Category	CID / PD [%]
P	$[Cu_2(dcpm)_2]^{2+}$	471	2			
F_1	$[Cu_2(dcpm)(PCy_2)]^+$	731	1	$(PCH_2Cy_2)^+$	IF	✓/✓ [2/50]
F_2	$[Cu_2(dcpm)(P_2CH_2Cy_3)H]^{2+}$	430	2	(Cy-H)	NL	✓/✓ [11/3]
	$[Cu_2(dcpm)(P_2CH_2Cy_3)]^{2+}$	(429.5)	2	(Cy)	NL	
F_3	$[Cu_2(dcpm)(P_2CH_2Cy_2)H]^{2+}$	388.5	2	(Cy), (Cy-H)	NL	✓/✓ [20/4]
F_4	$[Cu_2(dcpm)(P_2CH_2Cy)H_2]^{2+}$	347.5	2	(Cy), 2(Cy-H)	NL	✓/✓ [1/3]
	$[Cu_2(dcpm)(P_2CH_2Cy)H]^{2+}$	(347)	2	2(Cy), (Cy-H)	NL	
F_5	$[Cu(CH_2)_2P_2Cy_2H_2(H_2O)]^+$	325	1	$[Cu(dcpm)]^+$, 2(Cy-H), $+H_2O$	IF	✓/- [37/-]
F_6	$[Cu_2(CH_2)_2P_2(Cy)_4H_3]^{2+}$	306.5	2	(Cy), 3(Cy-H)	NL	✓/✓ [3/1]
F_7	$[Cu(CH_2)P_2CyH_3(H_2O)_3]^+$	279	1	$[Cu(dcpm)]^+$, 3(Cy-H), $+3H_2O$	IF	✓/- [9/-]
F_8	$[Cu_2(CH_2)_2P_4(Cy)_3H_4]^{2+}$	265.5	2	(Cy), 4(Cy-H)	NL	✓/✓ [1/0]
F_9	$[Cu(CH_2)P_4CyH_3(H_2O)]^+$	243	1	$[Cu(dcpm)]^+$, 3(Cy-H), $+H_2O$	IF	✓/- [4/-]
F_{10}	$[Cu_2(CH_2)_2P_4(Cy)_2H_6]^{2+}$	225	2	6(Cy-H)	NL	✓/✓ [2/0]
	$[Cu_2(CH_2)_2P_4(Cy)_2H_5]^{2+}$	(224.5)	2	(Cy), 5(Cy-H)	NL	
	$[Cu_2(CH_2)_2P_4(Cy)_2H_4]^{2+}$	(224)	2	2(Cy), 4(Cy-H)	NL	
F_{12}	$(PCH_2Cy_2)^+$	211	1	$[Cu_2(dcpm)(PCy_2)]^+$	IF	✓/✓ [6/32]

Tab. S2 Mass spectrometric PD and CID fragment assignments of $[CuAg(dcpm)_2]^{2+}$ dication. Nominal masses of isolated precursor P and fragment ions F_i are indicated. Charge states, fragment formula and losses are shown. Fragments are categorized into ionic and neutral losses. Percentages of total fragment yields were displayed for CID (excitation amplitude = 0.85 V) and UV PD (λ_{ex} = 290 nm, 2 μJ), respectively.

Label	Isolation	m/z	z	Loss	Category	CID / PD [%]
P	$[CuAg(dcpm)_2]^{2+}$	493	2			
F_1	$[CuAg(CH_2)P_3(Cy)_6]^+$	775	1	$(PCH_2Cy_2)^+$	IF	-/✓ [0/2]
F_2	$[Ag(CH_2)P_2(Cy)_4]^+$	515	1	$[Cu(CH_2)P_2(Cy)_4]^+$	IF	✓/- [64/-]
F_3	$[Cu(CH_2)P_2(Cy)_4]^+$	471	1	$[Ag(CH_2)P_2(Cy)_4]^+$	IF	✓/✓ [6/3]
F_4	$[CuP_2(Cy)_4]^+$	457	1	$[Ag(dcpm)(CH_2)]^+$	IF	✓/- [4/-]
F_5	$[CuAg(CH_2)_2P_4(Cy)_7H]^{2+}$	452	2	(Cy-H)	NL	✓/✓ [1/6]
	$[CuAg(CH_2)_2P_4(Cy)_7H]^{2+}$	(451.5)	2	(Cy)	NL	
F_6	$[Cu(CH_2)_2P_4(Cy)_8]^{2+}$	439.5	2	Ag^0	NL	-/✓ [0/67]
F_7	$[Ag(CH_2)P_2(Cy)_3H]^+$	433	1	$[Cu(CH_2)P_2(Cy)_4]^+$, (Cy-H)	IF	✓/- [1/-]
F_8	$[CuAg(CH_2)_2P_4(Cy)_6H]^{2+}$	410,5	2	(Cy), (Cy-H)	NL	✓/✓ [6/9]
F_9	$[CuAg(CH_2)_2P_4(Cy)_5H_2]^{2+}$	369.5	2	(Cy), 2(Cy-H)	NL	-/✓ [0/5]
F_{10}	$[CuAg(CH_2)_2P_4(Cy)_4H_3]^{2+}$	328.5	2	(Cy), 3(Cy-H)	NL	✓/✓ [10/7]
F_{11}	$(CH_2P_2(Cy)_3H)^+$	(326)	1	$[CuAg(dcpm)(Cy\text{-}H)]^+$	IF	
F_{12}	$(PCH_2Cy_2)^+$	211	1	$[CuAg(dcpm)(PCy_2)]^+$	IF	✓/✓ [1/1]

Tab. S3 Mass spectrometric PD and CID fragment assignments of $[CuAu(\textit{dcpm})_2]^{2+}$ dication. Nominal masses of isolated precursor P and fragment ions F_i are indicated. Charge states, fragment formula and losses are shown. Fragments are categorized into ionic and neutral losses. Percentages of total fragment yields were displayed for CID (excitation amplitude = 1.1 V) and UV PD (λ_{ex} = 296 nm, 2 µJ), respectively.

Label	Isolation	m/z	z	Loss	Category	CID /PD [%]
P	$[CuAu(\textit{dcpm})_2]^{2+}$	538	2			
F_1	$[CuAu(CH_2)P_3(Cy)_6]^+$	865	1	$(PCH_2Cy_2)^+$	IF	✓/✓ [6/27]
F_2	$[CuAu(CH_2)P_4(Cy)_6(Cy-H)]^{2+}$	497	2	(Cy), H	NL	✓/✓ [59/10]
	$[CuAu(CH_2)_2P_4(Cy)_7]^{2+}$	(496.5)	2	(Cy)	NL	
F_3	$[CuAu(CH_2)P_4(Cy)_6H_2]^{2+}$	456	2	2(Cy-H)	NL	✓/✓ [11/15]
	$[CuAu(CH_2)P_4(Cy)_6H]^{2+}$	(455.5)	2	(Cy), (Cy-H)	NL	
	$[CuAu(CH_2)P_4(Cy)_6]^{2+}$	(455)	2	2(Cy)		
F_4	$[CuAu(CH_2)P_4(Cy)_5H_3]^{2+}$	415	2	3(Cy-H)	NL	✓/✓ [3/14]
	$[CuAu(CH_2)P_4(Cy)_5H_2]^{2+}$	(414.5)	2	(Cy), 2(Cy-H)	NL	
	$[CuAu(CH_2)P_4(Cy)_5H]^{2+}$	(414)	2	2(Cy), (Cy-H)	NL	
F_5	$[CuAu(CH_2)P_4(Cy)_4H_4]^{2+}$	374	2	4(Cy-H)	NL	✓/✓ [5/10]
	$[CuAu(CH_2)P_4(Cy)_4H_3]^{2+}$	(373.5)	2	(Cy), 3(Cy-H)	NL	
	$[CuAu(CH_2)P_4(Cy)_4H_2]^{2+}$	(373)	2	2(Cy), 2(Cy-H)	NL	
F_6	$[CuAu(CH_2)P_4(Cy)_3H_4]^{2+}$	332.5	2	(Cy), 4(Cy-H)	NL	✓/✓ [2/1]
	$[CuAu(CH_2)P_4(Cy)_3H_3]^{2+}$	(332)	2	2(Cy), 3(Cy-H)	NL	
F_7	$[CuAu(CH_2)P_4(Cy)_2H_5]^{2+}$	291.5	2	(Cy), 5(Cy-H)	NL	✓/✓ [5/2]
	$[CuAu(CH_2)P_4(Cy)_2H_4]^{2+}$	(291)	2	2(Cy), 4(Cy-H)	NL	
F_8	$[CuAu(CH_2)P_4(Cy)H_7]^{2+}$	251	2	7(Cy-H)	NL	✓/✓ [4/1]
	$[CuAu(CH_2)P_4(Cy)H_6]^{2+}$	(250.5)	2	(Cy), 6(Cy-H)	NL	
F_9	$(PCH_2Cy_2)^+$	211	1	$[CuAu(\textit{dcpm})(PCy_2)]^+$	IF	✓/✓ [1/19]

Tab. S4 Mass spectrometric PD and CID fragment assignments of $[AgAu(\textit{dcpm})_2]^{2+}$ dication. Nominal masses of isolated precursor P and fragment ions F_i are indicated. Charge states, fragment formula and losses are shown. Fragments are categorized into ionic and neutral losses. Percentages of total fragment yields were displayed for CID (excitation amplitude = 1.2 V) and UV PD (λ_{ex} = 268 nm, 2 µJ), respectively.

Label	Isolation	m/z	z	Loss	Category	CID /PD [%]
P	$[AgAu(\textit{dcpm})_2]^{2+}$	560	2			
F_1	$[AgAu(CH_2)_2P_4(Cy)_6H]^+$	955	1	"(Cy), (Cy-H)"$^+$	IF	✓/- [0/-]
F_2	$[AgAu(CH_2)P_3(Cy)_6]^+$	909	1	$(PCH_2Cy_2)^+$	IF	✓/✓ [7/3]
F_3	$[AgAu(CH_2)P_3(Cy)_5H]^+$	827	1	"2(Cy), (Cy-H)"$^+$	IF	✓/- [1/-]
F_4	$[AgAu(CH_2)_2P_4(Cy)_7H]^{2+}$	519	2	(Cy-H)	NL	✓/✓ [54/21]
	$[AgAg(CH_2)_2P_4(Cy)_7]^{2+}$	(518.5)	2	(Cy)	NL	
	$[AgAg(CH_2)_2P_4(Cy)_6(Cy\text{-}H)]^{2+}$	(518)	2	(Cy), H	NL	
F_5	$[AuAg(CH_2)_2P_4(Cy)_6H]^{2+}$	477.5	2	(Cy), (Cy-H)	NL	✓/✓ [13/27]
	$[AuAg(CH_2)_2P_4(Cy)_6]^{2+}$	(477)	2	2(Cy)	NL	
F_6	$[Au(CH_2)_2P_4(Cy)_7H]^{2+}$	465.5		Ag^0, +H	NL	-/✓ [-/2]
F_7	$[AuAg(CH_2)_2P_4(Cy)_5H_3]^{2+}$	437	2	3(Cy-H)	NL	✓/✓ [4/25]
	$[AuAg(CH_2)_2P_4(Cy)_5H]^{2+}$	(436)	2	2(Cy), (Cy-H)	NL	
F_8	$[AuAg(CH_2)_2P_4(Cy)_4H_4]^{2+}$	396	2	4(Cy-H)	NL	✓/✓ [5/15]
	$[AuAg(CH_2)_2P_4(Cy)_4H_3]^{2+}$	(395.5)	2	(Cy), 3(Cy-H)	NL	
	$[AuAg(CH_2)_2P_4(Cy)_4H_2]^{2+}$	(395)	2	2(Cy), 2(Cy-H)	NL	
F_9	$[AuAg(CH_2)P_2(Cy)(Cy\text{-}H)_2]^{2+}$	313.5	2	(*dcpm*), 2H	NL	✓/✓ [3/0]
F_{10}	$[AuAg(CH_2)P_2(Cy)_2]^{2+}$	273	2	(*dcpm*), 2(Cy)	NL	✓/✓ [6/1]
	$[AuAg(CH_2)P_2(Cy)_2\text{-}H]^{2+}$	272.5	2	(*dcpm*), (Cy), (Cy-H)	NL	
F_{11}	$(PCH_2Cy_2)^+$	211	1	$[AgAu(\textit{dcpm})(PCy_2)]^+$	IF	✓/✓ [0/0]

Tab. S5 Mass spectrometric PD and CID fragment assignments of $[Au_2(dcpm)_2]^{2+}$ dication. Nominal masses of isolated precursor P and fragment ions F_i are indicated. Charge states, fragment formula and losses are shown. Fragments are categorized into ionic and neutral losses. Percentages of total fragment yields were displayed for CID (excitation amplitude = 1.25 V) and UV PD (λ_{ex} = 277 nm, 2 µJ), respectively.

Label	Isolation	m/z	z	Loss	Category	CID / PD [%]
P	$[Au_2(dcpm)_2]^{2+}$	605	2			
F_1	$[Au_2(CH_2)_2P_4(Cy)_7]^+$	1127	1	$(Cy)^+$	IF	✓/- [1/0]
F_2	$[Au_2(CH_2)_2P_4(Cy)_6H]^+$	1045	1	"(Cy), (Cy-H)"$^+$	IF	✓/- [1/0]
F_3	$[Au_2(CH_2)P_3(Cy)_6]^+$	999	1	$(PCH_2Cy_2)^+$	IF	✓/✓ [7/7]
F_4	$[Au_2(CH_2)_2P_4(Cy)_5H_2]^+$	963	1	"(Cy), -2(Cy-H)"$^+$	IF	✓/- [1/0]
	$[Au_2(CH_2)_2P_4(Cy)_5]^+$	(961)	1	"3(Cy)"$^+$	IF	
F_5	$[Au_2(CH_2)P_3(Cy)_5H]^+$	917	1	$(PCH_2Cy_2(Cy\text{-}H))^+$	IF	✓/- [1/0]
F_6	$[Au_2(CH_2)P_3(Cy)_4H_2]^+$	835	1	$(PCH_2Cy_2)^+$, 2(Cy-H)	IF	✓/- [1/0]
	$[Au_2(CH_2)P_3(Cy)_4]^+$	(833)	1	$(PCH_2Cy_2)^+$, 2(Cy)	IF	
F_7	$[Au_2(CH_2)_2P_4(Cy)_7H]^{2+}$	564	2	(Cy-H)	NL	✓/✓ [59/12]
	$[Au_2(CH_2)_2P_4(Cy)_7]^{2+}$	(563.5)	2	(Cy)	NL	
F_8	$[Au_2(CH_2)_2P_4(Cy)_6H_2]^{2+}$	523	2	2(Cy-H)	NL	✓/✓ [15/19]
	$[Au_2(CH_2)_2P_4(Cy)_6]^{2+}$	(522)	2	2(Cy)	NL	
F_9	$[Au_2(CH_2)_2P_4(Cy)_5H_4]^{2+}$	482	2	3(Cy-H), +H	NL	✓/✓ [4/23]
	$[Au_2(CH_2)_2P_4(Cy)_5H_2]^{2+}$	(481)	2	(Cy), 2(Cy-H)	NL	
F_{10}	$[Au_2(CH_2)_2P_4(Cy)_4H_4]^{2+}$	441	2	4(Cy-H)	NL	✓/✓ [3/24]
	$[Au_2(CH_2)_2P_4(Cy)_4H_3]^{2+}$	(440.5)	2	(Cy), 3(Cy-H)	NL	
	$[Au_2(CH_2)_2P_4(Cy)_4H_2]^{2+}$	(440)	2	2(Cy), 2(Cy-H)	NL	
F_{11}	$[Au_2(CH_2)_2P_4(Cy)_3H_5]^{2+}$	400		5(Cy-H)	NL	✓/- [0/-]
	$[Au_2(CH_2)_2P_4(Cy)_3H_4]^{2+}$	(399.5)	2	(Cy), 4(Cy-H)	NL	
	$[Au_2(CH_2)_2P_4(Cy)_3H_3]^{2+}$	(399)	2	2(Cy), 3(Cy-H)	NL	
F_{12}	$[Au_2(CH_2)_2P_4(Cy)_2H_6]^{2+}$	359	2	6(Cy-H)	NL	✓/- [2/5]
	$[Au_2(CH_2)_2P_4(Cy)_2H_5]^{2+}$	(358.5)	2	(Cy), 5(Cy-H)	NL	
F_{13}	$[Au_2(CH_2)_2P_4(Cy)H_7]^{2+}$	318	2	7(Cy-H)	NL	✓/- [3/-]
	$[Au_2(CH_2)_2P_4(Cy)H_6]^{2+}$	(317.5)	2	(Cy), -6(Cy-H)	NL	
F_{14}	$(PCH_2Cy_2)^+$	211	1	$[Au_2(dcpm)(PCy_2)]^+$	IF	-/✓ [-/5]

1.2.3 Mass spectrometric isotope patterns of CID fragment channels

Tab. S6 Top: Isotope patterns of isolated $[Cu_2(dcpm)_2]^{2+}$ precursor ion mass-signals and its CID products. Bottom: Simulated isotope patterns (Gaussian profile, *m/z* = 0.2 fwhm). Mass-signals normalized to unity for comparison.

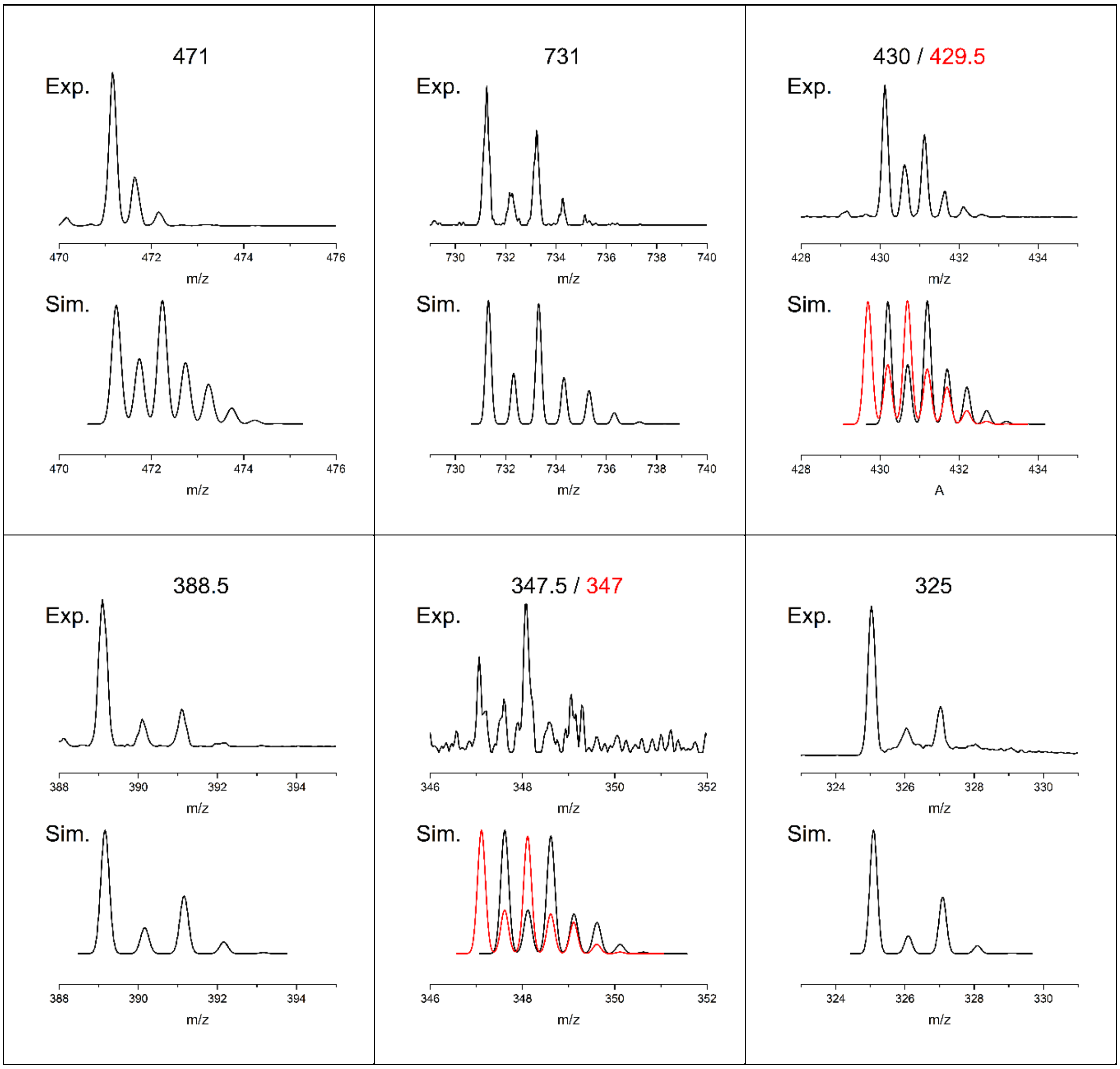

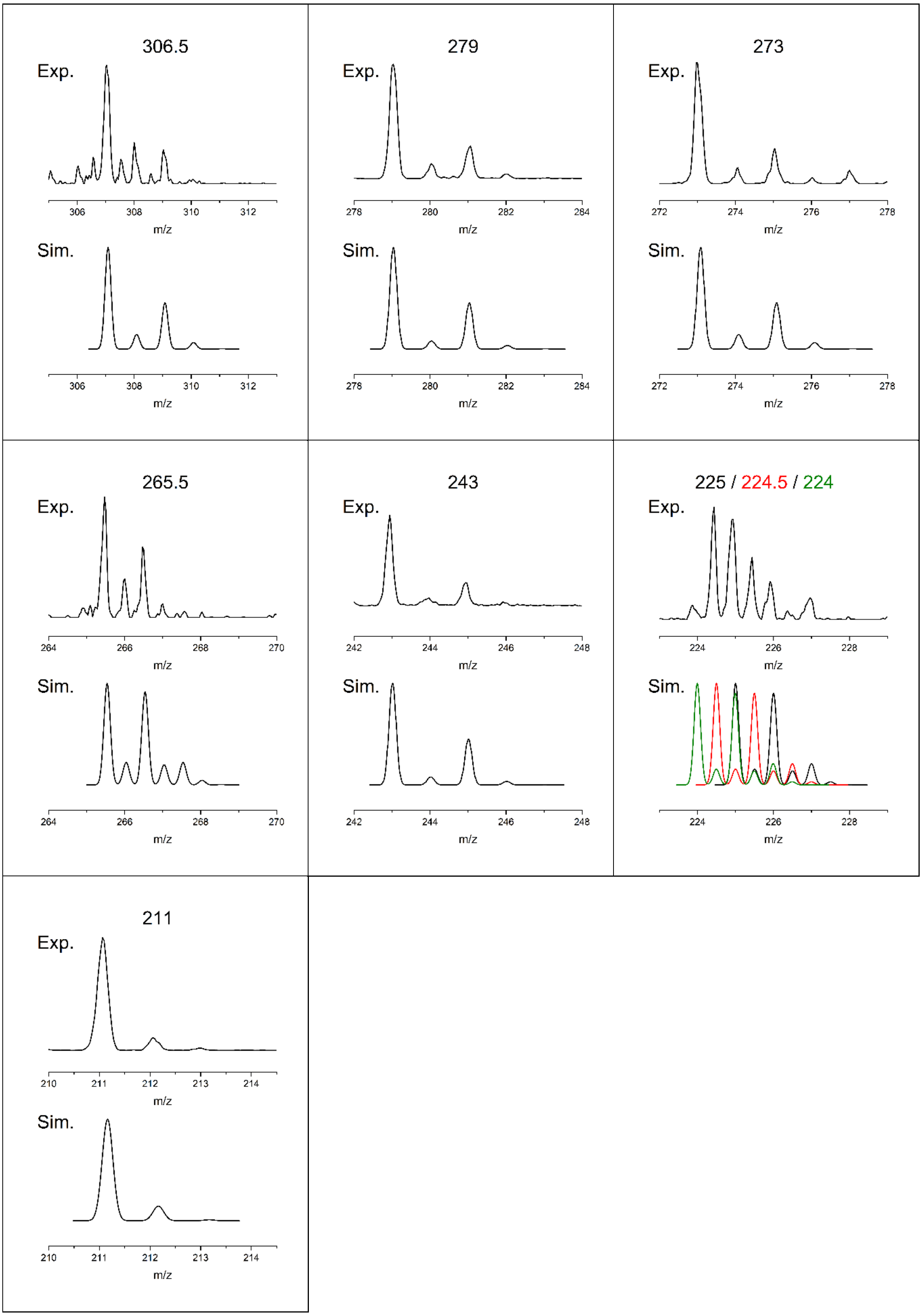
306.5
Exp.
306
308
310
312
m/z
Sim.
306
308
310
312
m/z
279
Exp.
278
280
282
284
m/z
Sim.
278
280
282
284
m/z
273
Exp.
272
274
276
278
m/z
Sim.
272
274
276
278
m/z
265.5
Exp.
264
266
268
270
m/z
Sim.
264
266
268
270
m/z
243
Exp.
242
244
246
248
m/z
Sim.
242
244
246
248
m/z
225 / 224.5 / 224
Exp.
224
226
228
m/z
Sim.
224
226
228
m/z
211
Exp.
210
211
212
213
214
m/z
Sim.
210
211
212
213
214
m/z

Tab. S7 Top: Isotope patterns of isolated [CuAg(*dcpm*)$_2$]$^{2+}$ precursor ion mass-signals and its CID products. Bottom: Simulated isotope patterns (Gaussian profile, *m/z* = 0.2 fwhm). Mass-signals normalized to unity for comparison.

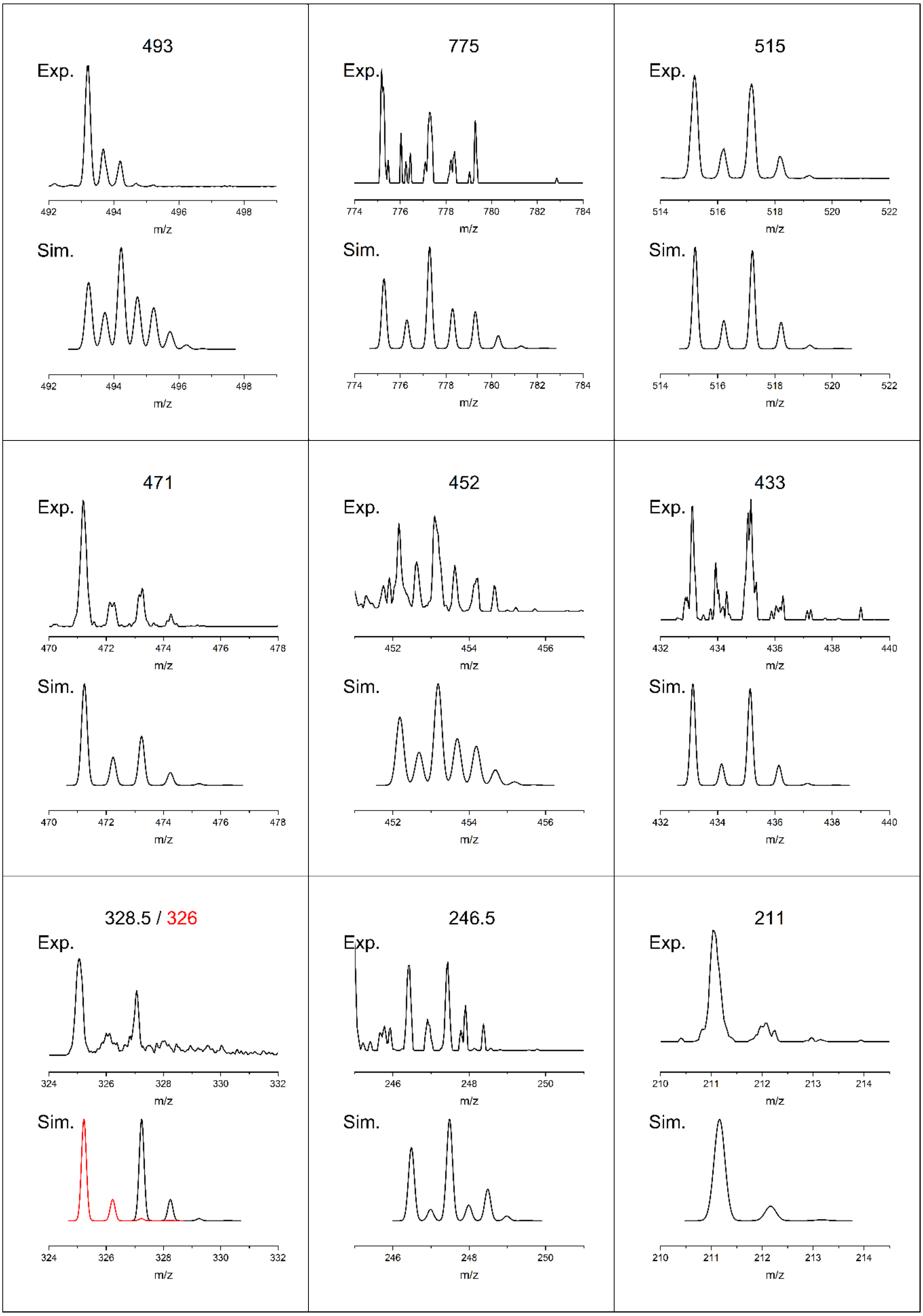

Tab. S8 Top: Isotope patterns of isolated $[CuAu(dcpm)_2]^{2+}$ precursor ion mass-signals and its CID products. Bottom: Simulated isotope patterns (Gaussian profile, *m/z* = 0.2 fwhm). Mass-signals normalized to unity for comparison.

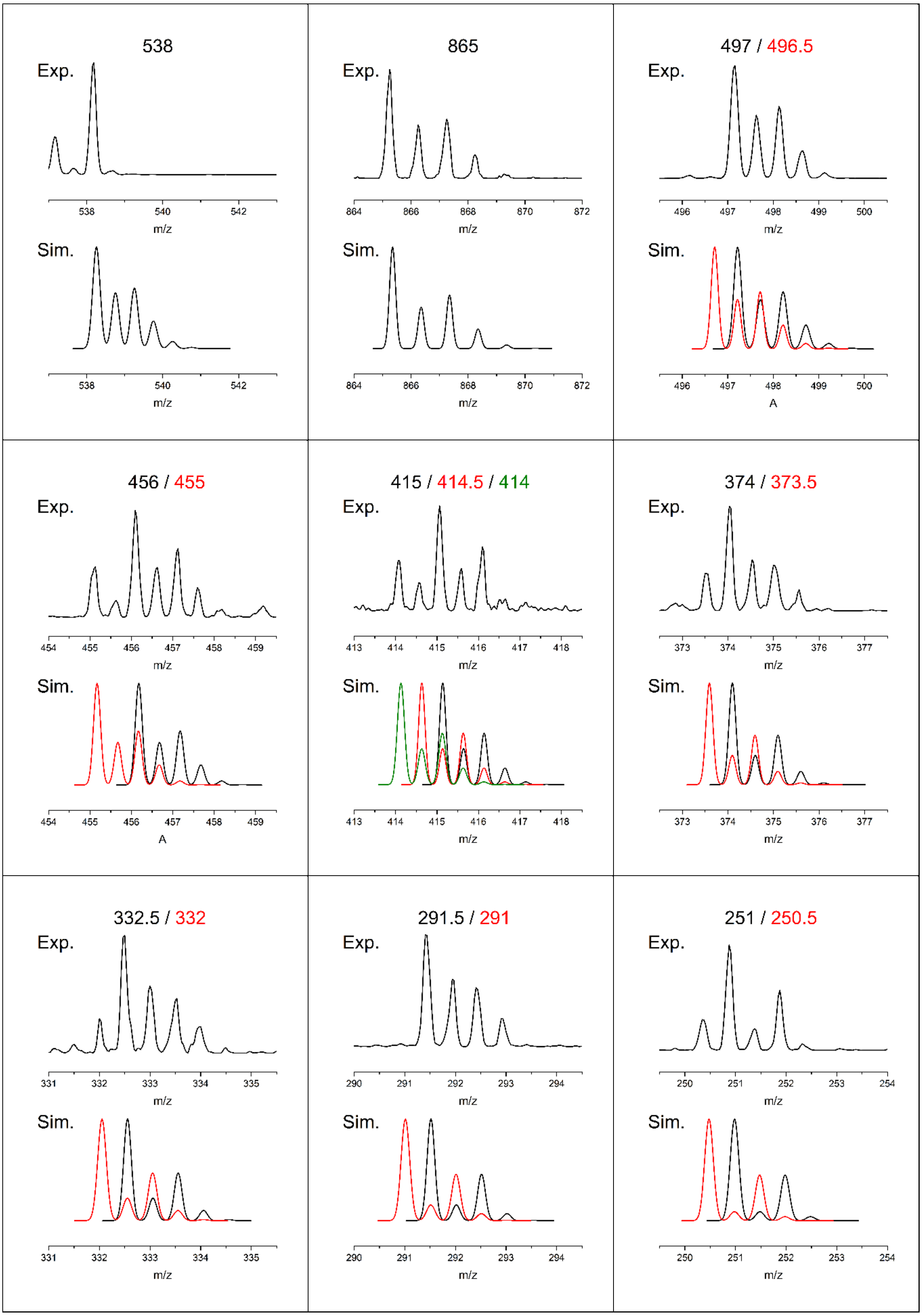

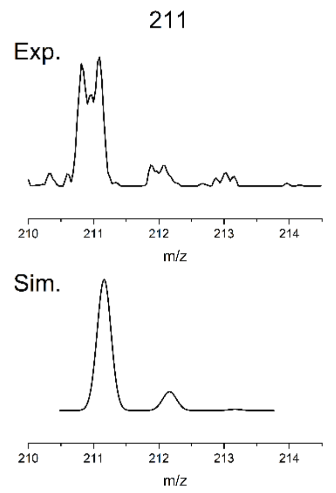
211
Exp.
210
211
212
213
214
m/z
Sim.
210
211
212
213
214
m/z

Tab. S9 Top: Isotope patterns of isolated $[AgAu(dcpm)_2]^{2+}$ precursor ion mass-signals and its CID products. Bottom: Simulated isotope patterns (Gaussian profile, m/z = 0.2 fwhm). Mass-signals normalized to unity for comparison.

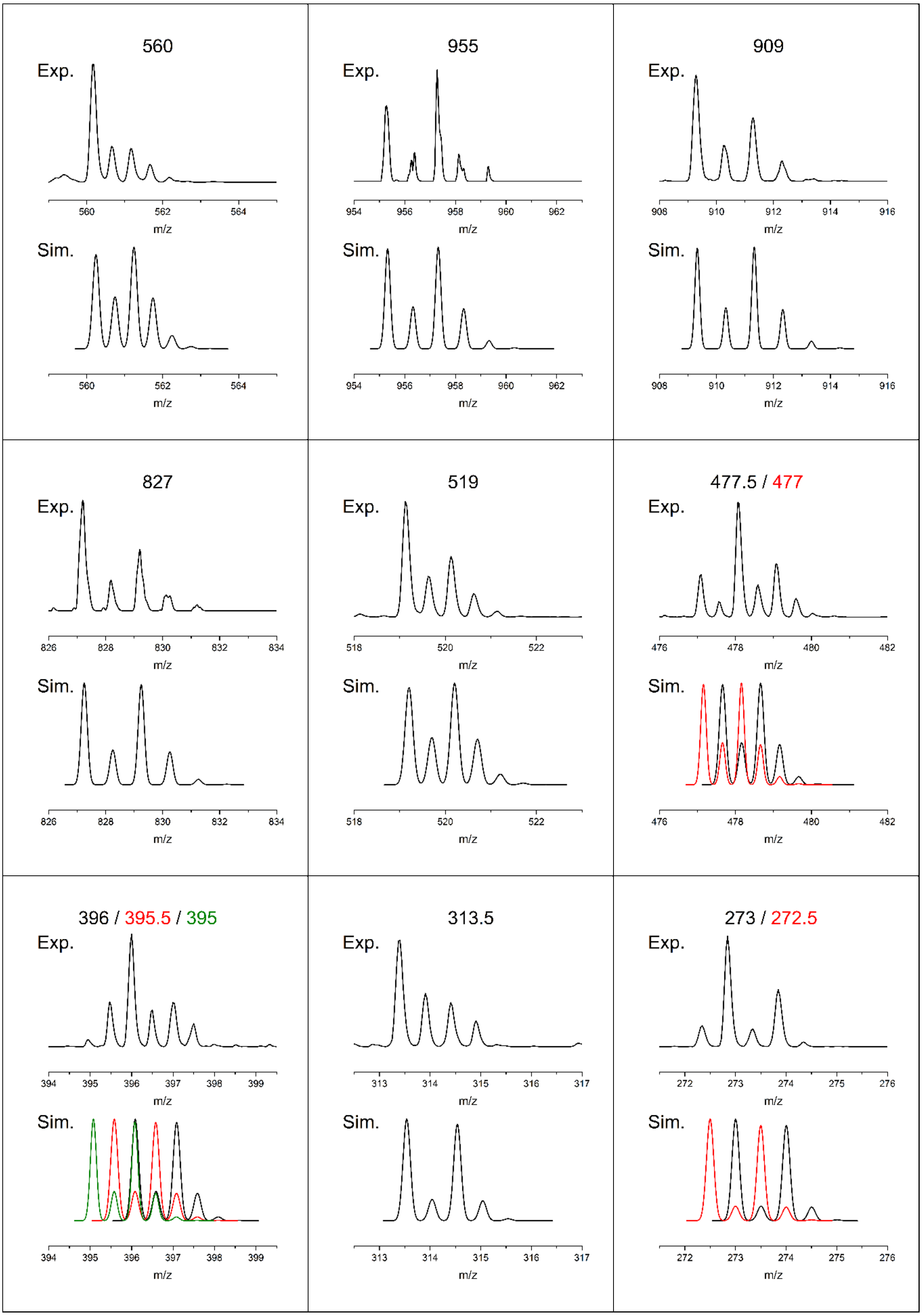

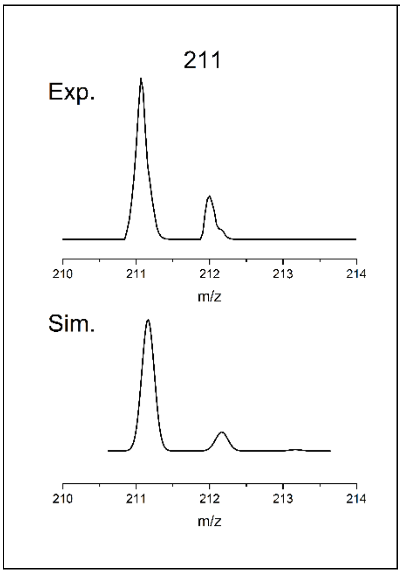
211
Exp.
210
211
212
213
214
m/z
Sim.
210
211
212
213
214
m/z

Tab. S10 Top: Isotope patterns of isolated $[Au_2(\mathit{dcpm})_2]^{2+}$ precursor ion mass-signals and its CID products. Bottom: Simulated isotope patterns (Gaussian profile, *m/z* = 0.2 fwhm). Mass-signals normalized to unity for comparison.

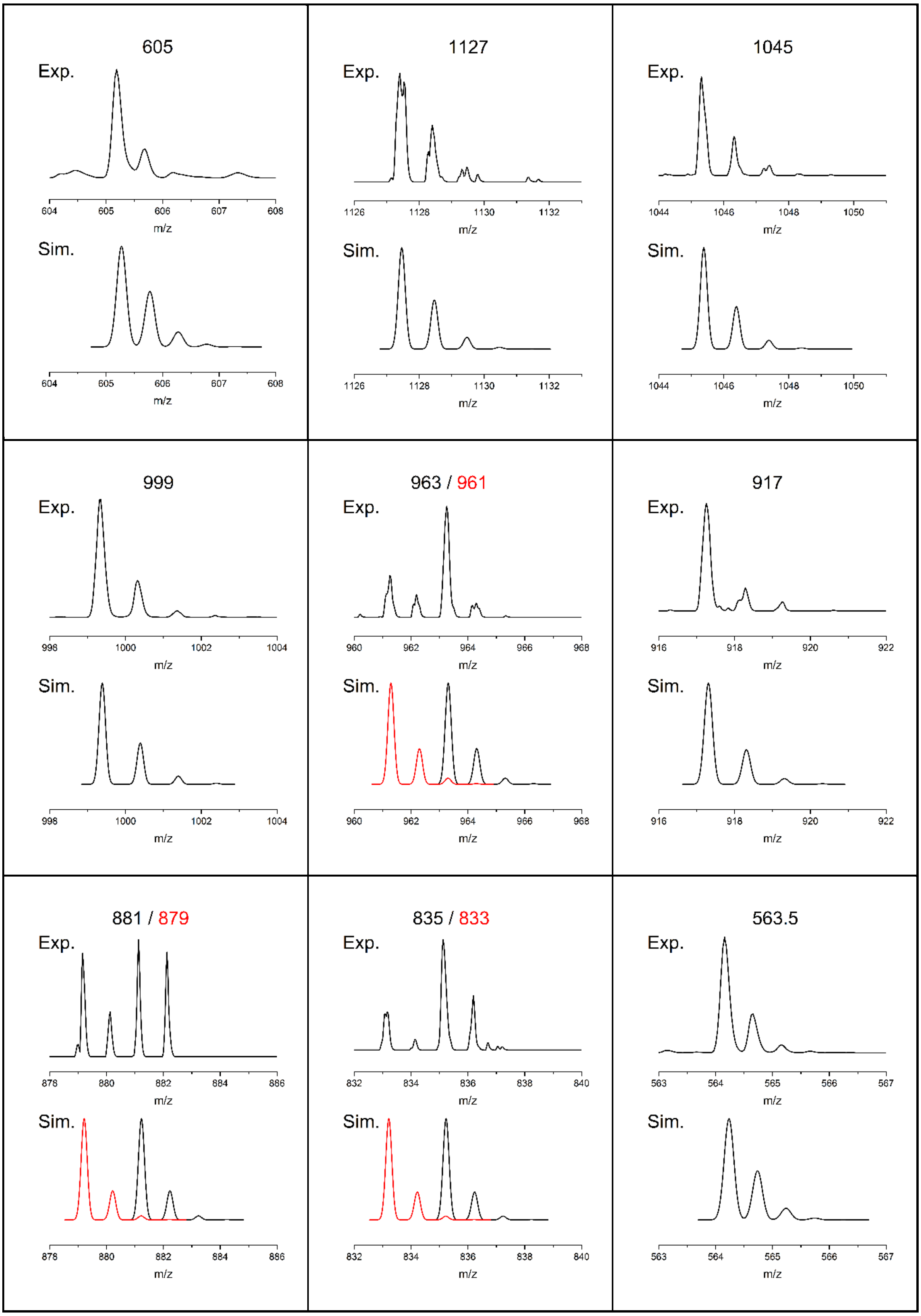

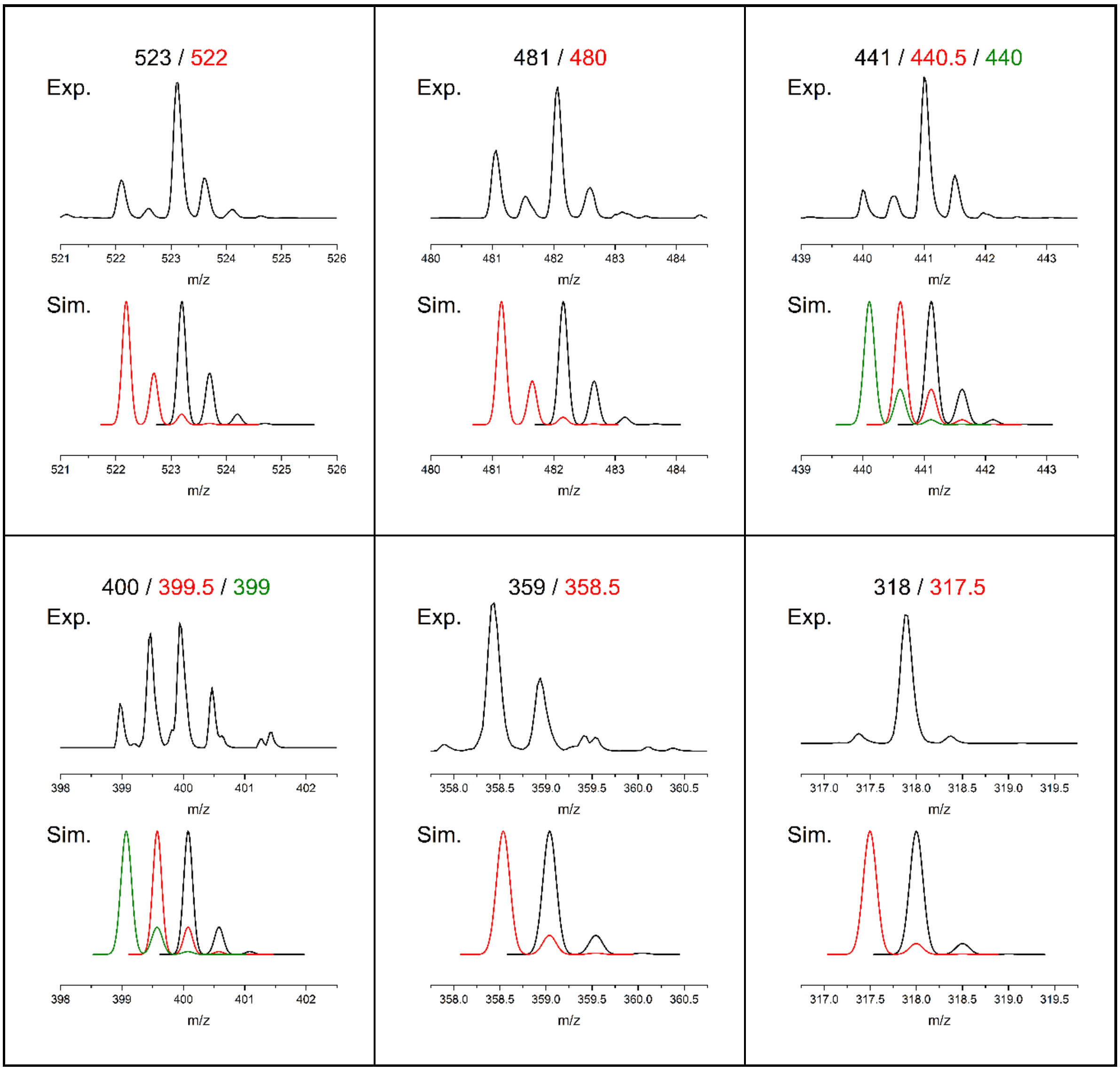
523 / 522
Exp.
Sim.
481 / 480
Exp.
Sim.
441 / 440.5 / 440
Exp.
Sim.
400 / 399.5 / 399
Exp.
Sim.
359 / 358.5
Exp.
Sim.
318 / 317.5
Exp.
Sim.
m/z

1.2.4 CID breakdown and appearance curves of heterobimetallic species

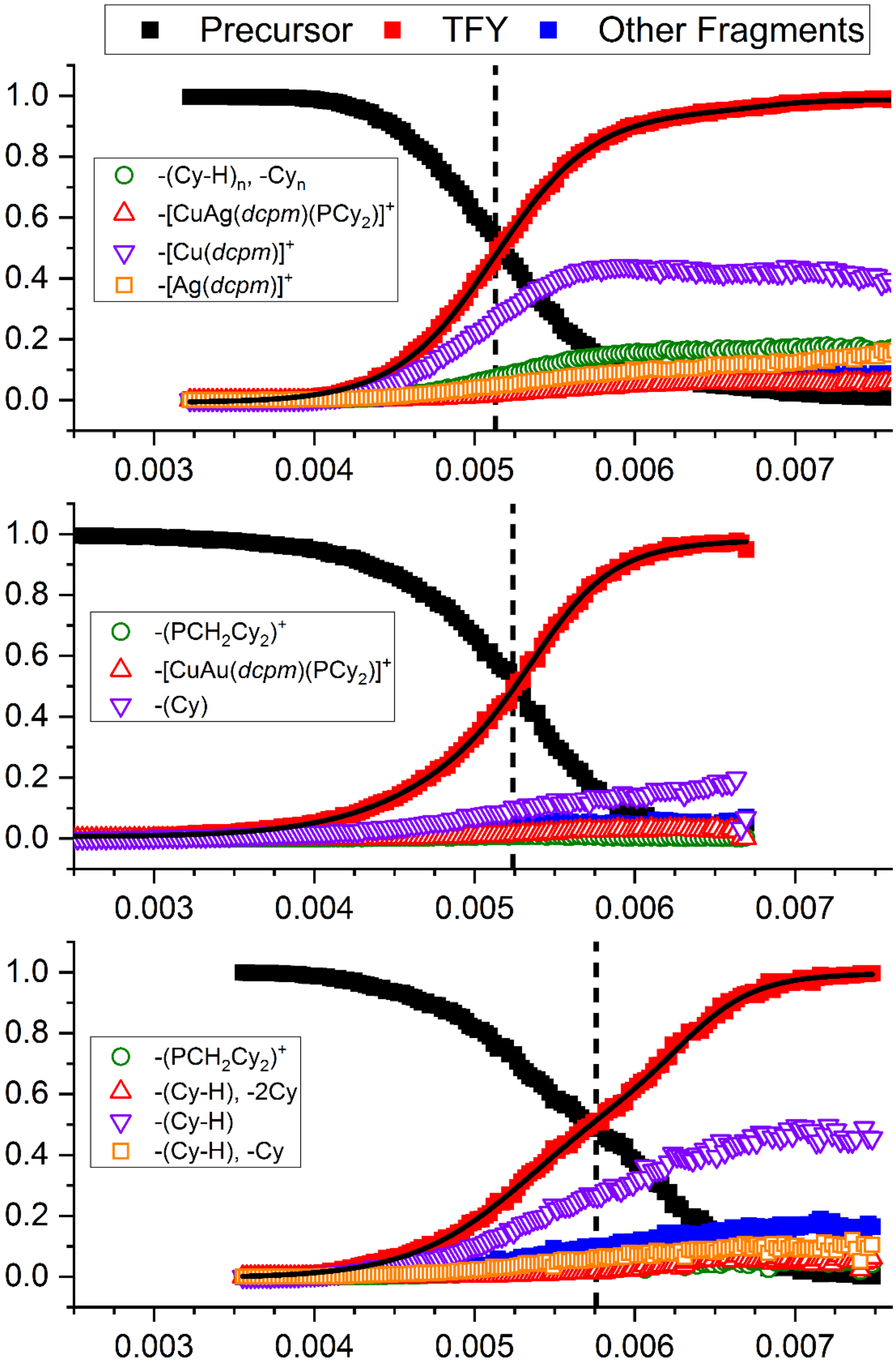

Fig. S7 CID breakdown (black squares), total fragment yield (red squares) and fragment-specific appearance curves (open symbols) of a) [CuAg(*dcpm*)$_2$]$^{2+}$, b) [CuAu(*dcpm*)$_2$]$^{2+}$ and c) [AgAu(*dcpm*)$_2$]$^{2+}$. Dashed vertical lines indicate $E_{COM}^{50\%}$ values ($E_{COM} \propto$ collisional energy, frag. time = 40 ms).

1.2.5 Mass spectrometric isotope patterns of femtosecond PD fragment channels

Tab. S11 Top: Isotope patterns of isolated $[Cu_2(\mathit{dcpm})_2]^{2+}$ precursor ion mass-signals and its photofragment products (λ_{ex} = 297.5 nm, E = 2 µJ, ~118 pulses), recorded with femtosecond laser system. Bottom: Simulated isotope patterns (Gaussian profile, *m/z* = 0.2 fwhm). Mass-signals normalized to unity for comparison.

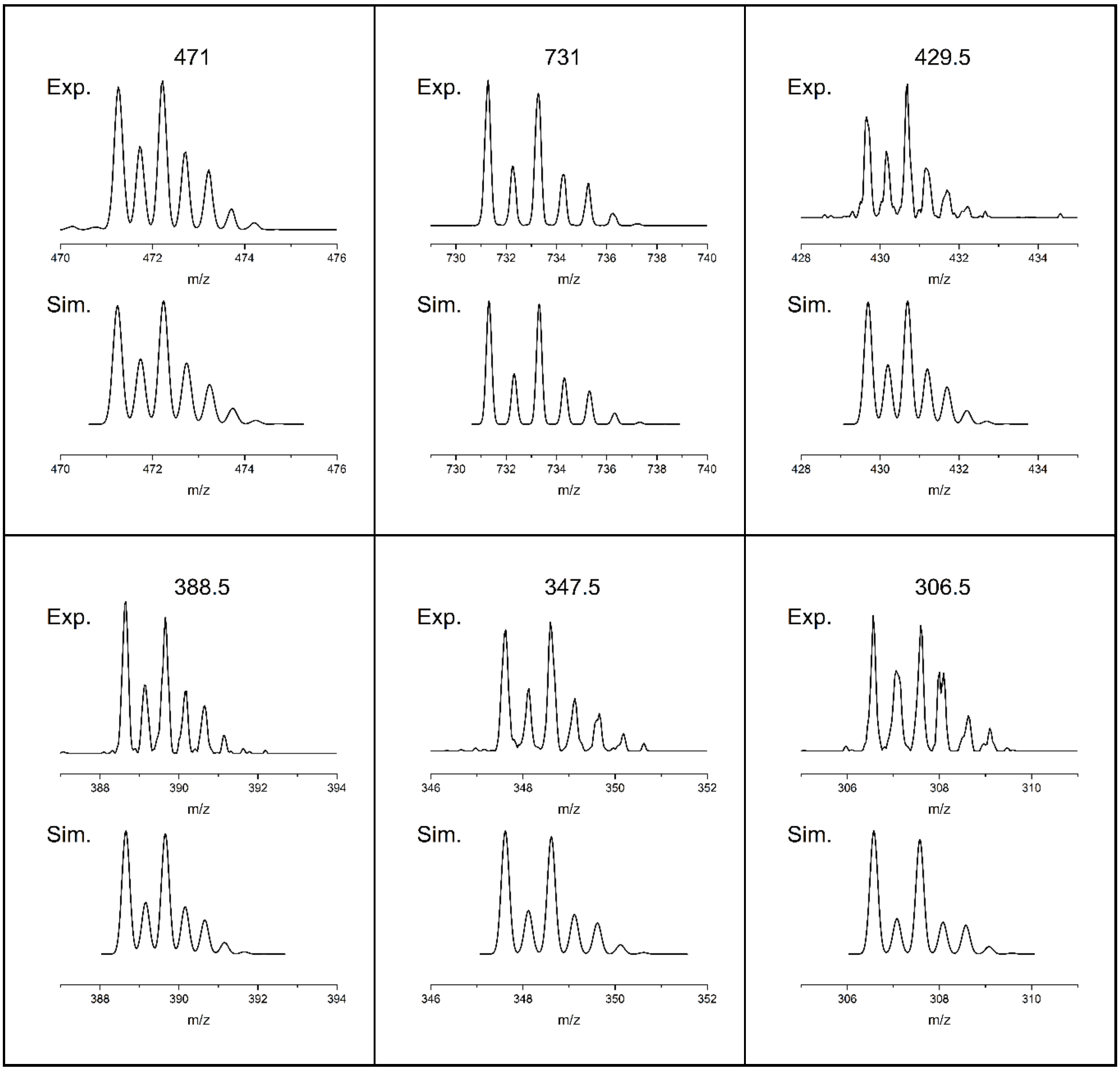

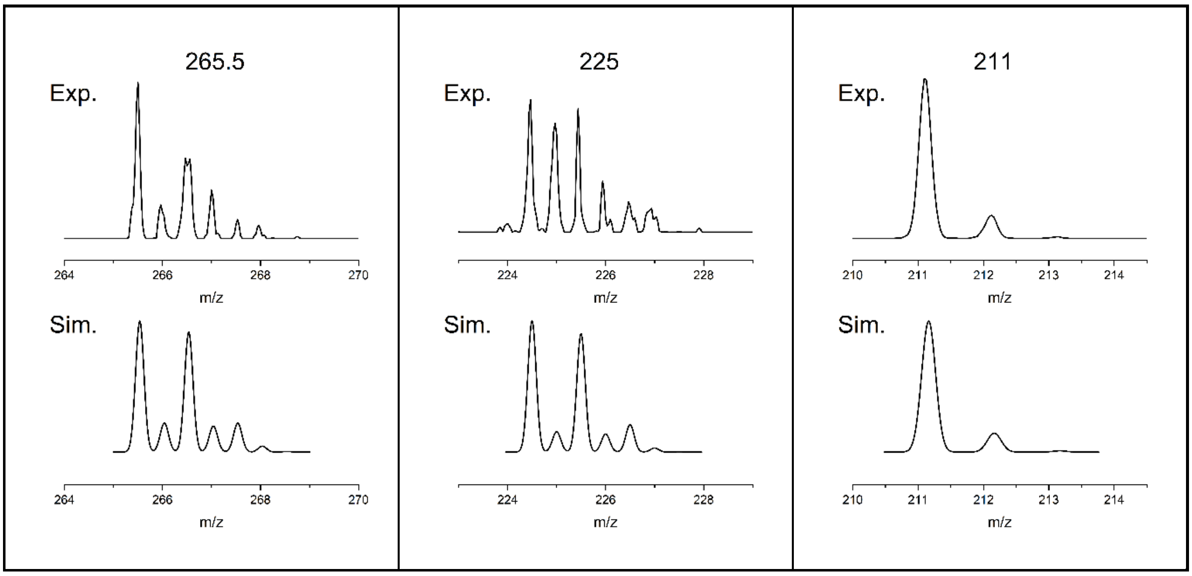

265.5
Exp.
264
266
268
270
m/z
Sim.
264
266
268
270
m/z
225
Exp.
224
226
228
m/z
Sim.
224
226
228
m/z
211
Exp.
210
211
212
213
214
m/z
Sim.
210
211
212
213
214
m/z

Tab. S12 Top: Isotope patterns of isolated $[CuAg(\mathit{dcpm})_2]^{2+}$ precursor ion mass-signals and its photofragment products (λ_{ex} = 294.5 nm, E = 2 µJ, ~118 pulses)), recorded with femtosecond laser system. Bottom: Simulated isotope patterns (Gaussian profile, *m/z* = 0.2 fwhm). Mass-signals normalized to unity for comparison.

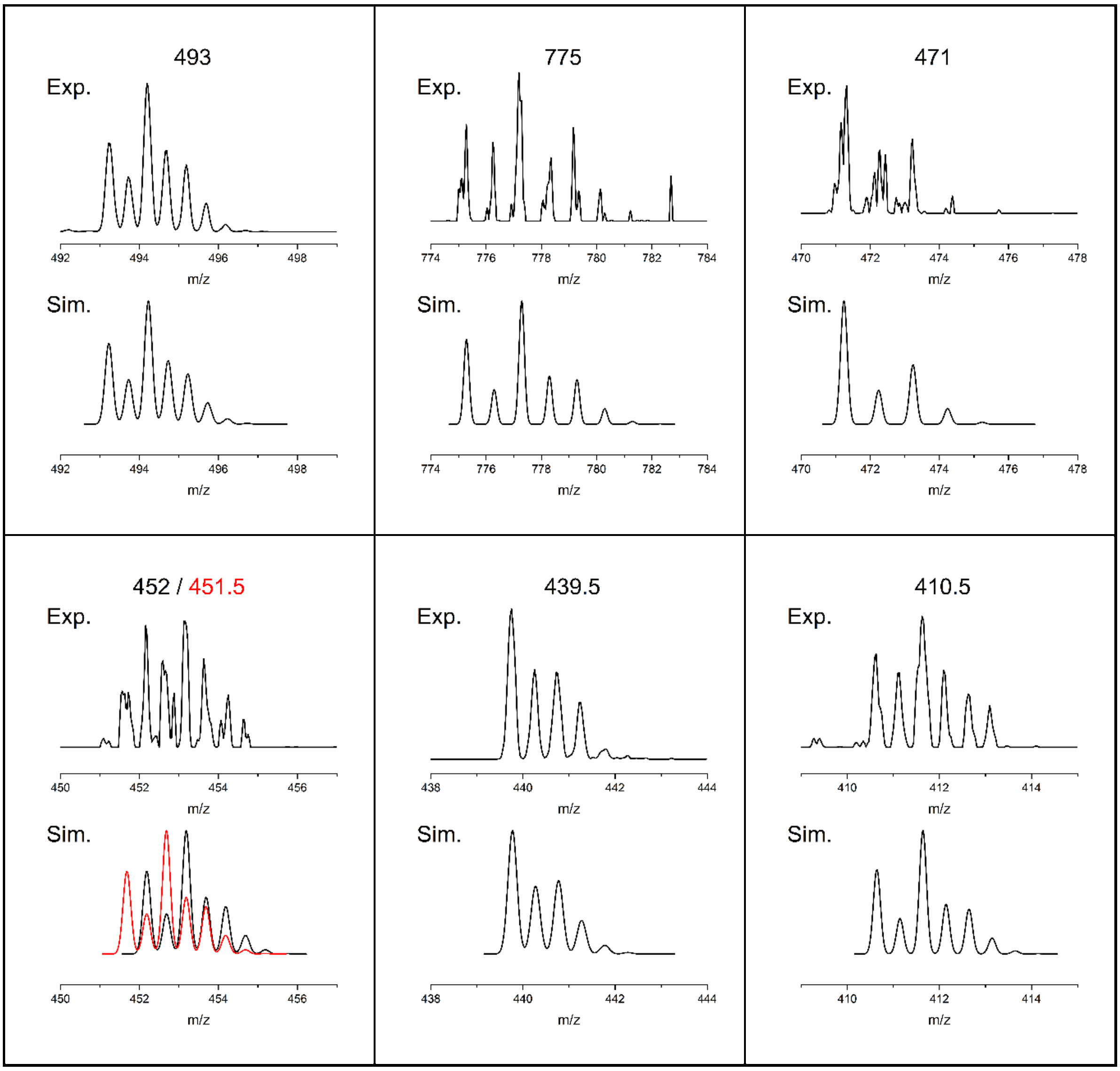

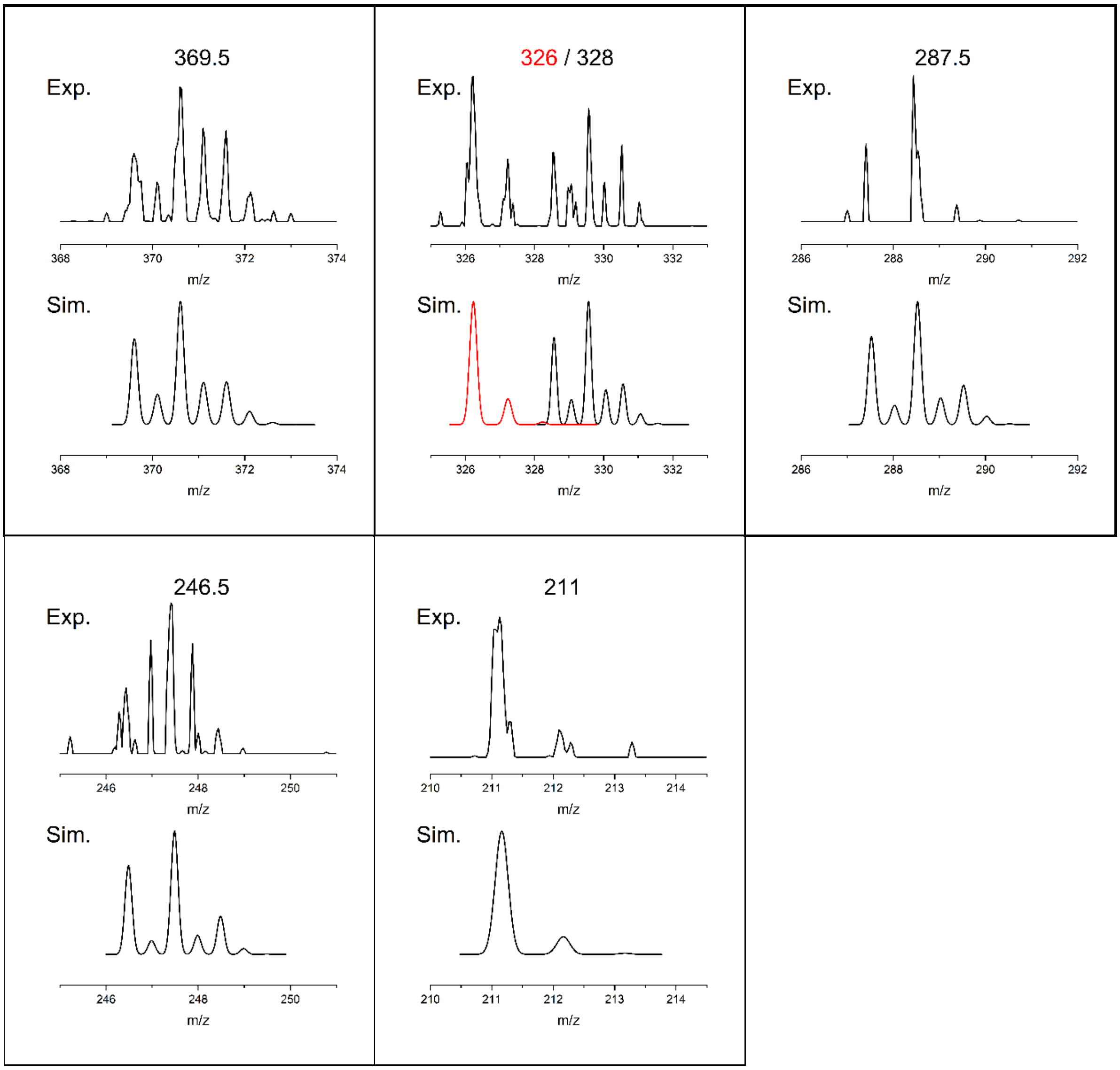
369.5
Exp.
368 370 372 374
m/z
Sim.
368 370 372 374
m/z
326 / 328
Exp.
326 328 330 332
m/z
Sim.
326 328 330 332
m/z
287.5
Exp.
286 288 290 292
m/z
Sim.
286 288 290 292
m/z
246.5
Exp.
246 248 250
m/z
Sim.
246 248 250
m/z
211
Exp.
210 211 212 213 214
m/z
Sim.
210 211 212 213 214
m/z

Tab. S13 Top: Isotope patterns of isolated [CuAu(*dcpm*)$_2$]$^{2+}$ precursor ion mass-signals and its photofragment products (λ_{ex} = 289 nm, E = 2 µJ, ~118 pulses)), recorded with femtosecond laser system. Bottom: Simulated isotope patterns (Gaussian profile, *m/z* = 0.2 fwhm). Mass-signals normalized to unity for comparison.

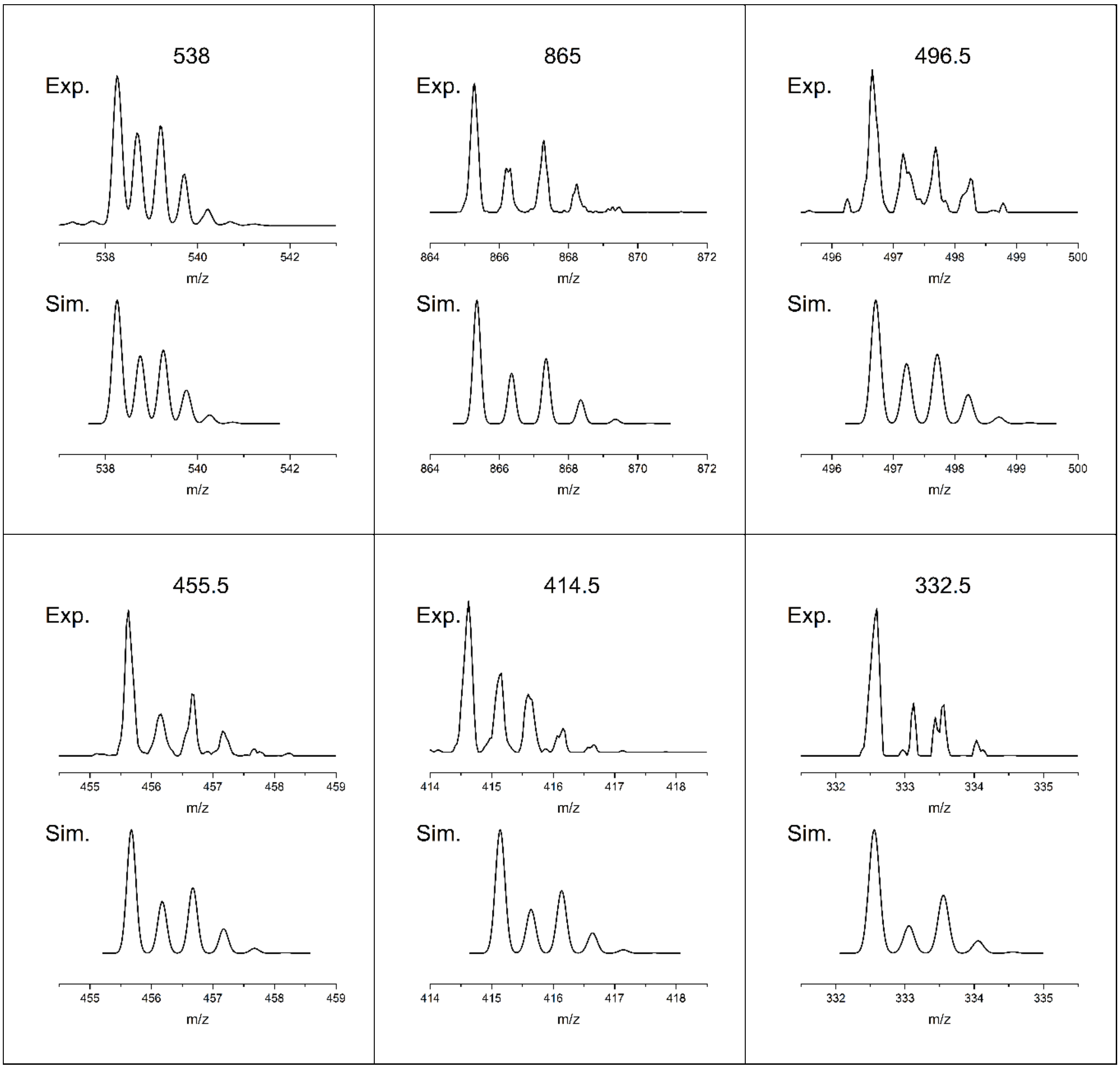

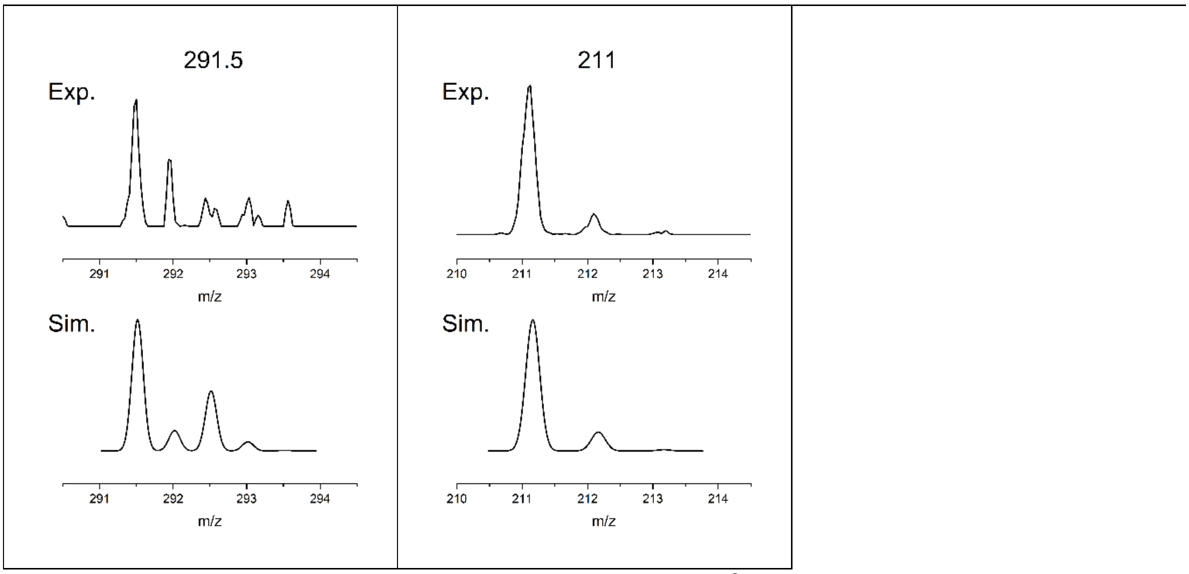

Tab. S14 Top: Isotope patterns of isolated $[AgAu(\mathit{dcpm})_2]^{2+}$ precursor ion mass-signals and its photofragment products (λ_{ex} = 268 nm, E = 2 µJ, ~118 pulses)), recorded with femtosecond laser system. Bottom: Simulated isotope patterns (Gaussian profile, *m/z* = 0.2 fwhm). Mass-signals normalized to unity for comparison.

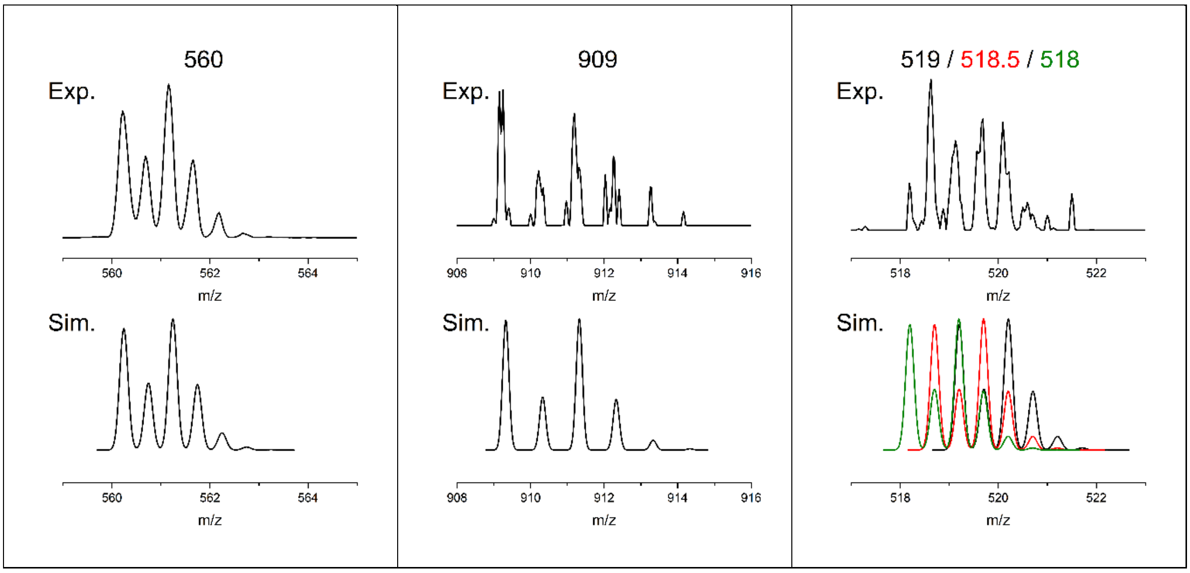

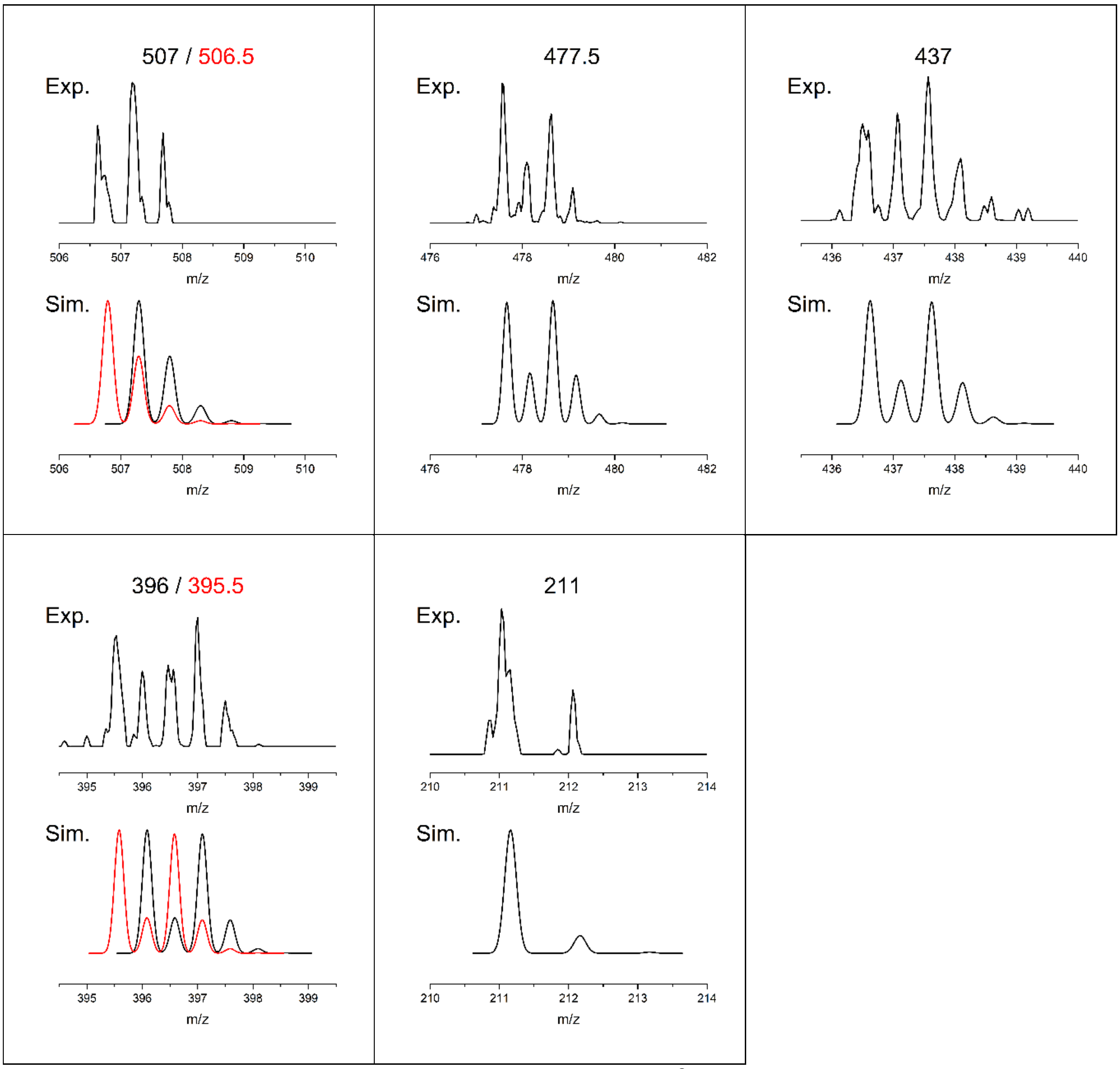

Tab. S15 Top: Isotope patterns of isolated $[Au_2(dcpm)_2]^{2+}$ precursor ion mass-signals and its photofragment products (λ_{ex} = 277 nm, E = 2 µJ, ~118 pulses)), recorded with femtosecond laser system. Bottom: Simulated isotope patterns (Gaussian profile, *m/z* = 0.2 fwhm). Mass-signals normalized to unity for comparison.

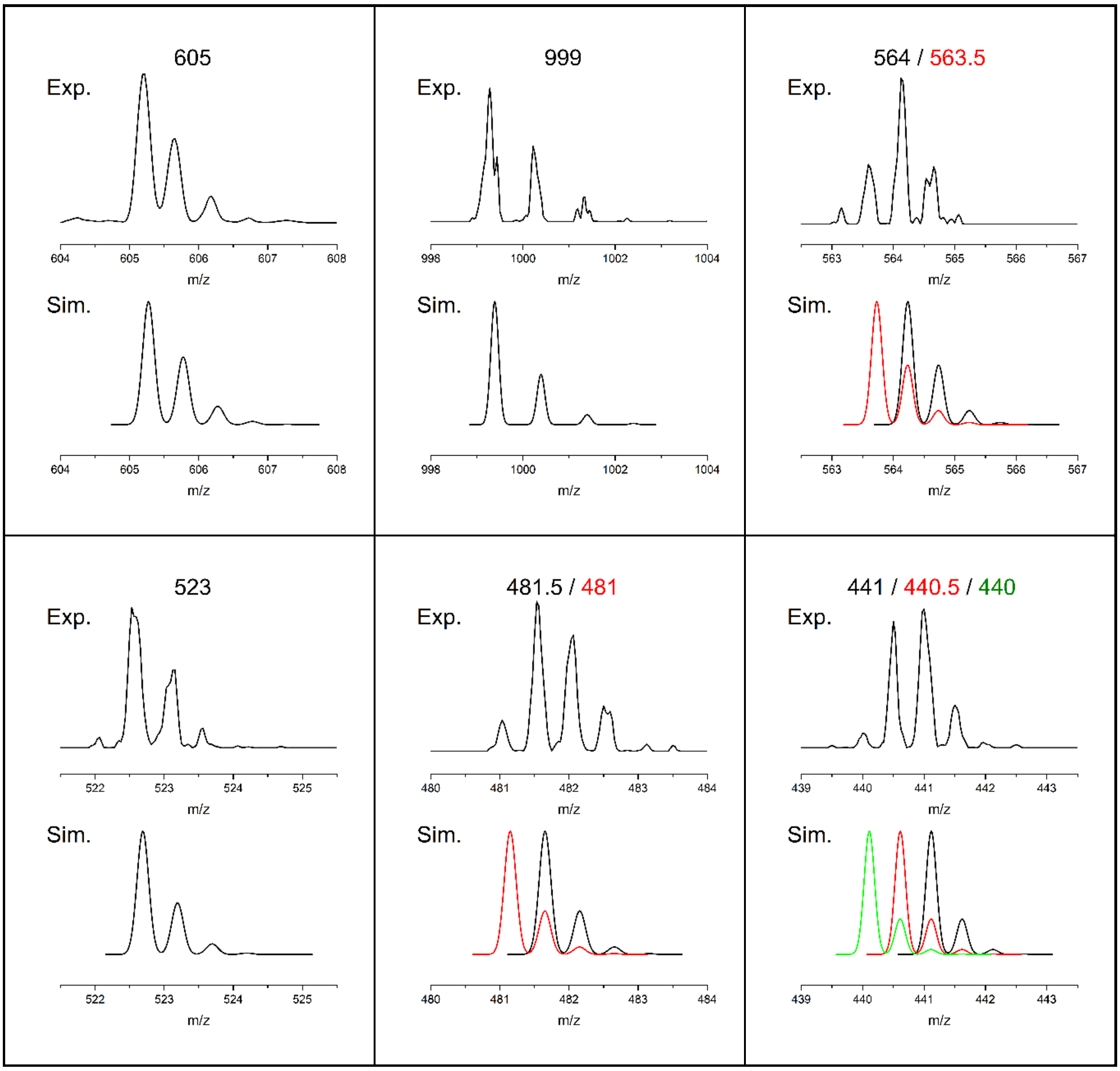
605
Exp.
Sim.
m/z
999
564 / 563.5
523
481.5 / 481
441 / 440.5 / 440

1.2.5 Mass spectrometric isotope patterns of nanosecond PD fragment channels

Tab. S16 Top: Isotope patterns of isolated $[Cu_2(\mathit{dcpm})_2]^{2+}$ precursor ion mass-signals and its photofragment products (λ_{ex} = 297 nm, E = 2 µJ, ~118 pulses)), recorded with nanosecond laser system. Bottom: Simulated isotope patterns (Gaussian profile, *m/z* = 0.2 fwhm). Mass-signals normalized to unity for comparison.

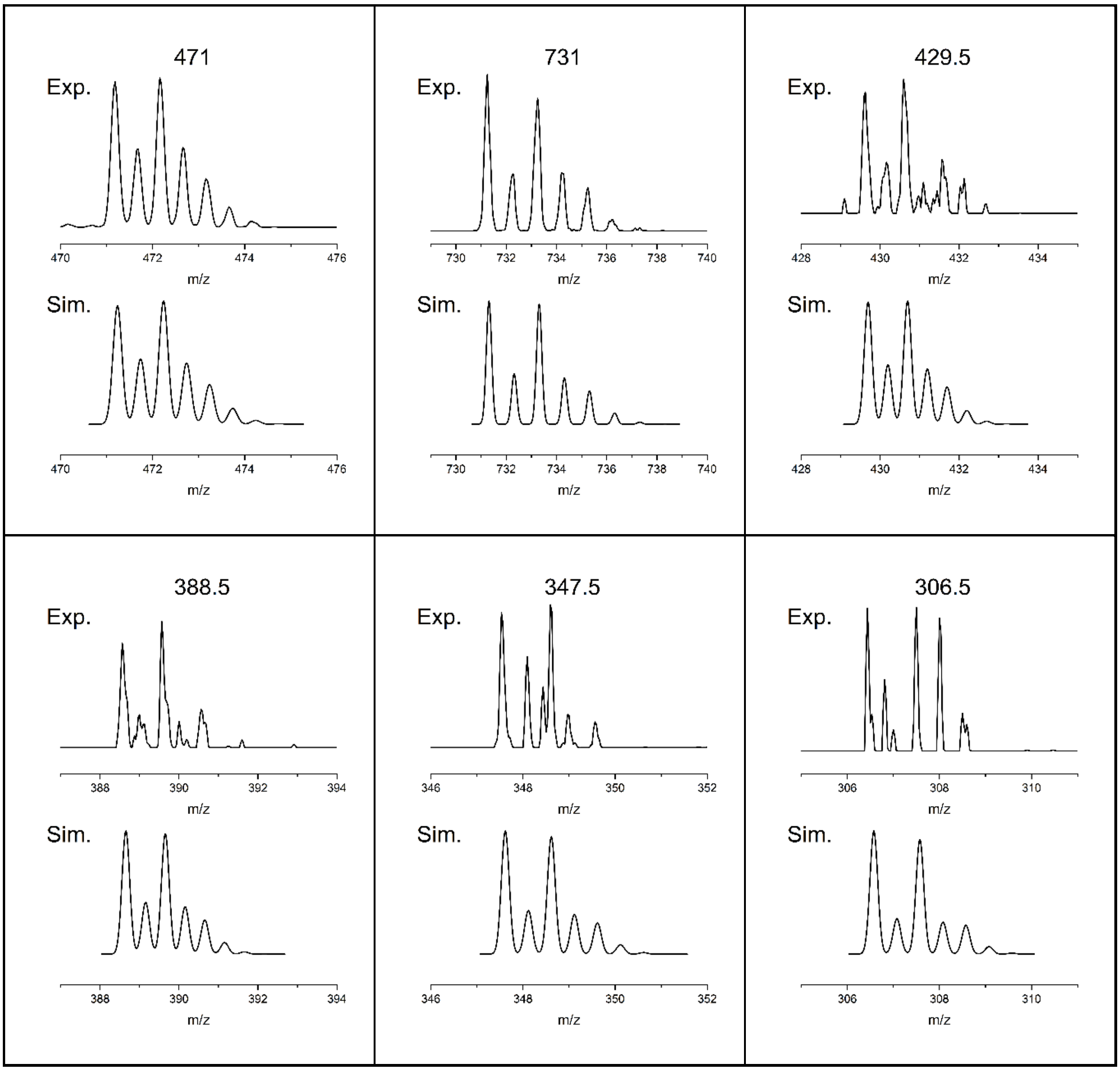

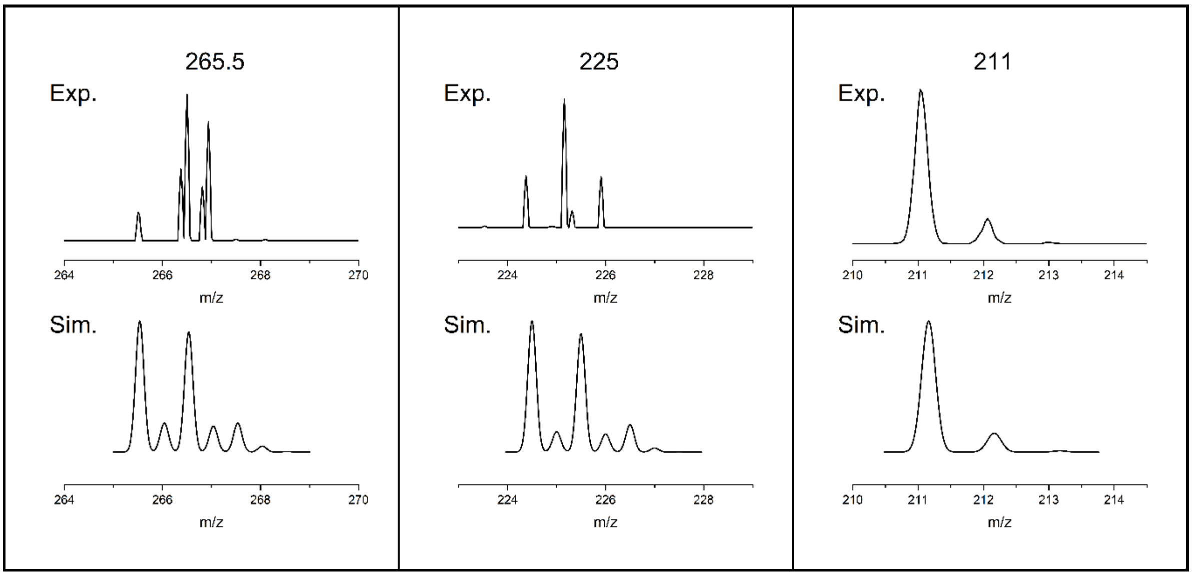
265.5
Exp.
264
266
268
270
m/z
Sim.
264
266
268
270
m/z
225
Exp.
224
226
228
m/z
Sim.
224
226
228
m/z
211
Exp.
210
211
212
213
214
m/z
Sim.
210
211
212
213
214
m/z

Tab. S17 Top: Isotope patterns of isolated [CuAg(*dcpm*)$_2$]$^{2+}$ precursor ion mass-signals and its photofragment products (λ_{ex} = 294 nm, E = 2 µJ, ~118 pulses)), recorded with nanosecond laser system. Bottom: Simulated isotope patterns (Gaussian profile, *m/z* = 0.2 fwhm). Mass-signals normalized to unity for comparison.

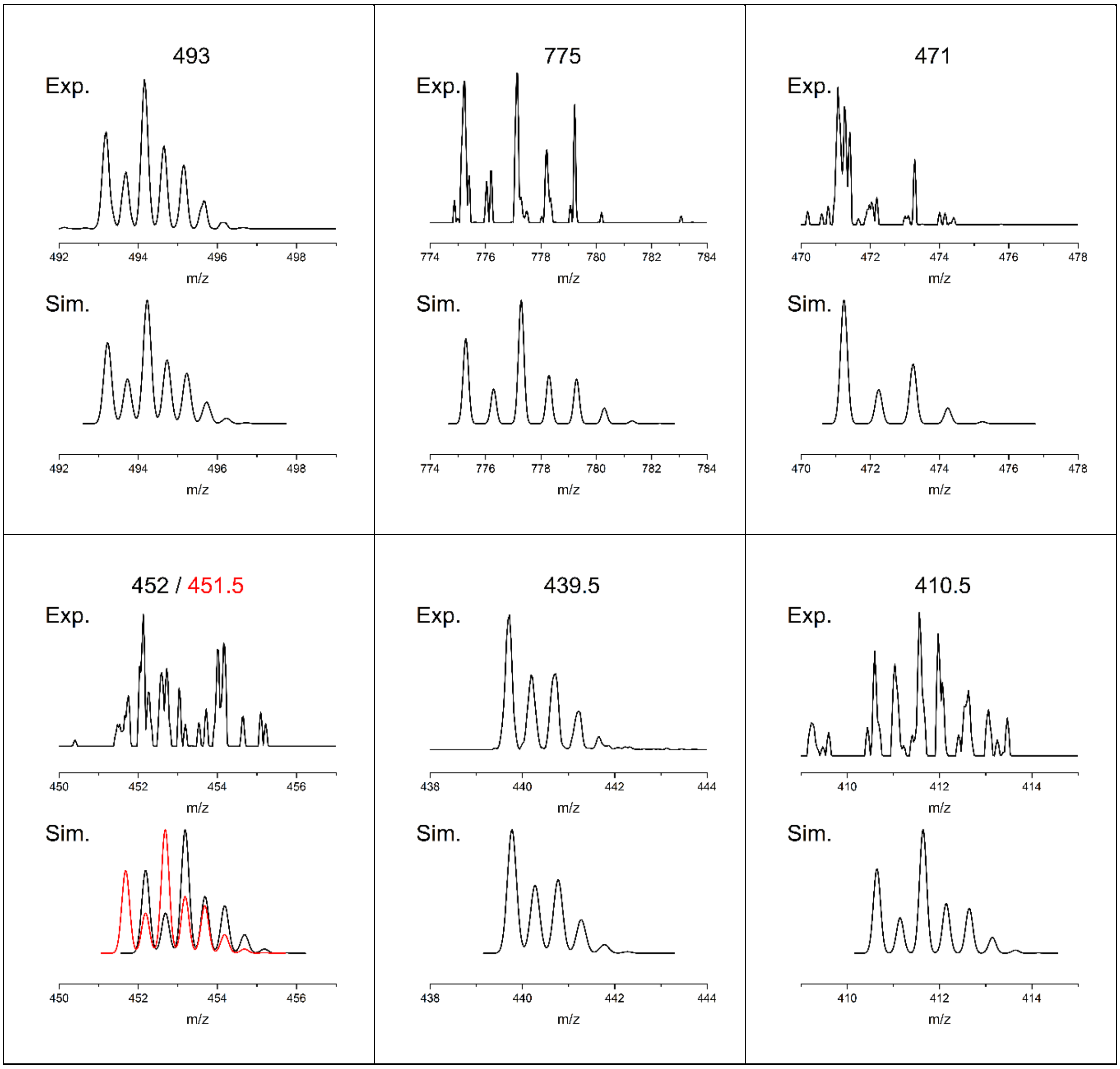

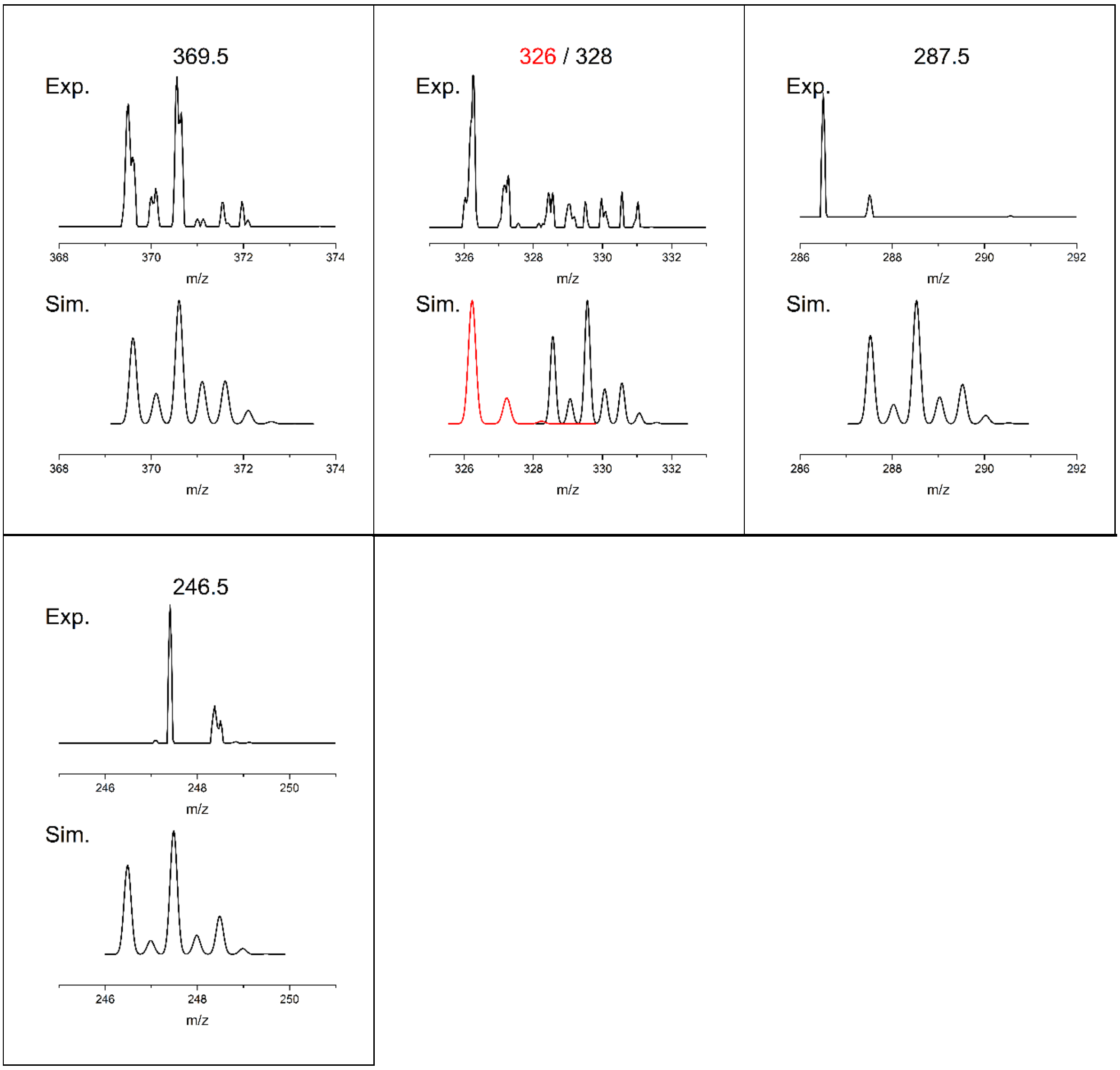
369.5
Exp.
368
370
372
374
m/z
Sim.
368
370
372
374
m/z
326 / 328
Exp.
326
328
330
332
m/z
Sim.
326
328
330
332
m/z
287.5
Exp.
286
288
290
292
m/z
Sim.
286
288
290
292
m/z
246.5
Exp.
246
248
250
m/z
Sim.
246
248
250
m/z

Tab. S18 Top: Isotope patterns of isolated [CuAu(*dcpm*)$_2$]$^{2+}$ precursor ion mass-signals and its photofragment products (λ_{ex} = 285 nm, E = 2 µJ, ~118 pulses)), recorded with nanosecond laser system. Bottom: Simulated isotope patterns (Gaussian profile, *m/z* = 0.2 fwhm). Mass-signals normalized to unity for comparison.

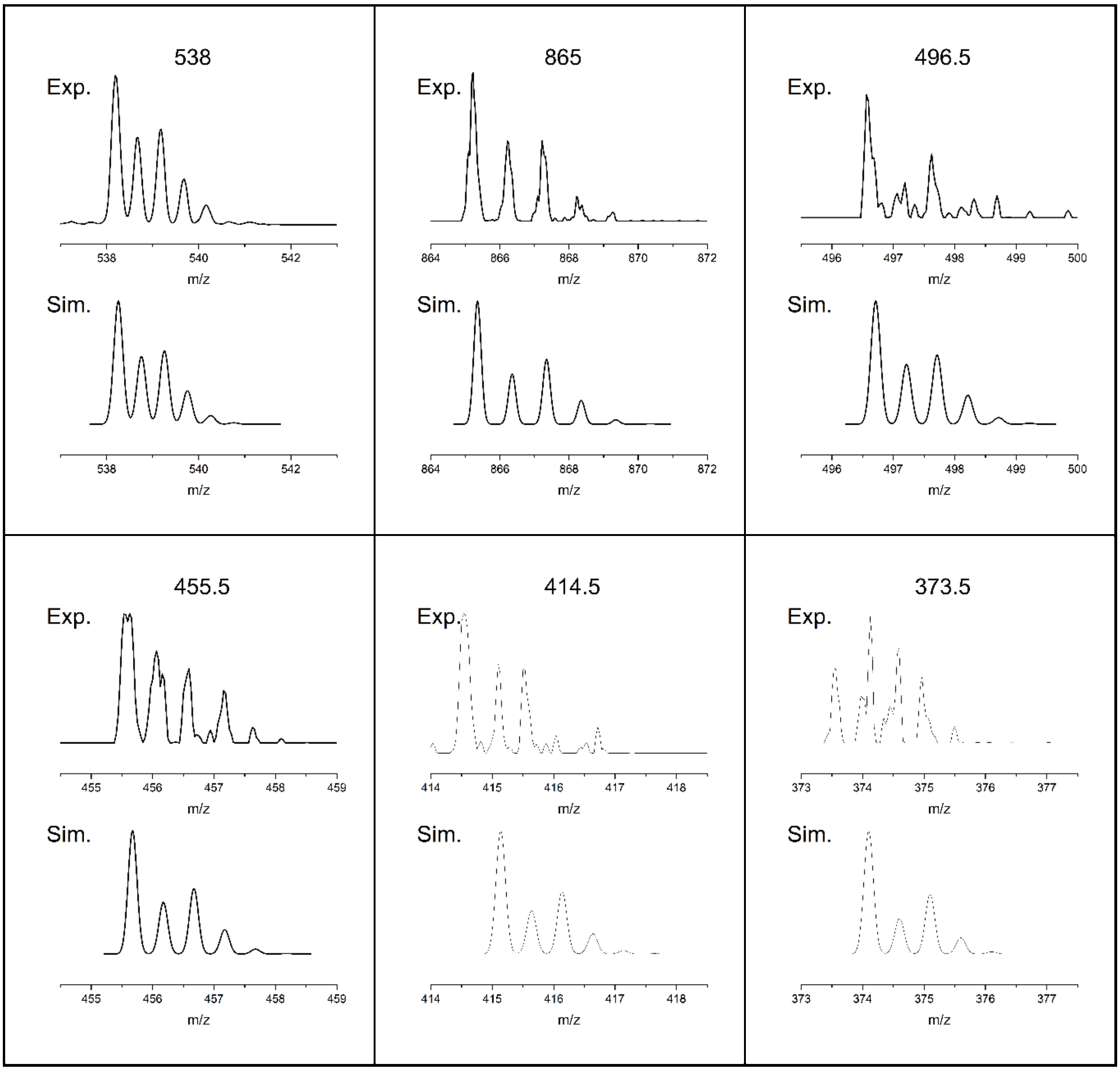

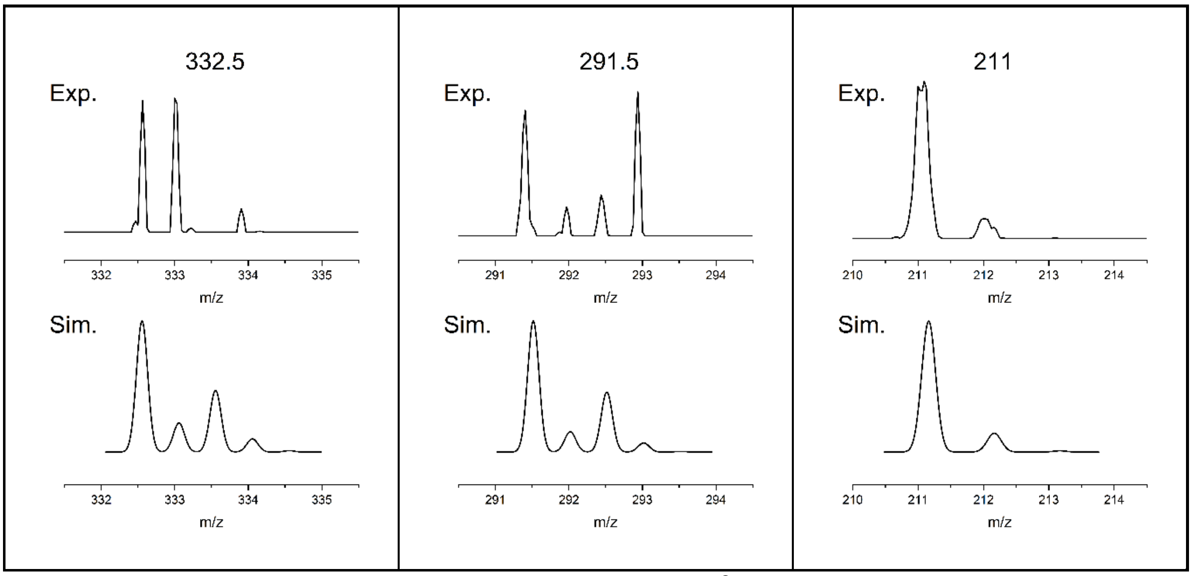

Tab. S19 Top: Isotope patterns of isolated $[Ag_2(dcpm)_2]^{2+}$ precursor ion mass-signals and its photofragment products (λ_{ex} = 258 nm, E = 2 µJ, ~118 pulses)), recorded with nanosecond laser system. Bottom: Simulated isotope patterns (Gaussian profile, *m/z* = 0.2 fwhm). Mass-signals normalized to unity for comparison.

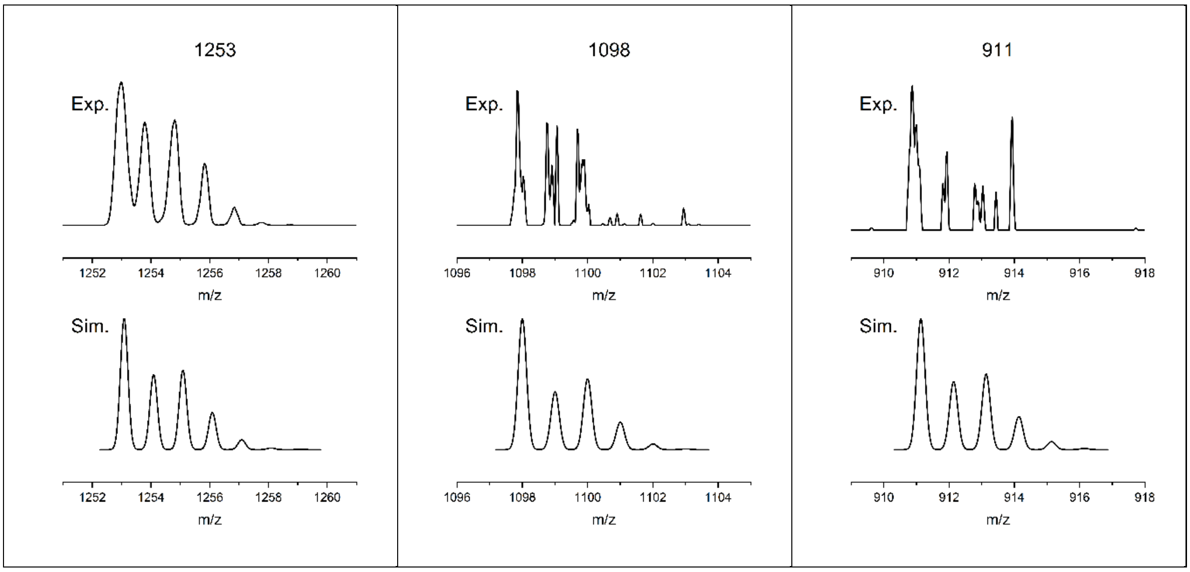

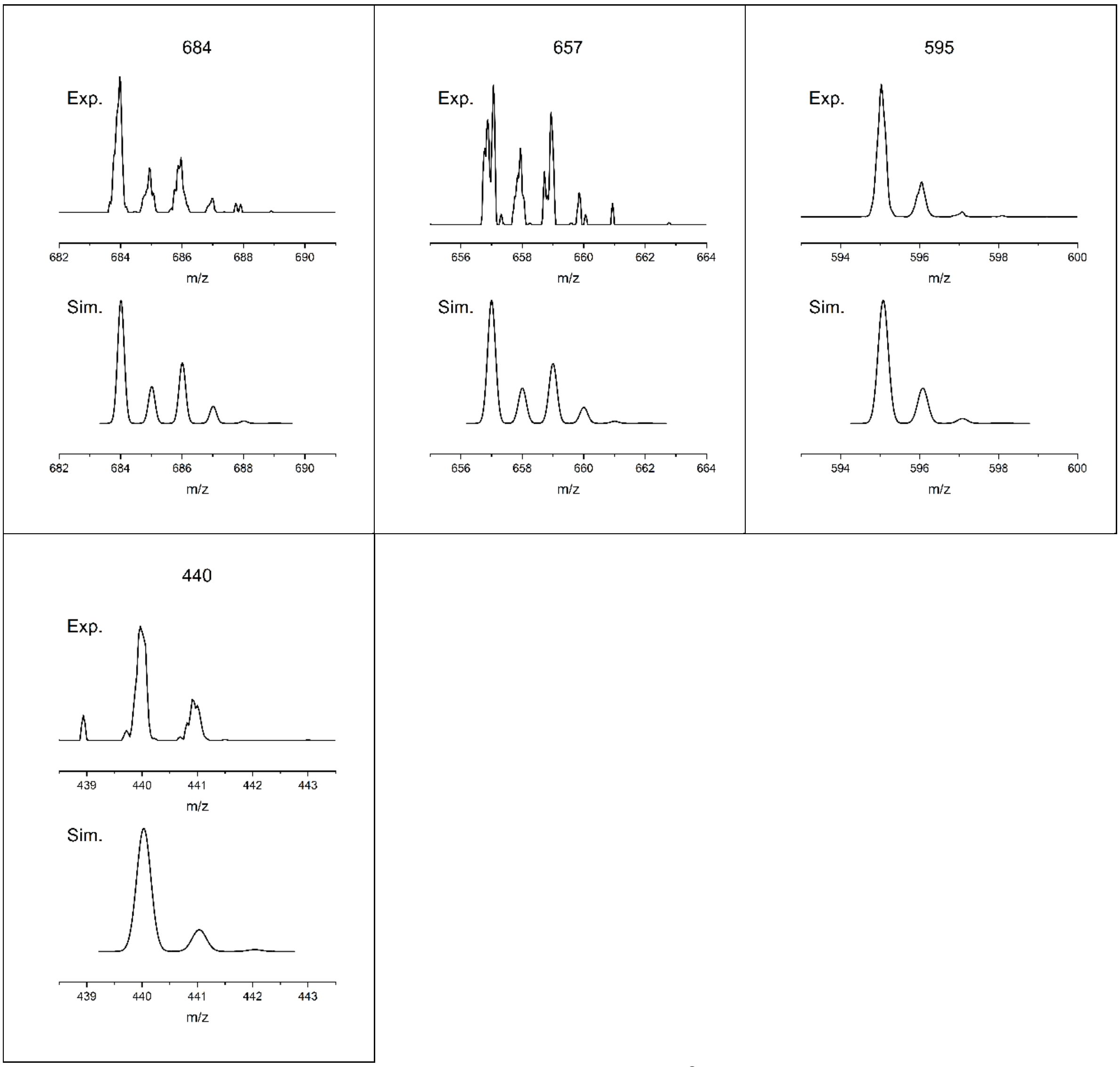

Tab. S20 Top: Isotope patterns of isolated [AgAu(*dcpm*)$_2$]$^{2+}$ precursor ion mass-signals and its photofragment products (λ_{ex} = 267 nm, E = 2 µJ, ~118 pulses)), recorded with nanosecond laser system. Bottom: Simulated isotope patterns (Gaussian profile, *m/z* = 0.2 fwhm). Mass-signals normalized to unity for comparison.

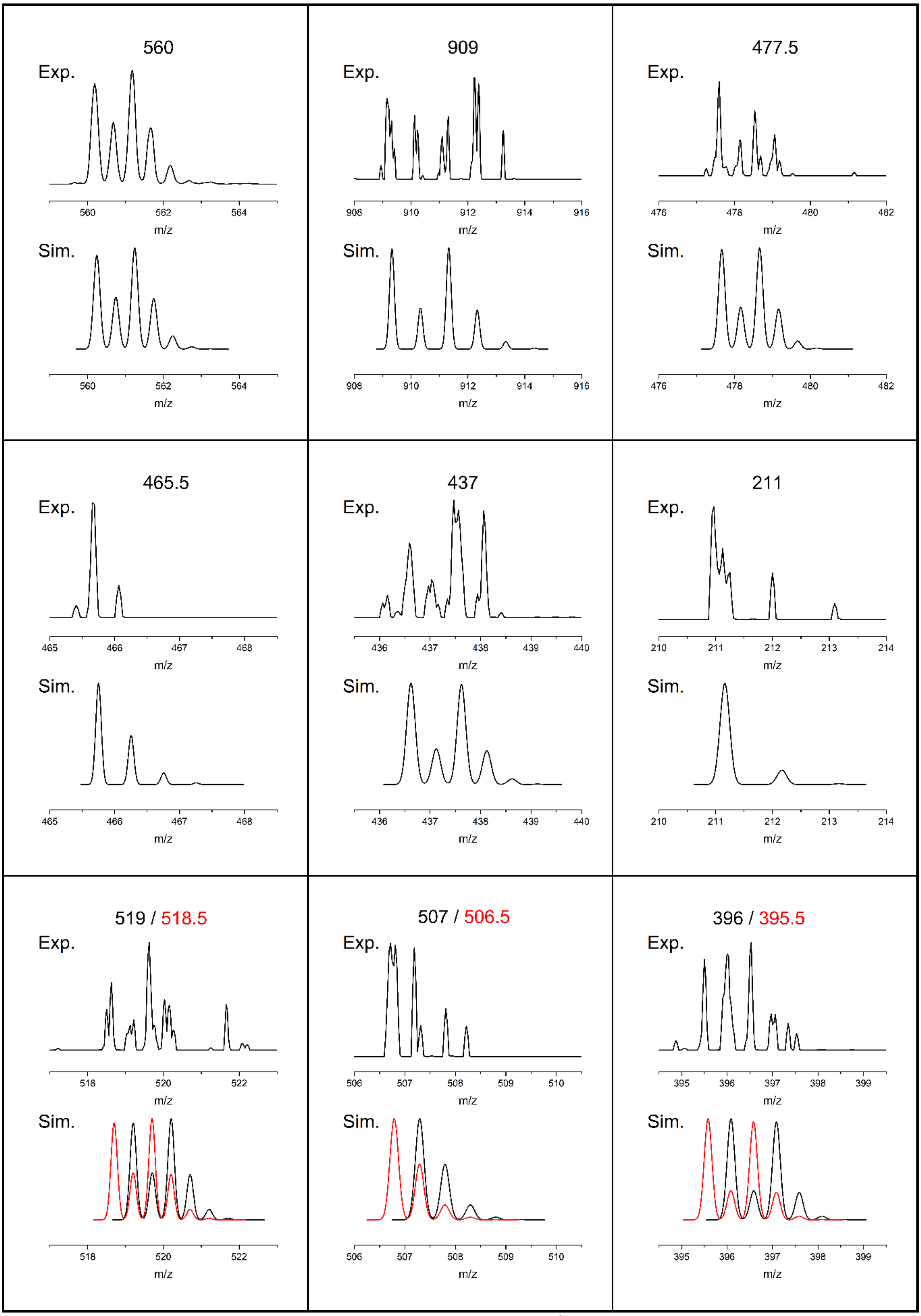

Tab. S21 Top: Isotope patterns of isolated $[Au_2(dcpm)_2]^{2+}$ precursor ion mass-signals and its photofragment products (λ_{ex} = 276 nm, E = 2 µJ, ~118 pulses)), recorded with nanosecond laser system. Bottom: Simulated isotope patterns (Gaussian profile, *m/z* = 0.2 fwhm). Mass-signals normalized to unity for comparison.

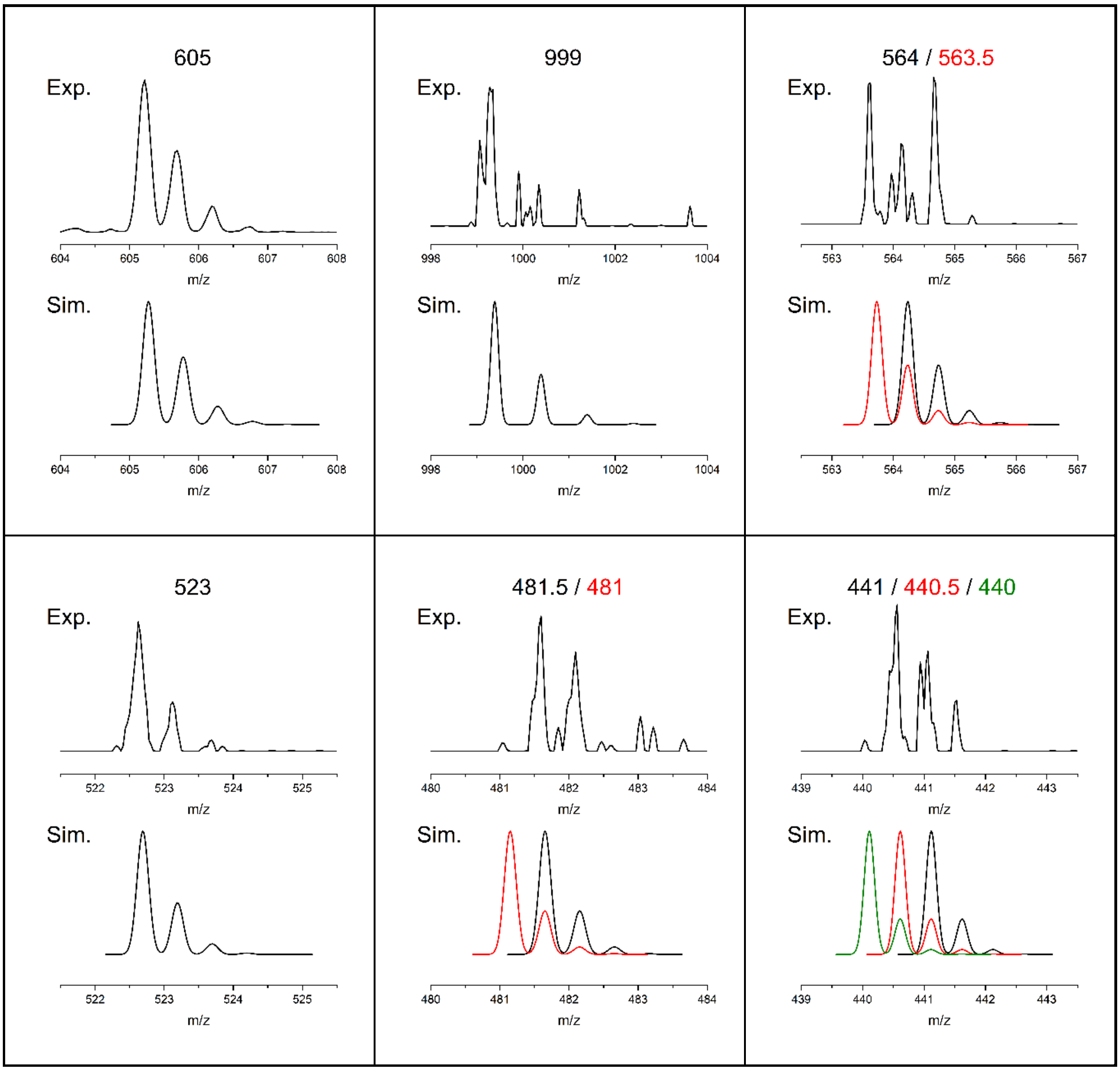
605
Exp.
Sim.
m/z
999
564 / 563.5
523
481.5 / 481
441 / 440.5 / 440

2. Fragment channel specific UV PD spectra

2.1 Femtosecond Laser System

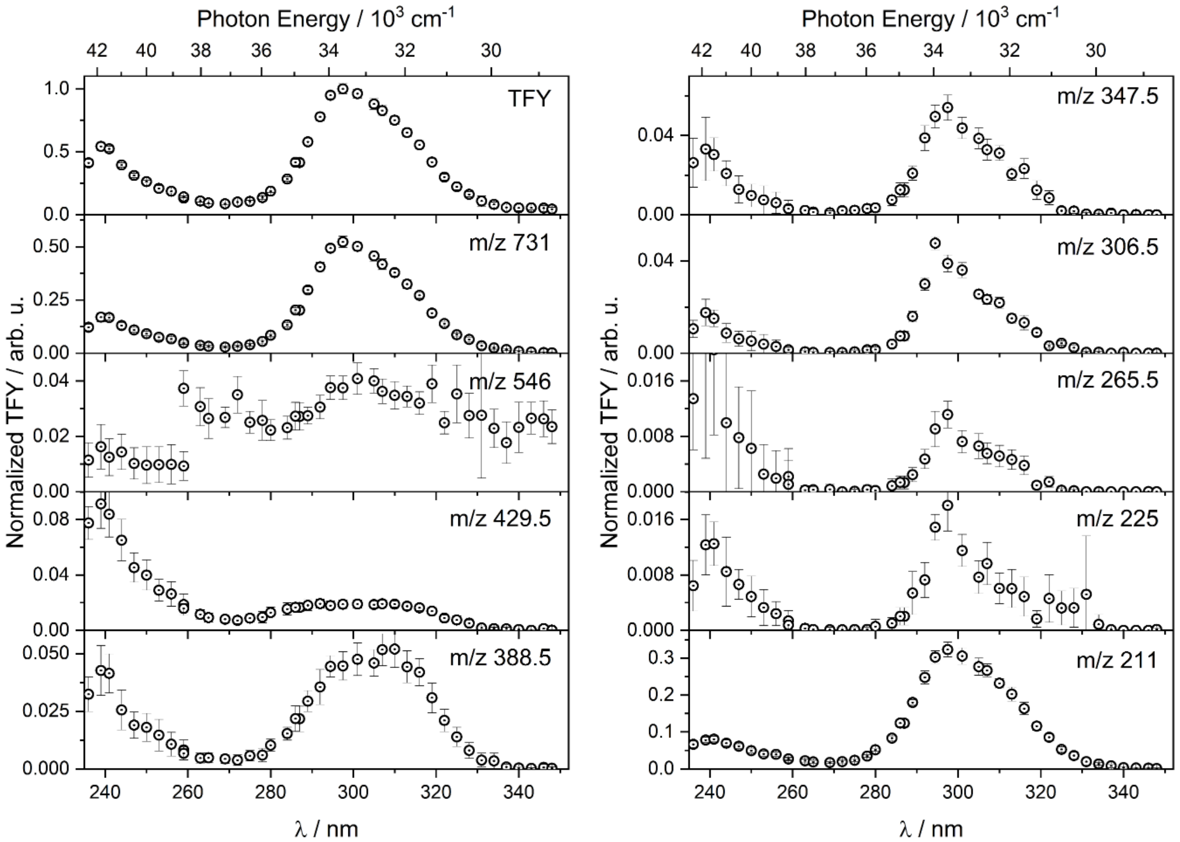

Fig. S8 Channel-specific UV PD spectra (E_{pulse} = 2µJ) of isolated $[Cu_2(\mathit{dcpm})_2]^{2+}$. Spectra were normalized to the maximum of the TFY. Integer nominal masses of the individual PD product channels are indicated, and error bars represent one standard deviation (±1σ).

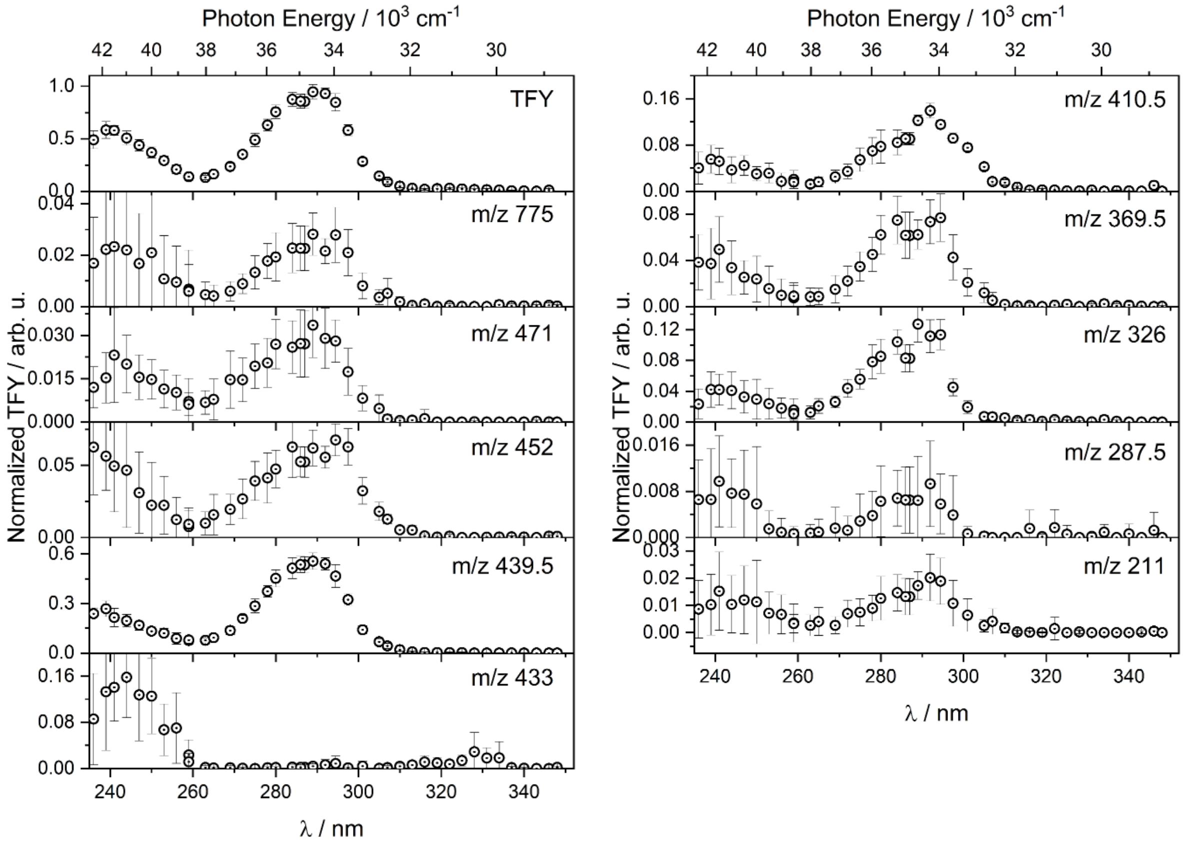

Fig. S9 Channel-specific UV PD spectra (E_{pulse} = 2μJ) of isolated [CuAg(*dcpm*)$_2$]$^{2+}$. Spectra were normalized to the maximum of the TFY. Integer nominal masses of the individual PD product channels are indicated, and error bars represent one standard deviation (±1σ).

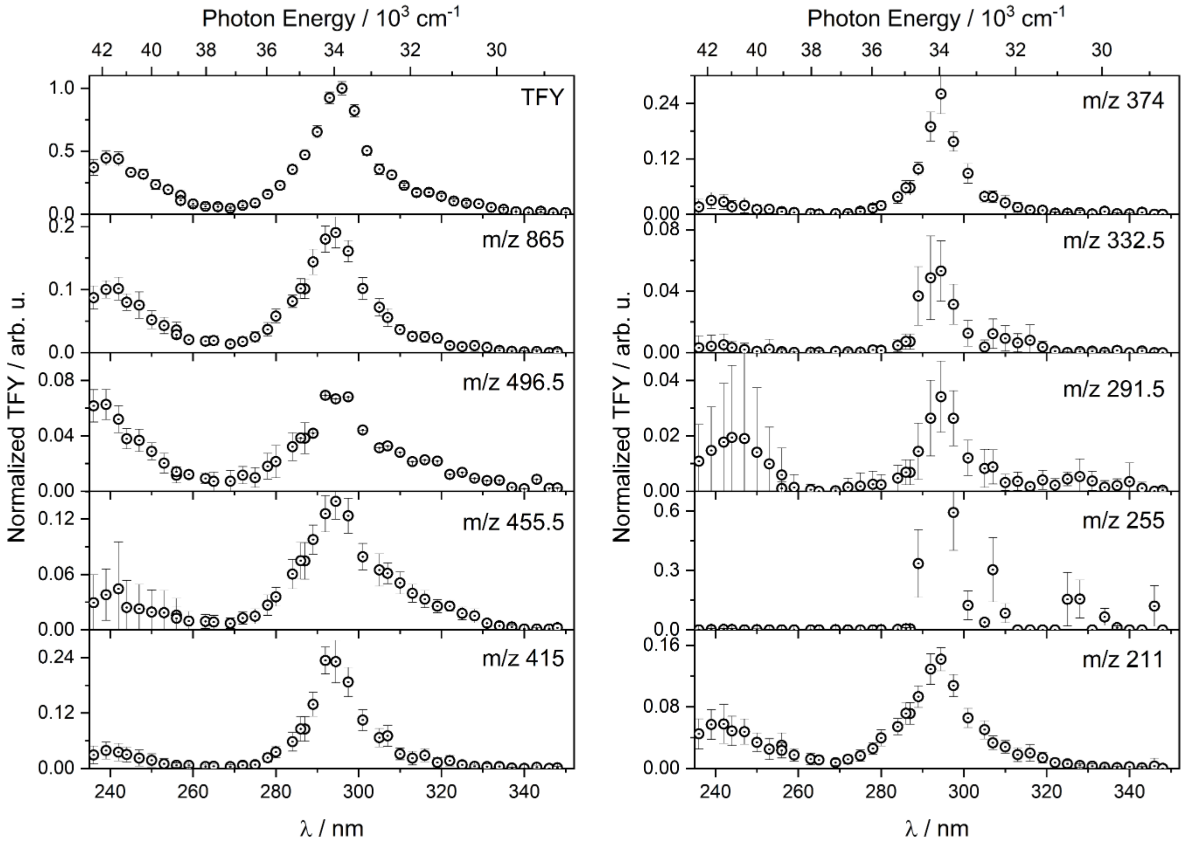

Fig. S10 Channel-specific UV PD spectra (E_{pulse} = 2µJ) of isolated $[CuAu(\textit{dcpm})_2]^{2+}$. Spectra were normalized to the maximum of the TFY. Integer nominal masses of the individual PD product channels are indicated, and error bars represent one standard deviation (±1σ).

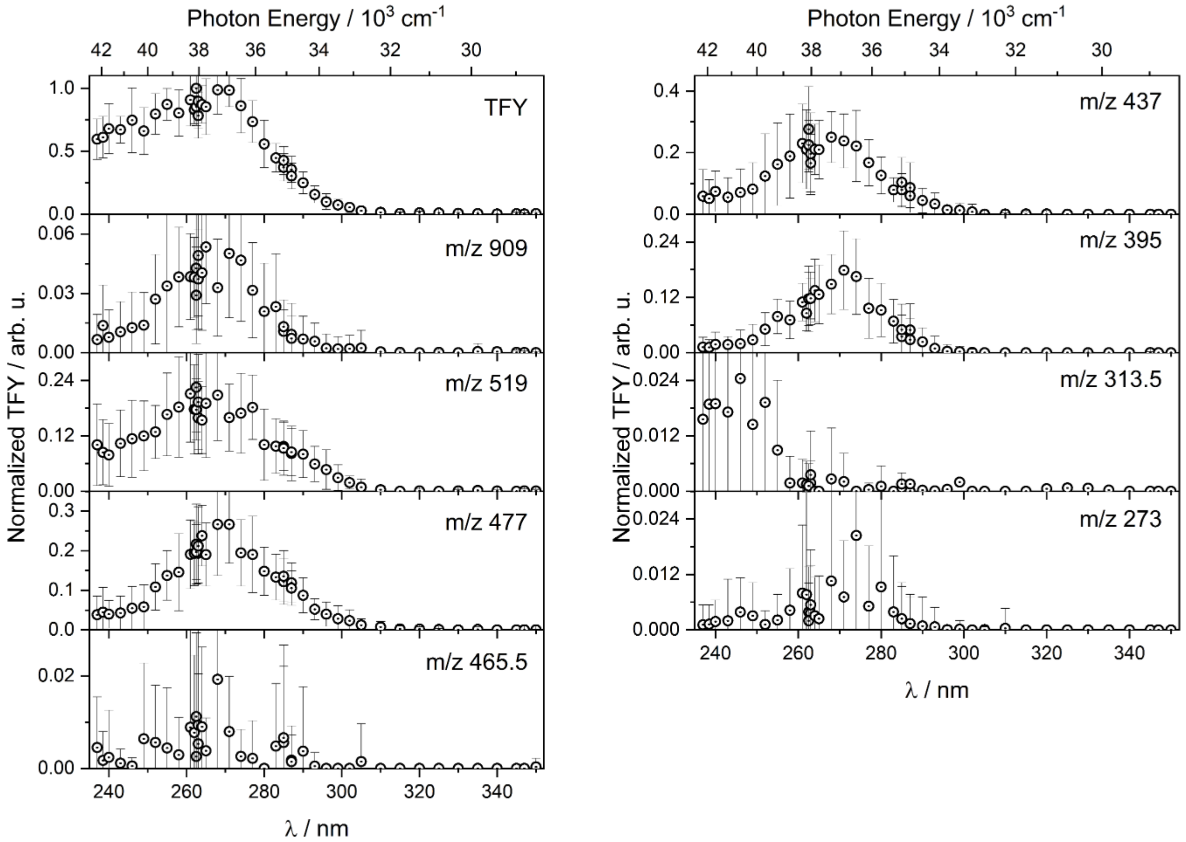

Fig. S11 Channel-specific UV PD spectra (E_{pulse} = 2µJ) of isolated $[AgAu(dcpm)_2]^{2+}$. Spectra were normalized to the maximum of the TFY. Integer nominal masses of the individual PD product channels are indicated, and error bars represent one standard deviation (±1σ).

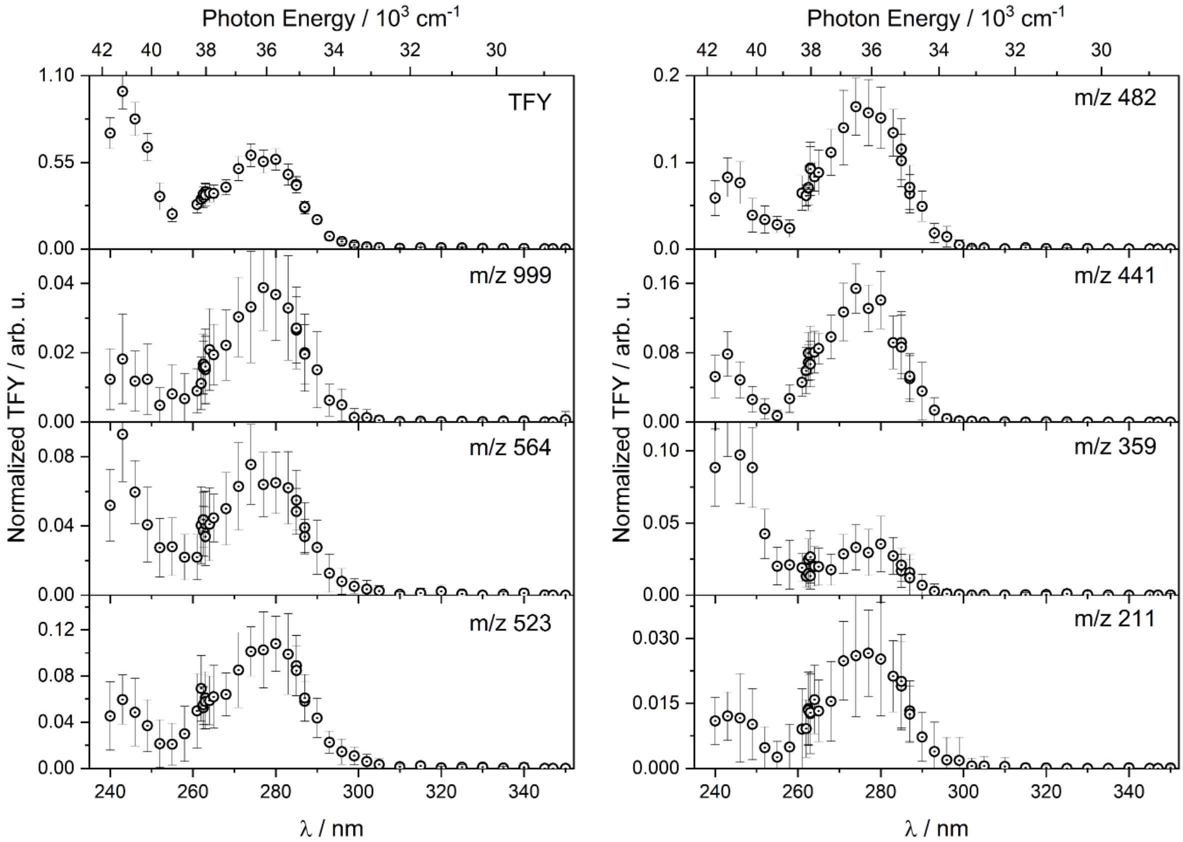

Fig. S12 Channel-specific UV PD spectra (E_{pulse} = 2µJ) of isolated $[Au_2(dcpm)_2]^{2+}$. Spectra were normalized to the maximum of the TFY. Integer nominal masses of the individual PD product channels are indicated, and error bars represent one standard deviation (±1σ).

2.2 Nanosecond laser system

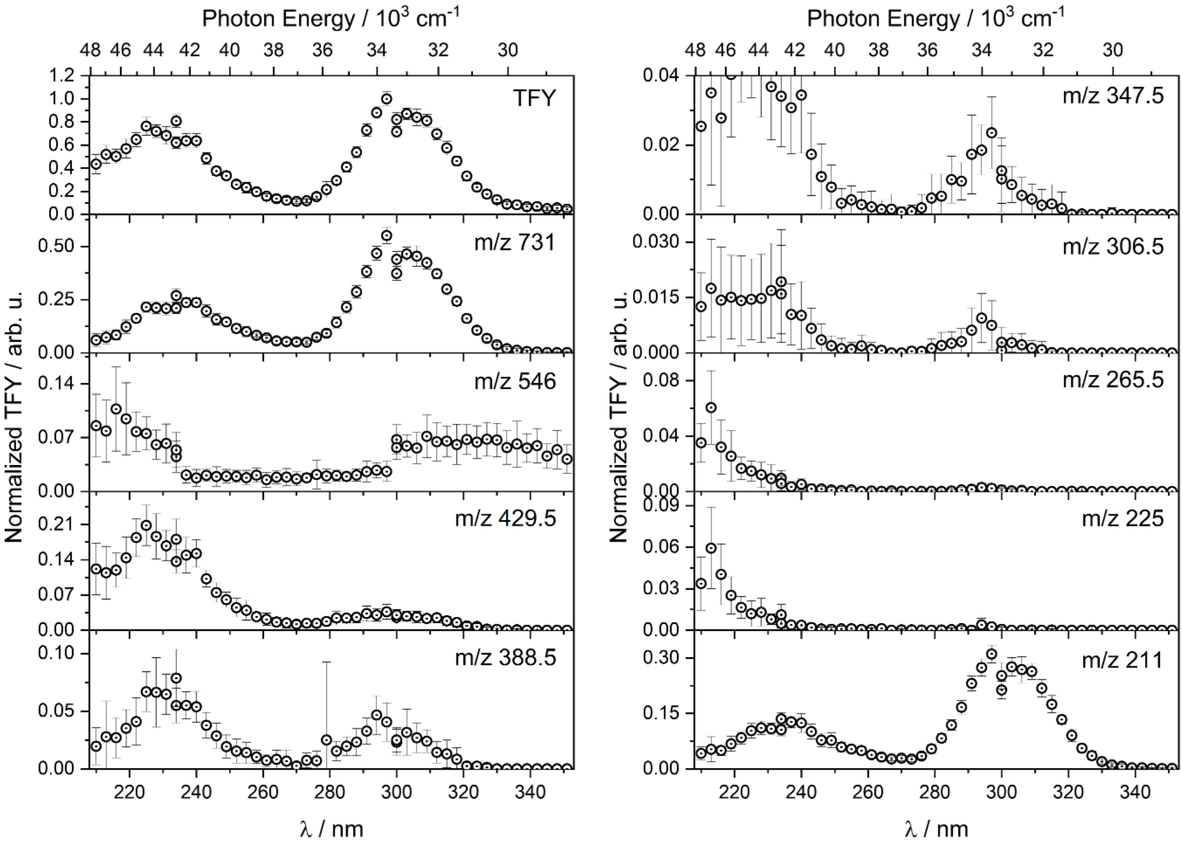

Fig. S13 Channel-specific UV PD spectra (E_{pulse} = 2μJ) of isolated $[Cu_2(dcpm)_2]^{2+}$. Spectra were normalized to the maximum of the TFY. Integer nominal masses of the individual PD product channels are indicated, and error bars represent one standard deviation (±1σ).

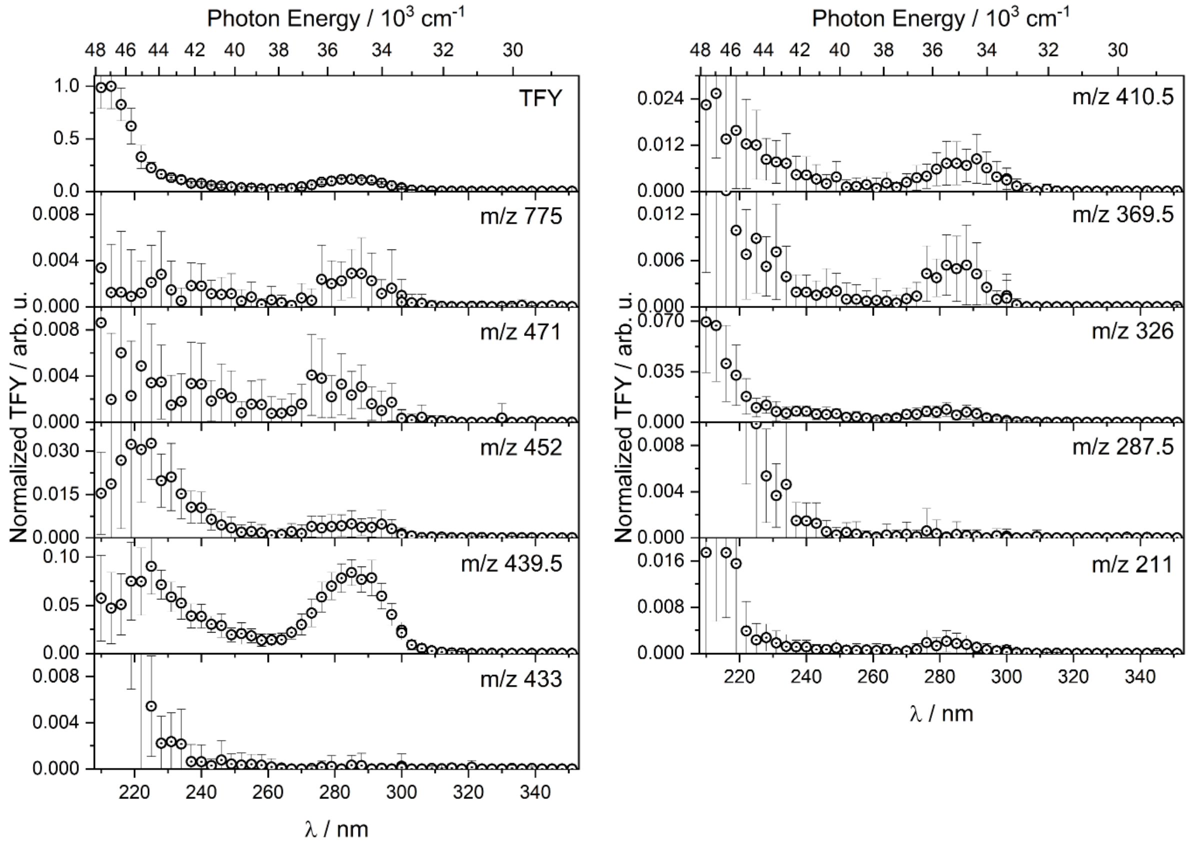

Fig. S14 Channel-specific UV PD spectra (E_{pulse} = 2µJ) of isolated [CuAg(*dcpm*)$_2$]$^{2+}$. Spectra were normalized to the maximum of the TFY. Integer nominal masses of the individual PD product channels are indicated, and error bars represent one standard deviation (±1σ).

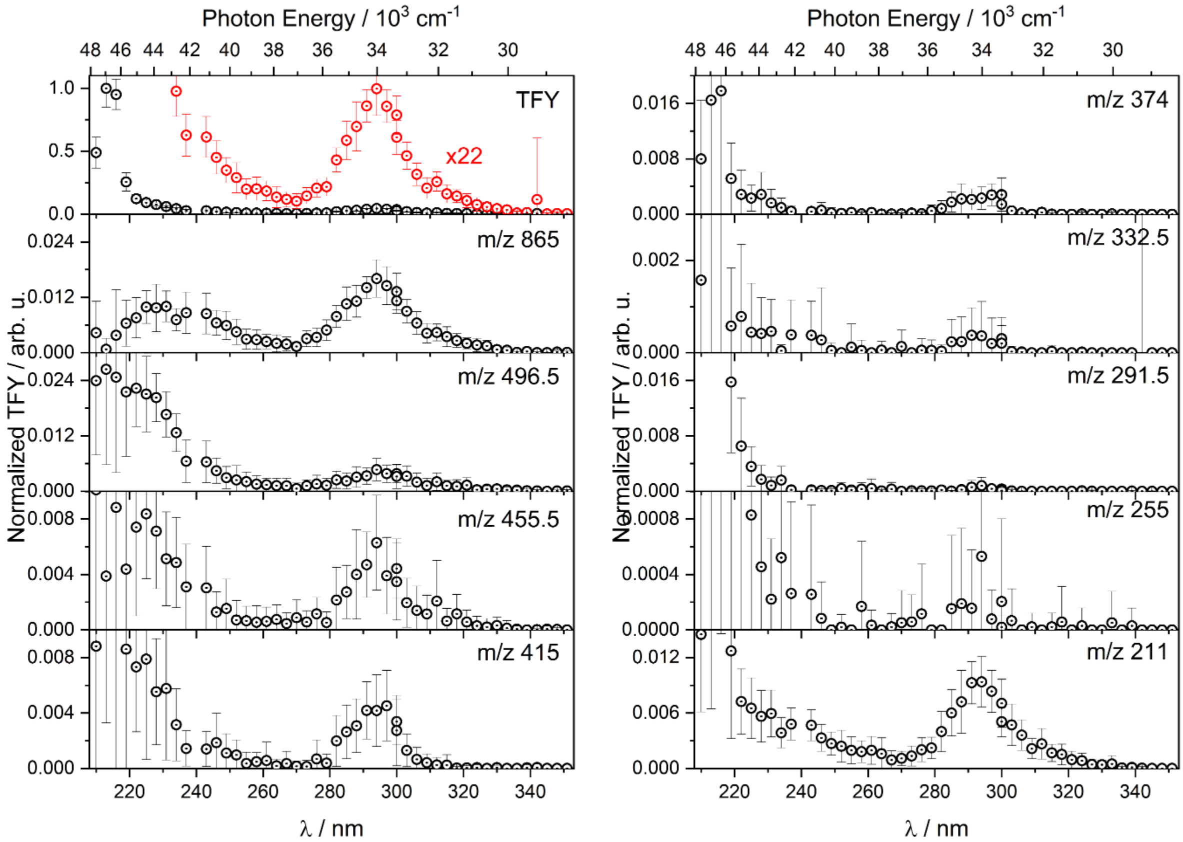

Fig. S15 Channel-specific UV PD spectra (E_{pulse} = 2µJ) of isolated [CuAu(*dcpm*)$_2$]$^{2+}$. Spectra were normalized to the maximum of the TFY. Integer nominal masses of the individual PD product channels are indicated, and error bars represent one standard deviation (±1σ).

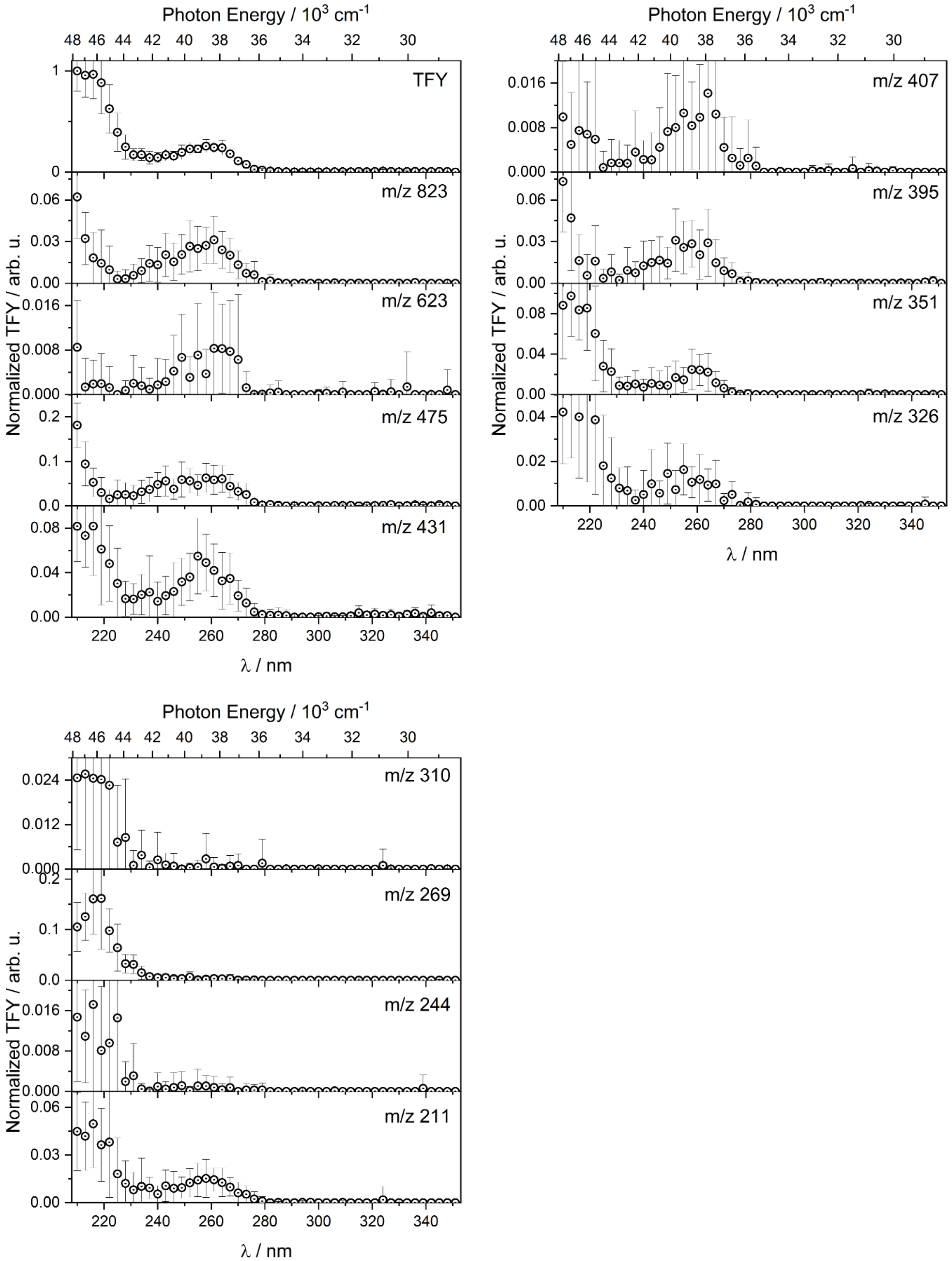

Fig. S16 Channel-specific UV PD spectra (E_{pulse} = 2μJ) of isolated $[Ag_2(dcpm)_2]^{2+}$. Spectra were normalized to the maximum of the TFY. Integer nominal masses of the individual PD product channels are indicated, and error bars represent one standard deviation (±1σ).

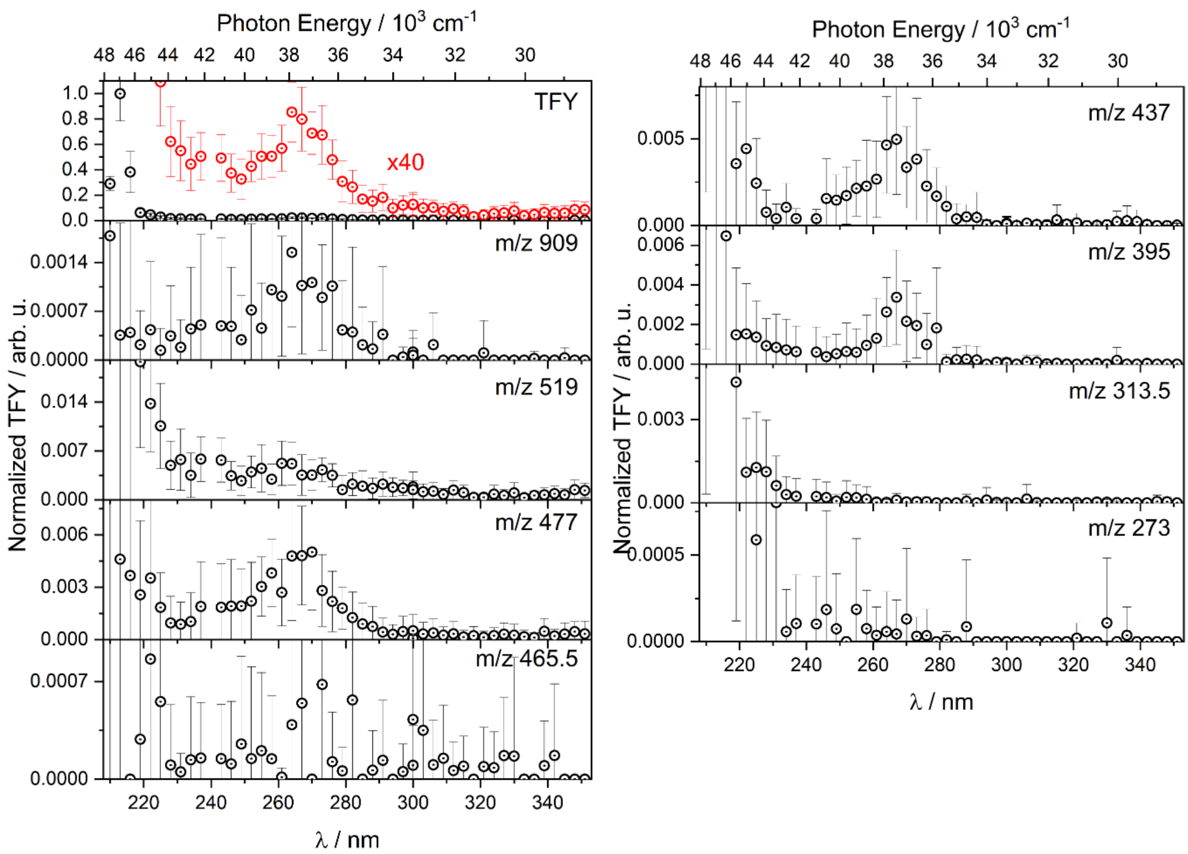

Fig. S17 Channel-specific UV PD spectra (E_{pulse} = 2µJ) of isolated [AgAu(*dcpm*)$_2$]$^{2+}$. Spectra were normalized to the maximum of the TFY. Integer nominal masses of the individual PD product channels are indicated, and error bars represent one standard deviation (±1σ).

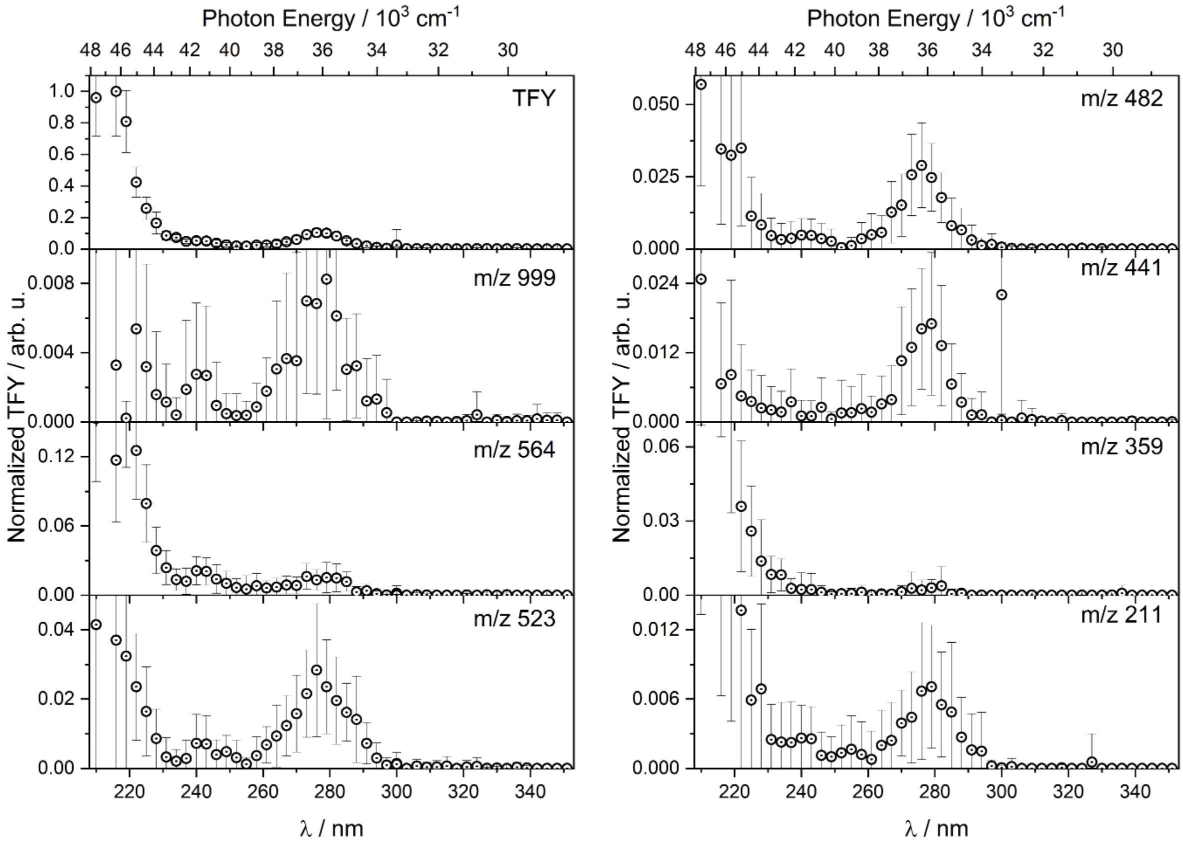

Fig. S18 Channel-specific UV PD spectra (E_{pulse} = 2µJ) of isolated $[Au_2(dcpm)_2]^{2+}$. Spectra were normalized to the maximum of the TFY. Integer nominal masses of the individual PD product channels are indicated, and error bars represent one standard deviation (±1σ).

3. Dependence of total fragment yield on laser pulse energy

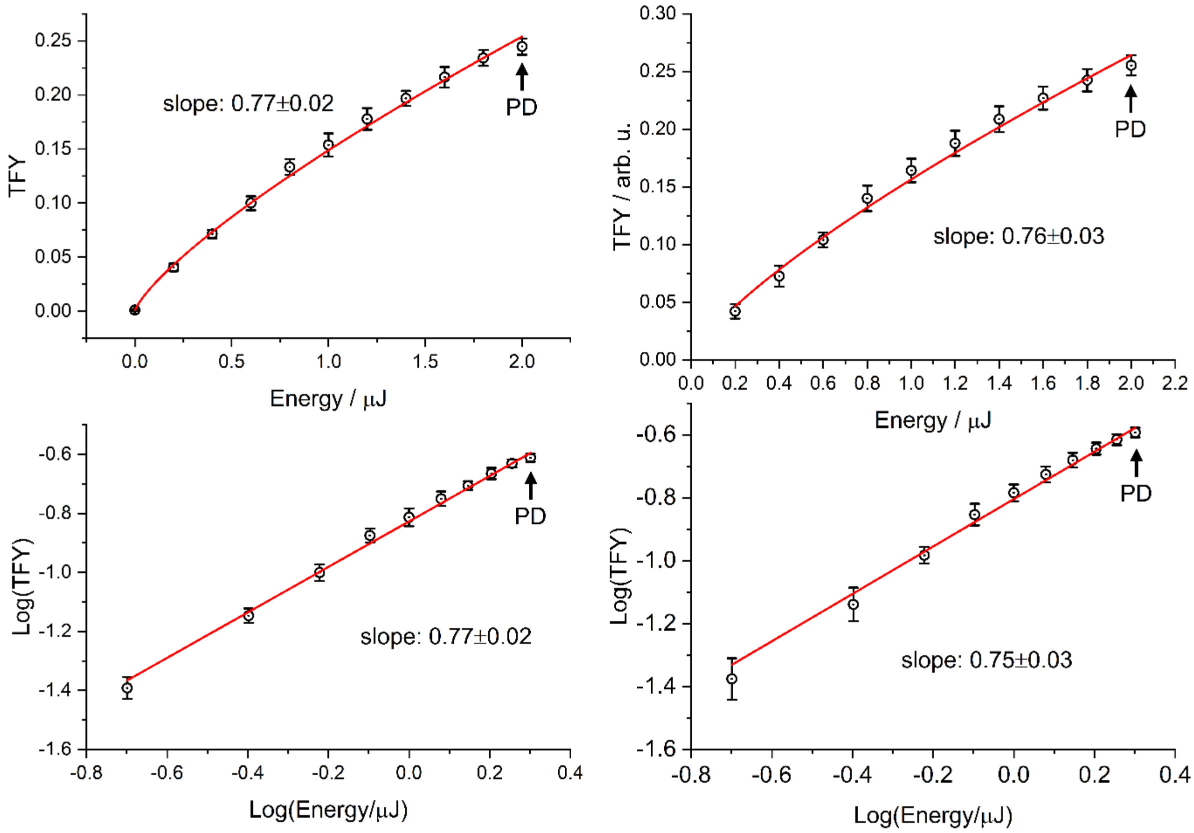

Fig. S19 Pulse energy dependence of the total fragment yield of isolated $[Cu_2(dcpm)_2]^{2+}$ ions (λ_{ex} = 297 nm, 118 pulses). Dependencies determined according to a) $Y = A \cdot E^n$ and b) $Y = A \cdot E$. Linear fits in panel below indicate a single-photon absorption process for photofragmentation. Arrows indicate E_{pulse} = 2μJ for UV PD spectra. Femtosecond (left) and nanosecond data (right) are displayed.

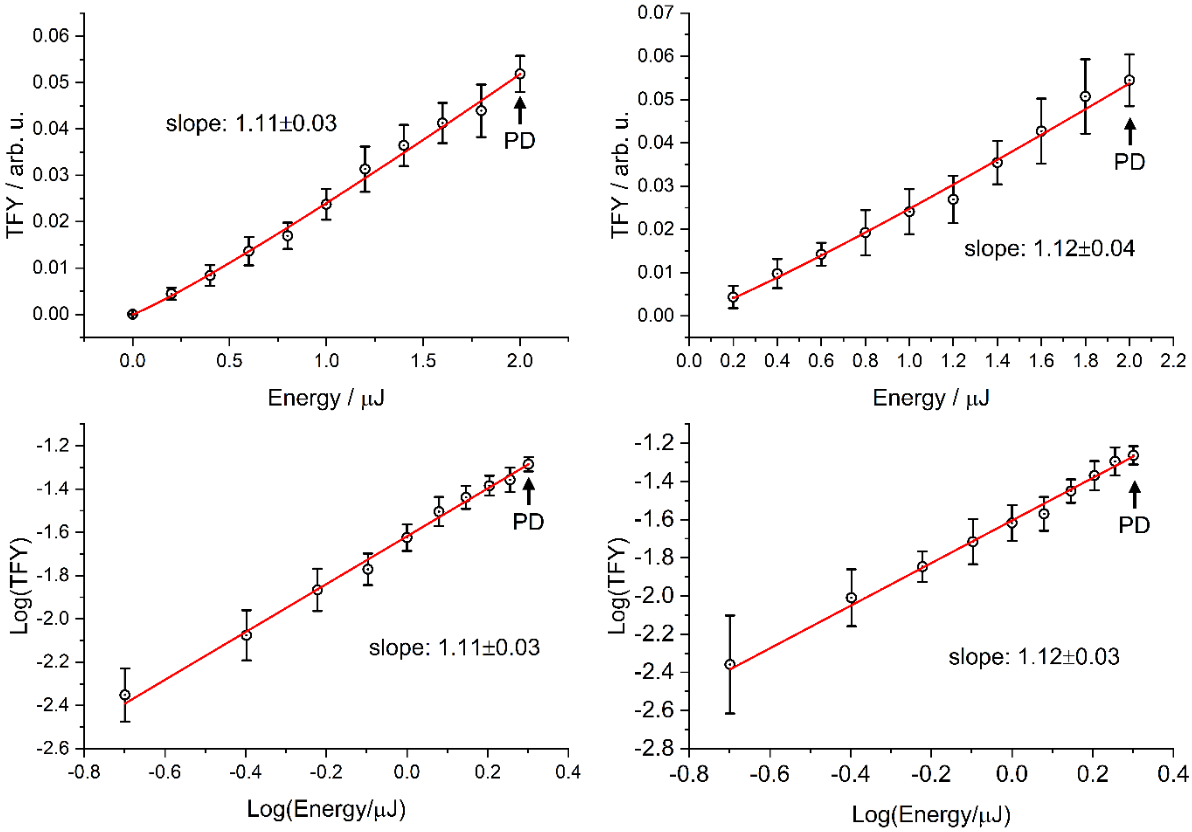

Fig. S20 Pulse energy dependence of the total fragment yield of isolated $[CuAg(\textit{dcpm})_2]^{2+}$ ions (λ_{ex} = 294 nm, 118 pulses). Dependencies determined according to a) $Y = A \cdot E^n$ and b) $Y = A \cdot E$. Linear fits in panel below indicate a single-photon absorption process for photofragmentation. Arrows indicate E_{pulse} = 2µJ for UV PD spectra. Femtosecond (left) and nanosecond data (right) are displayed.

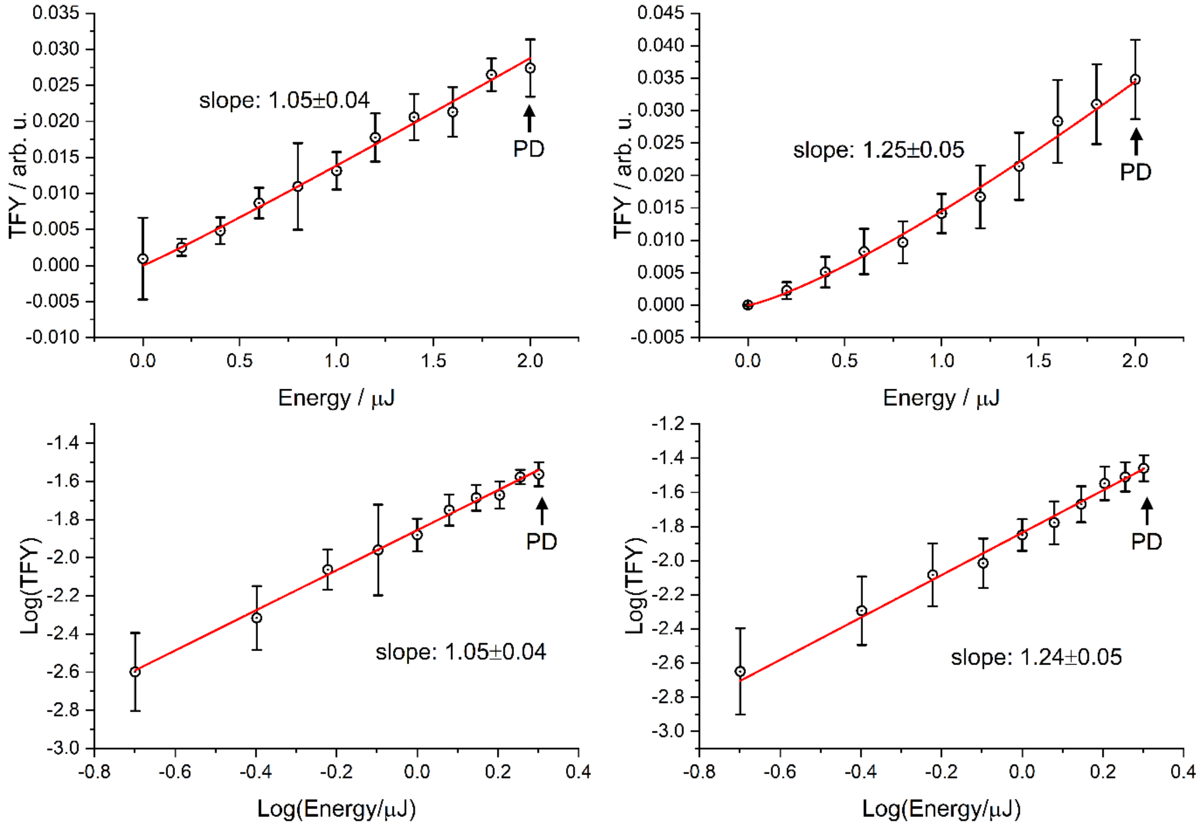

Fig. S21 Pulse energy dependence of the total fragment yield of isolated [CuAu(*dcpm*)$_2$]$^{2+}$ ions (λ_{ex} = 289 nm, 118 pulses). Dependencies determined according to a) $Y = A \cdot E^n$ and b) $Y = A \cdot E$. Linear fits in panel below indicate a single-photon absorption process for photofragmentation. Arrows indicate E_{pulse} = 2µJ for UV PD spectra. Femtosecond (left) and nanosecond data (right) are displayed.

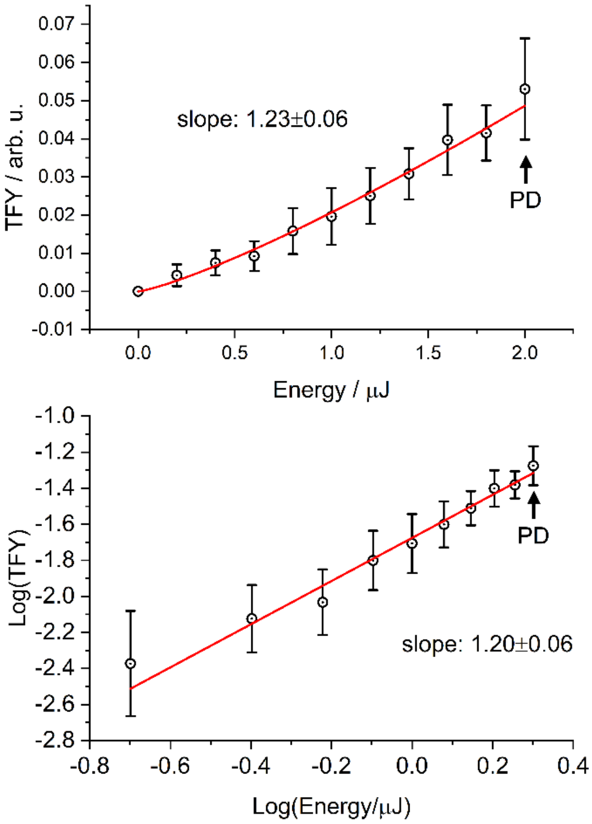

Fig. S22 Pulse energy dependence of the total fragment yield of isolated $[Ag_2(dcpm)_2]^{2+}$ ions (λ_{ex} = 258 nm, 118 pulses). Dependencies determined according to a) $Y = A \cdot E^n$ and b) $Y = A \cdot E$. Linear fits in panel below indicate a single-photon absorption process for photofragmentation. Arrows indicate E_{pulse} = 2µJ for UV PD spectra. Nanosecond data are displayed.

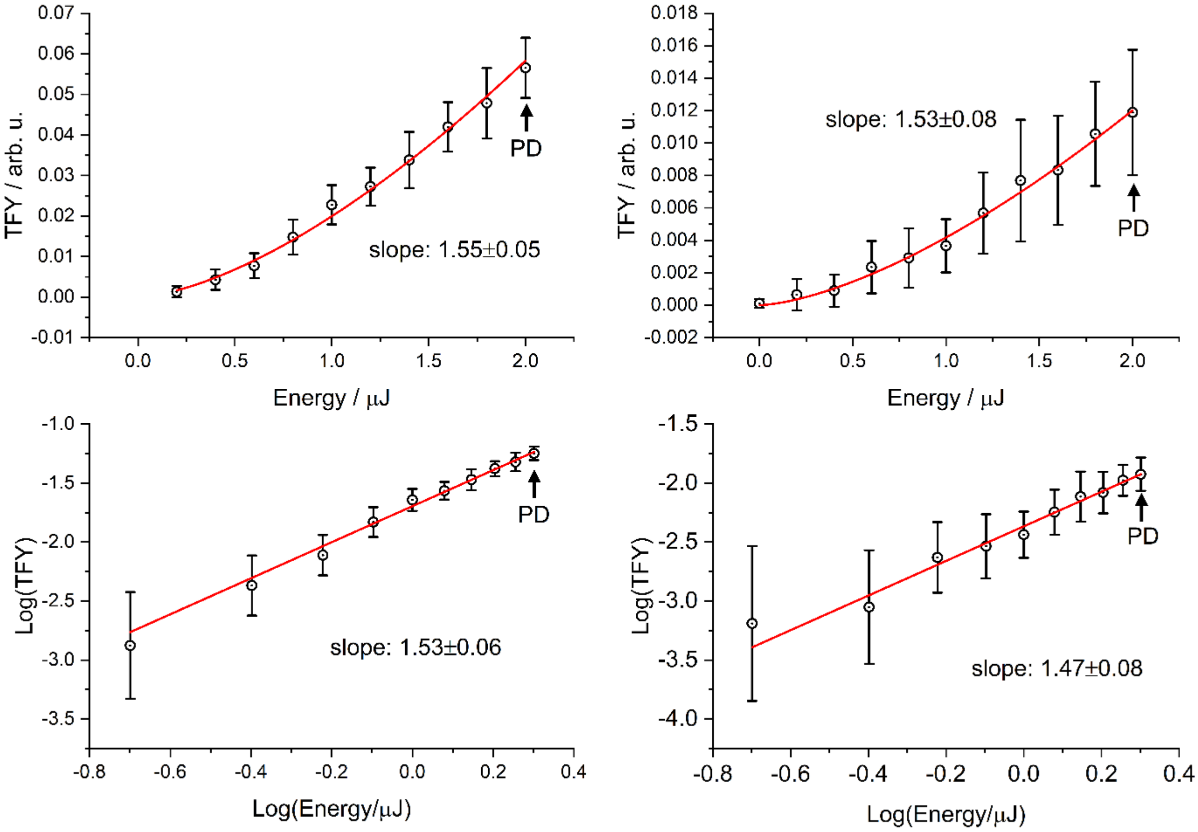

Fig. S23 Pulse energy dependence of the total fragment yield of isolated [AgAu(*dcpm*)$_2$]$^{2+}$ ions (λ_{ex} = 268 nm, 118 pulses). Dependencies determined according to a) $Y = A \cdot E^n$ and b) $Y = A \cdot E$. Linear fits in panel below indicate a single-photon absorption process for photofragmentation. Arrows indicate E_{pulse} = 2μJ for UV PD spectra. Femtosecond (left) and nanosecond data (right) are displayed.

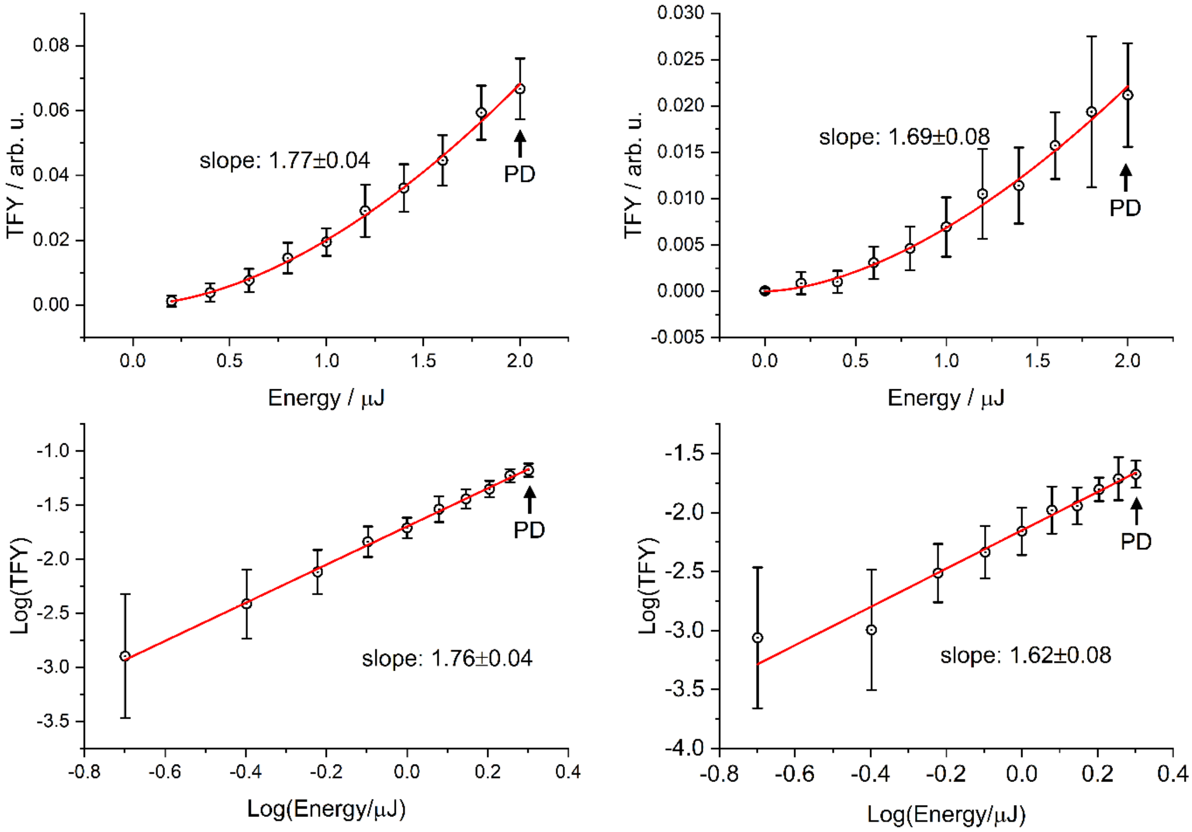

Fig. S24 Pulse energy dependence of the total fragment yield of isolated $[Au_2(dcpm)_2]^{2+}$ ions (λ_{ex} = 277 nm, 118 pulses). Dependencies determined according to a) $Y = A \cdot E^n$ and b) $Y = A \cdot E$. Linear fits in panel below indicate a single-photon absorption process for photofragmentation. Arrows indicate E_{pulse} = 2µJ for UV PD spectra. Femtosecond (left) and nanosecond data (right) are displayed.

4. Comparison of femto- and nanosecond data

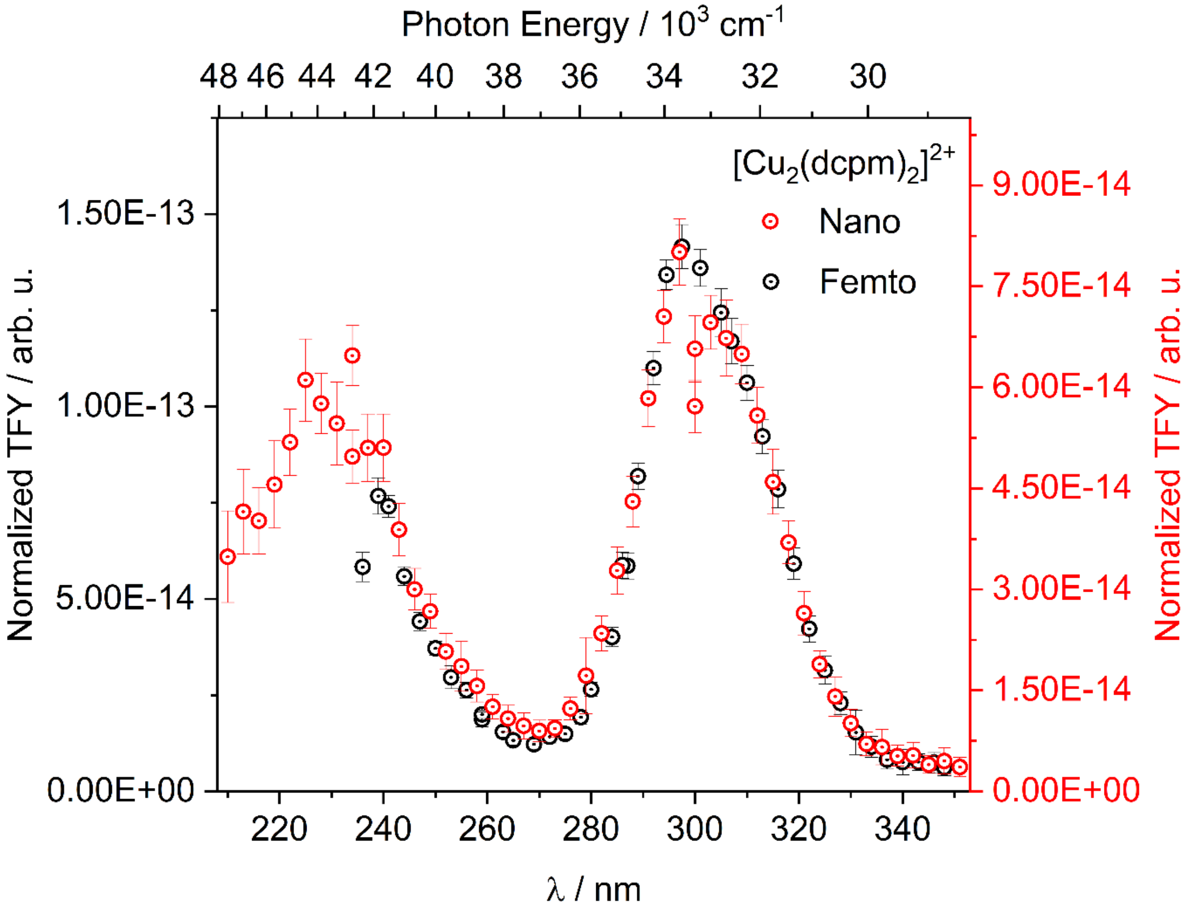

Fig. S25 Comparison of femtosecond (black circles) and nanosecond (red circles) UV PD total yield spectra of $[Cu_2(dcpm)_2]^{2+}$ ions (2 µJ, 118 pulses). Spectra were normalized to number of photons. Error bars indicate one standard deviation (±1σ).

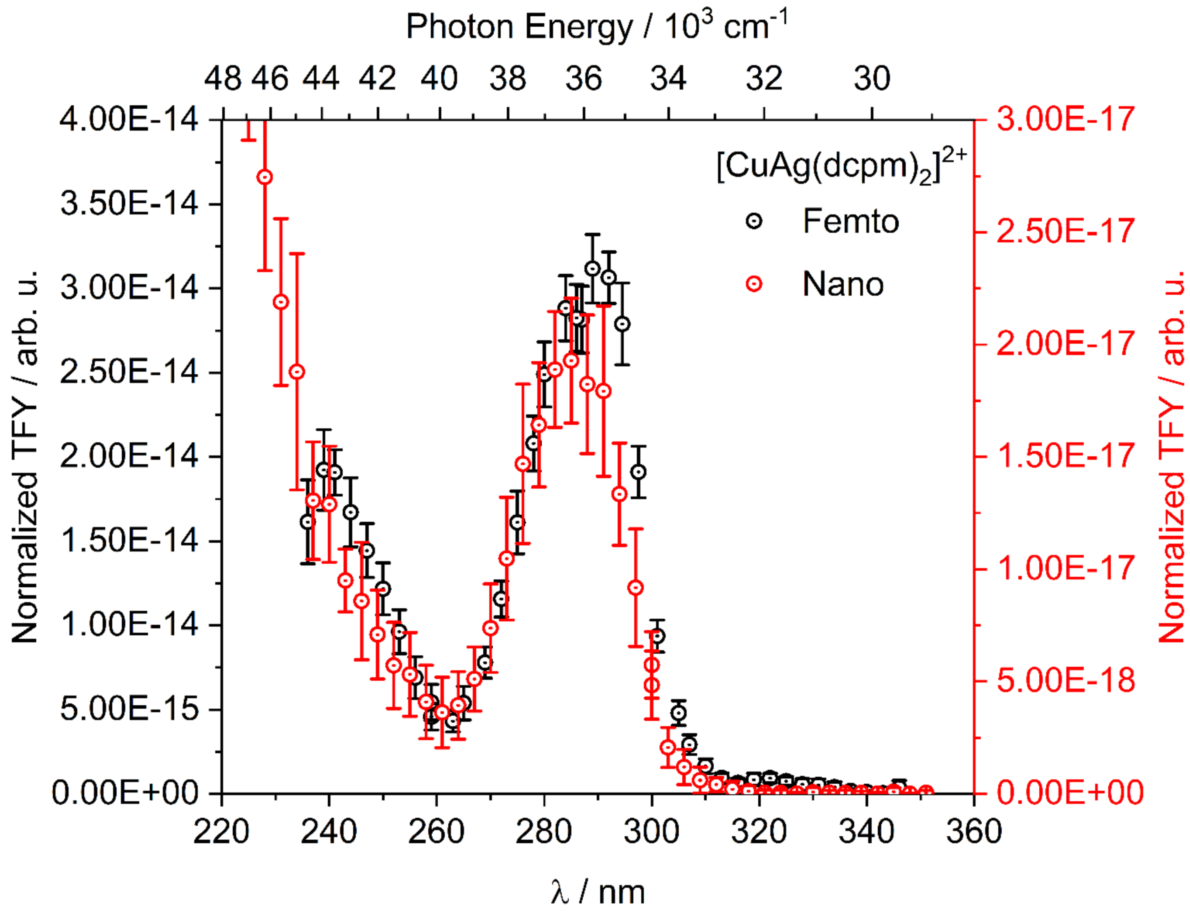

Fig. S26 Comparison of femtosecond (black circles) and nanosecond (red circles) UV PD total yield spectra of $[CuAg(\mathit{dcpm})_2]^{2+}$ ions (2 µJ, 118 pulses). Spectra were normalized to number of photons. Error bars indicate one standard deviation (±1σ).

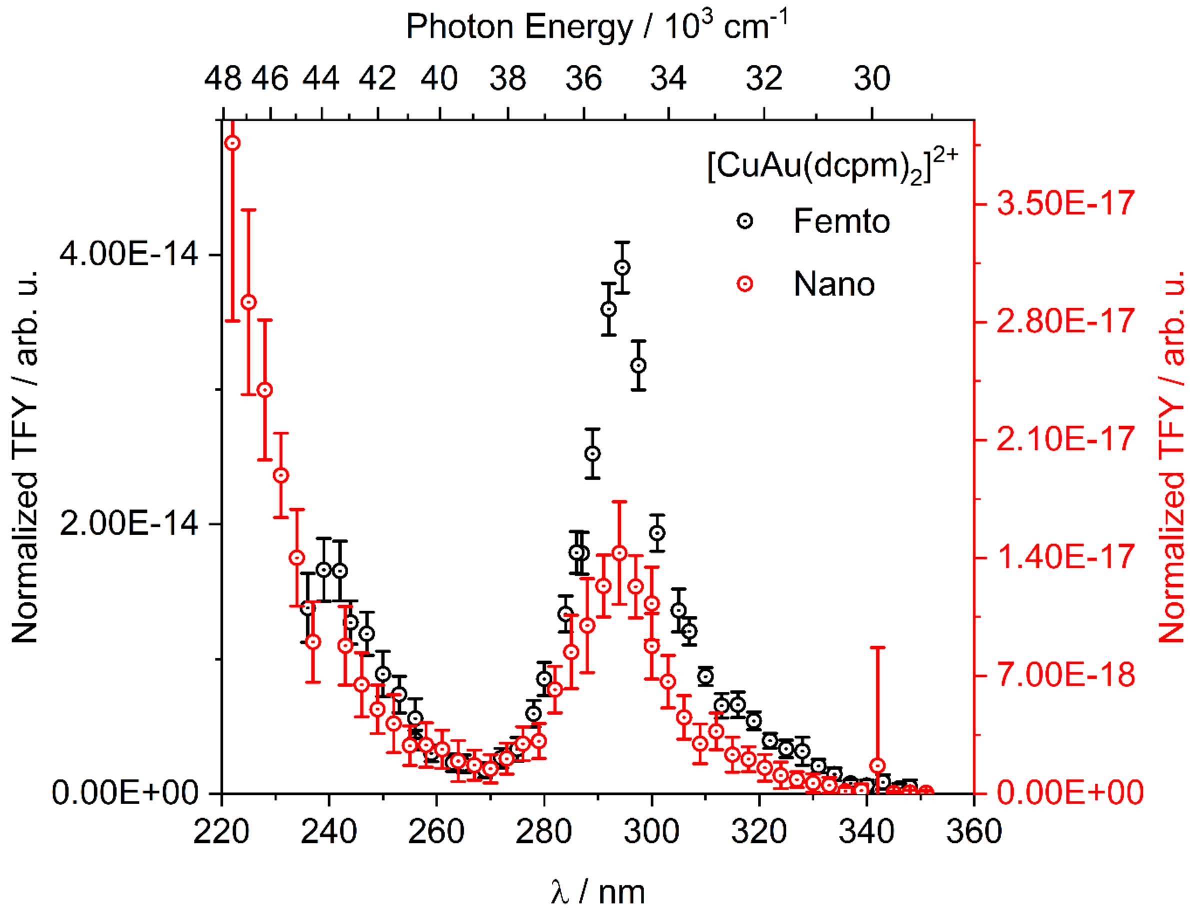

Fig. S27 Comparison of femtosecond (black circles) and nanosecond (red circles) UV PD total yield spectra of $[CuAu(\textit{dcpm})_2]^{2+}$ ions (2 µJ, 118 pulses). Spectra were normalized to number of photons. Error bars indicate one standard deviation (±1σ).

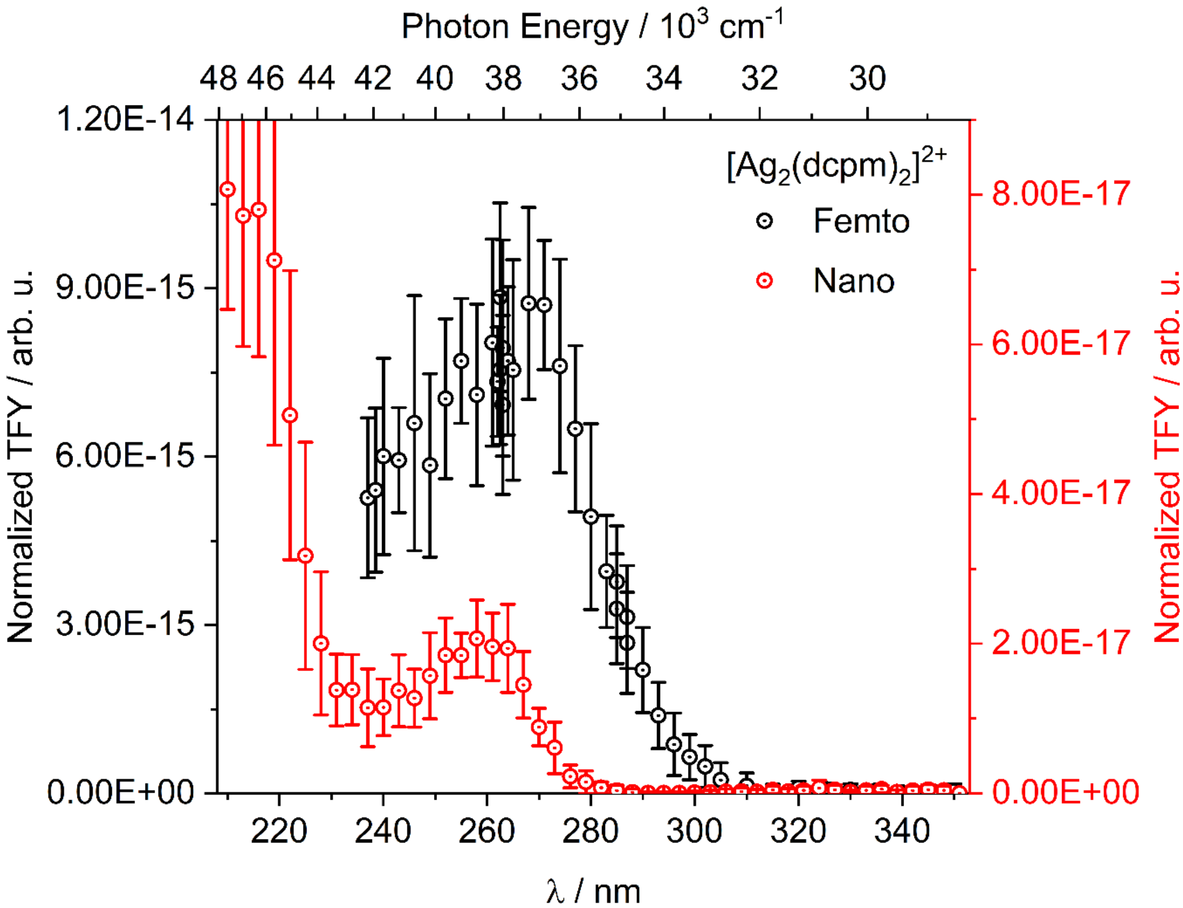

Fig. S28 Comparison of femtosecond (black circles) and nanosecond (red circles) UV PD total yield spectra of $[Ag_2(dcpm)_2]^{2+}$ ions (2 µJ, 118 pulses). Spectra were normalized to number of photons. Error bars indicate one standard deviation (±1σ).

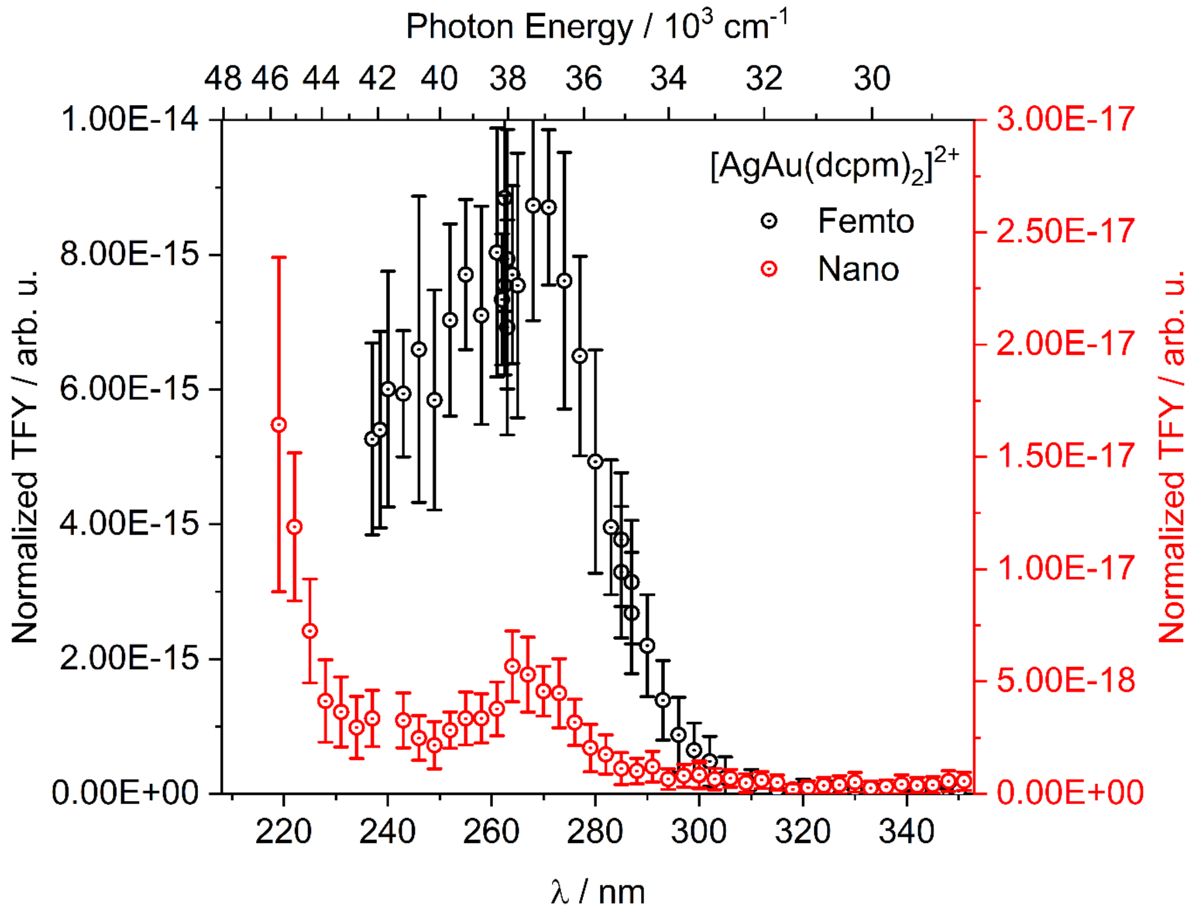

Fig. S29 Comparison of femtosecond (black circles) and nanosecond (red circles) UV PD total yield spectra of $[AgAu(\mathit{dcpm})_2]^{2+}$ ions (2 µJ, 118 pulses). Spectra were normalized to number of photons. Error bars indicate one standard deviation (±1σ).

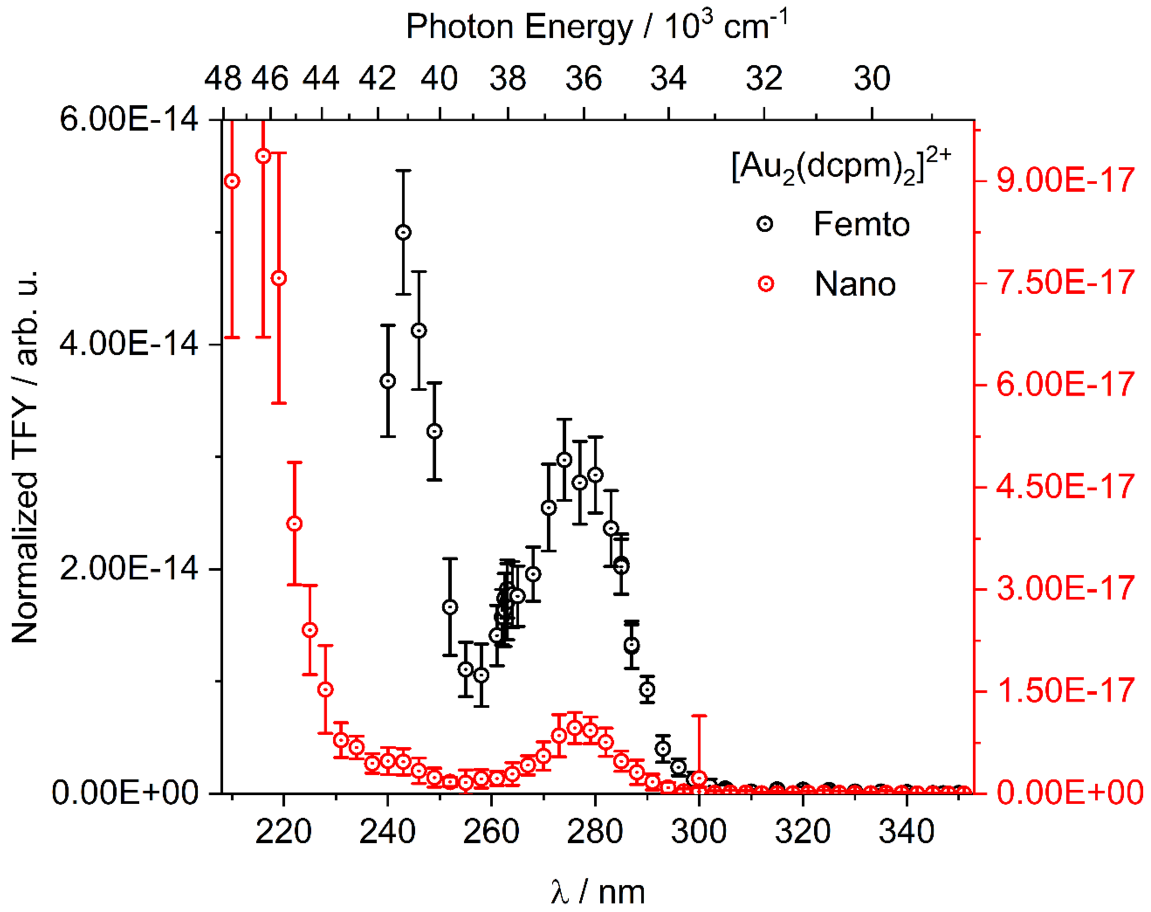

Fig. S30 Comparison of femtosecond (black circles) and nanosecond (red circles) UV PD total yield spectra of $[Au_2(\mathit{dcpm})_2]^{2+}$ ions (2 µJ, 118 pulses). Spectra were normalized to number of photons. Error bars indicate one standard deviation (±1σ).

5. Trends of electronic transitions

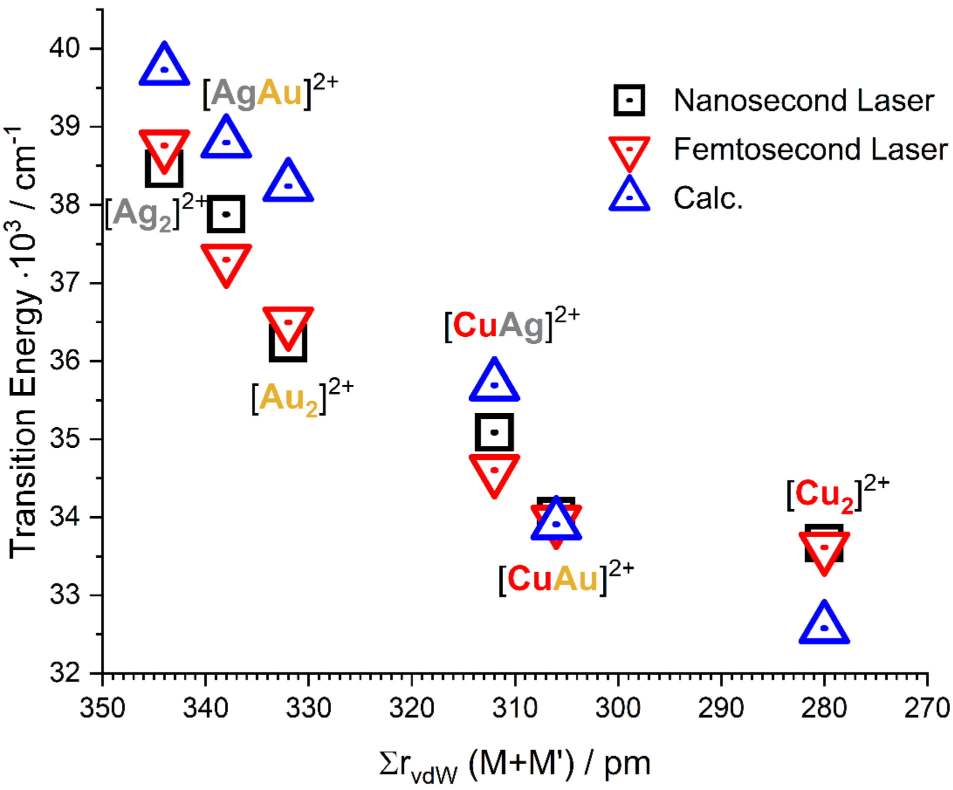

Fig. S31 Trend of (lowest-energy) bright electronic transitions taken as maximum of UV band position of PD results: nanosecond laser maxima (black open squares), femtosecond laser maxima (red open triangles), and calculated transition energies (blue open triangles) at *GW*-BSE (PBE0/x2c-TZVPall-2c) level of theory vs. sum of van-der-Waals-radii. Different metal-metal compositions are indicated.

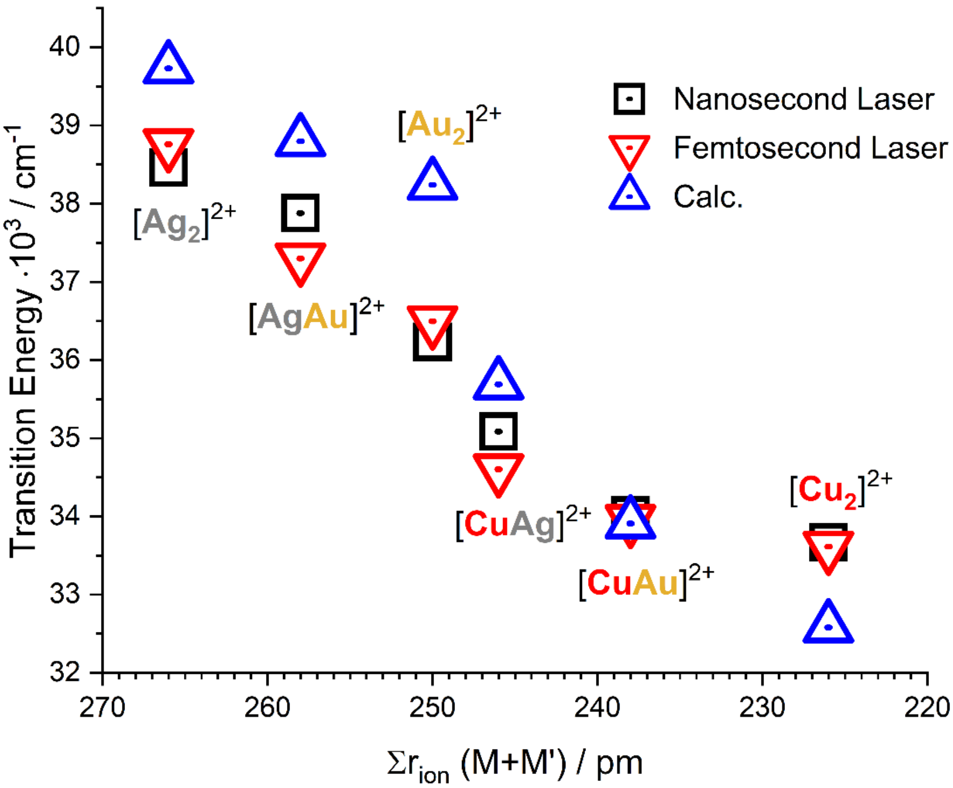

Fig. S32 Trend of (lowest-energy) bright electronic transitions taken as maximum of UV band position of PD results: nanosecond laser maxima (black open squares), femtosecond laser maxima (red open triangles), and calculated transition energies (blue open triangles) at *GW*-BSE (PBE0/x2c-TZVPall-2c) level of theory vs. sum of ion-radii. Different metal-metal compositions are indicated.

6. Calculated natural population analysis and natural transition orbitals (NTOs)

Tab. S22 Natural population analysis of the hole and particle unrelaxed difference densities of the bright state of the coinage metal and phosphorus atoms in the model complexes $[M_1M_2(\mathit{dcpm})_2]^{2+}$ (M_1, M_2 = Cu, Ag, Au). Negative values refer to a loss of electrons, positive values refer to a gain. The metal atom between parentheses indicates the metal atom to which the phosphorus atom is coordinated.

		Hole Density			**Particle Density**		
Comple	**Atom**	**s**	**p**	**d**	**s**	**p**	**d**
Ag_2	Ag1	–0.106	–0.045	–0.180	0.003	0.296	0.022
(S_1)	Ag2	–0.081	–0.032	–0.178	0.005	0.318	0.018
	P (Ag1)	–0.009	–0.050	–0.003	0.003	0.011	0.012
	P (Ag2)	–0.005	–0.041	–0.002	0.003	0.011	0.011
AgAu	Ag1	–0.078	–0.030	–0.230	0.002	0.209	0.022
(S_1)	Au2	–0.098	–0.065	–0.170	0.002	0.419	0.026
	P (Ag1)	–0.007	–0.065	–0.002	0.003	0.012	0.009
	P (Au2)	–0.002	–0.023	–0.003	0.000	0.008	0.013
Au_2	Au1	–0.123	–0.052	–0.219	0.002	0.301	0.028
(S_2)	Au2	–0.120	–0.056	–0.220	0.002	0.327	0.025
	P (Au1)	–0.002	–0.028	–0.002	0.001	0.009	0.011
	P(Au2)	–0.001	–0.021	–0.003	0.001	0.008	0.011
CuAg	Cu1	–0.061	–0.010	–0.391	0.002	0.387	0.011
(S_1)	Ag2	–0.053	–0.041	–0.137	0.003	0.245	0.031
	P (Cu1)	–0.004	–0.055	–0.002	0.000	0.010	0.014
	P (Ag2)	–0.005	–0.033	–0.002	0.004	0.013	0.007
CuAu	Cu1	–0.061	–0.010	–0.436	0.002	0.273	0.009
	Au2	–0.064	–0.055	–0.120	0.005	0.372	0.035
	P (Cu1)	–0.008	–0.056	–0.003	0.001	0.011	0.011
	P (Au2)	–0.001	–0.013	–0.002	0.000	0.011	0.011
Cu_2	Cu1	–0.046	–0.014	–0.292	0.002	0.325	0.020

(S_1)	Cu2	–0.044	–0.016	–0.298	0.002	0.334	0.018
	P (Cu1)	–0.008	–0.046	–0.002	0.001	0.015	0.010
	P (Cu2)	–0.007	–0.037	–0.002	0.002	0.015	0.009

Tab. S23 Natural population analysis of the hole and particle unrelaxed difference densities of the dark state of the coinage metal and phosphorus atoms in the model complexes $[M_1M_2(\textit{dcpm})_2]^{2+}$ (M_1, M_2 = Cu, Ag, Au). Negative values refer to a loss of electrons, positive values refer to a gain. The metal atom between parentheses indicates the metal atom to which the phosphorus atom is coordinated.

		Hole Density			Particle Density		
Comple	**Atom**	**S**	**p**	**d**	**S**	**p**	**d**
Ag_2	Ag1	–0.075	–0.044	–0.189	0.000	0.306	0.011
(S_2)	Ag2	–0.073	–0.043	–0.186	0.001	0.299	0.010
	P (Ag1)	–0.007	–0.065	–0.001	0.001	0.005	0.016
	P (Ag2)	–0.006	–0.047	–0.002	0.000	0.005	0.017
AgAu	Ag1	–0.068	–0.031	–0.232	0.000	0.258	0.008
(S_2)	Au2	–0.101	–0.068	–0.184	0.000	0.375	0.013
	P (Ag1)	–0.007	–0.065	–0.002	0.001	0.004	0.014
	P (Au2)	–0.002	–0.024	–0.002	0.000	0.004	0.018
Au_2	Au1	–0.122	–0.054	–0.231	0.000	0.329	0.013
(S_1)	Au2	–0.117	–0.059	–0.227	0.000	0.322	0.012
	P (Au1)	–0.002	–0.029	–0.002	0.001	0.004	0.015
	P(Au2)	–0.001	–0.022	–0.002	0.000	0.003	0.015
CuAg	Cu1	–0.060	–0.010	–0.402	0.001	0.436	0.011
(S_2)	Ag2	–0.047	–0.046	–0.139	0.000	0.191	0.015
	P (Cu1)	–0.007	–0.055	–0.001	0.001	0.006	0.019
	P (Ag2)	–0.005	–0.035	–0.001	0.000	0.003	0.011
CuAu	Cu1	–0.053	–0.010	–0.445	0.001	0.387	0.006
	Au2	–0.064	–0.057	–0.122	0.000	0.256	0.018
	P (Cu1)	–0.009	–0.057	–0.002	0.001	0.005	0.018
	P (Au2)	–0.000	–0.016	–0.001	0.000	0.002	0.009
Cu_2	Cu1	–0.048	–0.017	–0.298	0.002	0.333	0.011
(S_2)	Cu2	–0.045	–0.019	–0.294	0.000	0.303	0.011
	P (Cu1)	–0.008	–0.048	–0.001	0.001	0.004	0.014
	P (Cu2)	–0.008	–0.038	–0.001	0.000	0.005	0.015

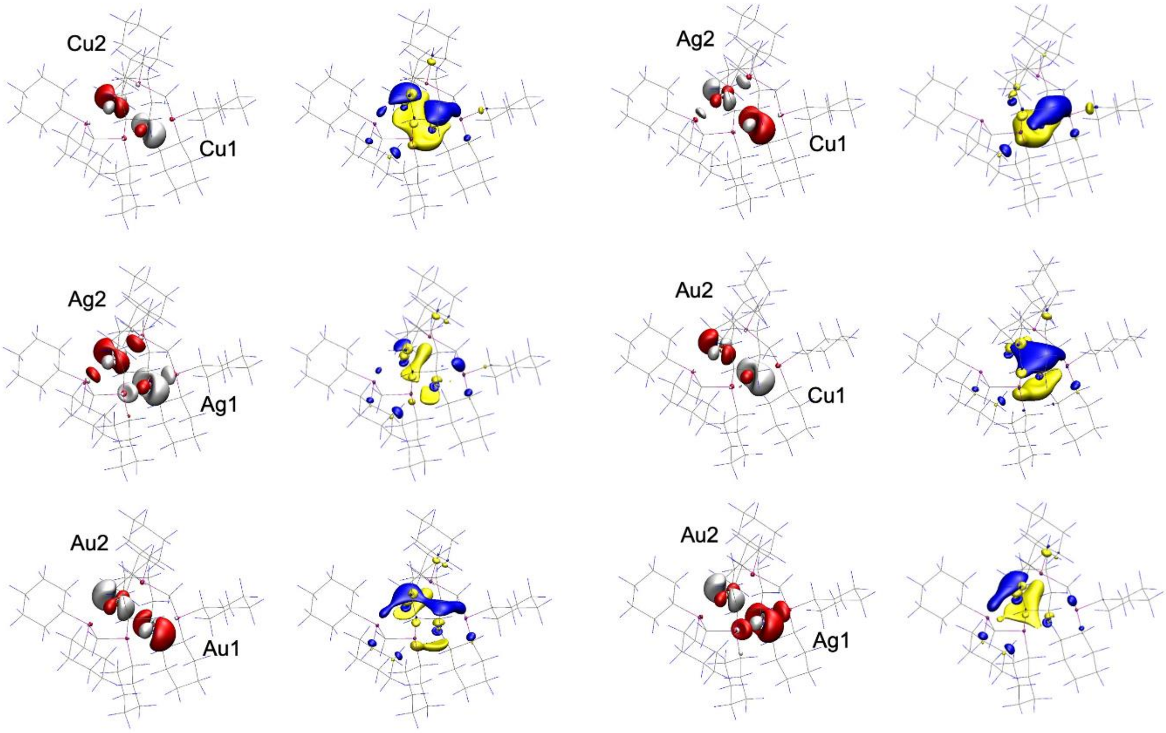

Fig. S33 Hole (1. and 3. column, red/white) and particle (2. and 4. column, blue/yellow) natural transition orbitals (NTOs) of the dark state, plotted with an isovalue of $\pm 0.05\, a_0^{-3/2}$. Homometallic (left) and heterometallic (right) species are displayed.

7. Calculated *GW* quasiparticle energies

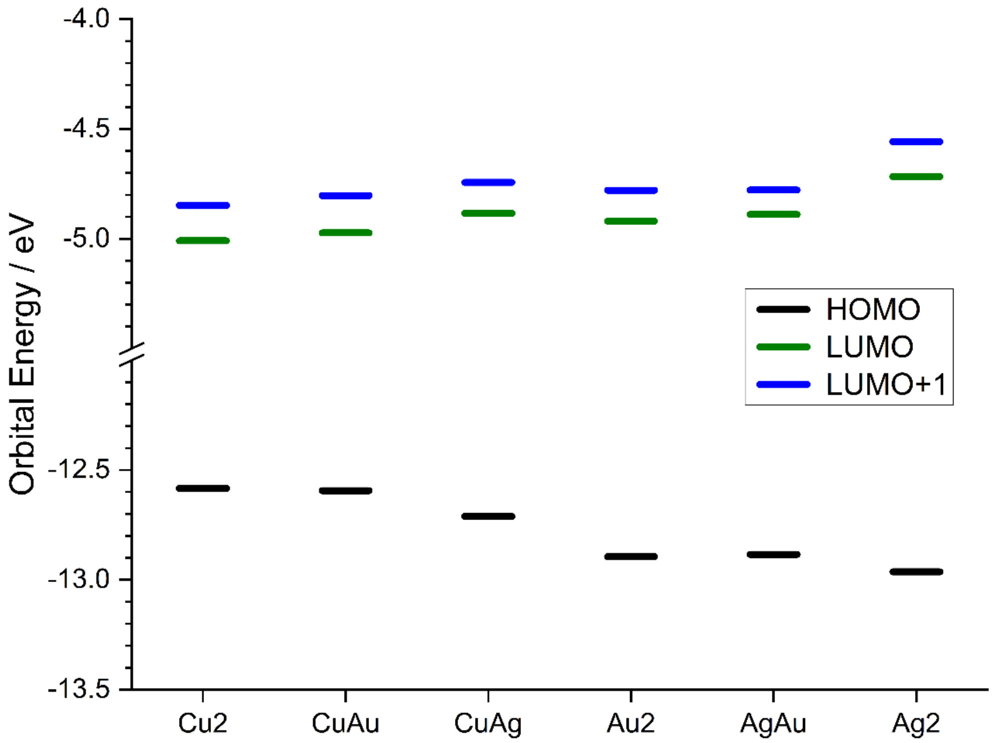

Fig. S34 HOMO (black), LUMO (green), and LUMO+1 (blue) quasiparticle energies in eV of the metal complexes [MM'(*dcpm*)$_2$]$^{2+}$ at the *GW* (PBE0/x2c-TZVPall-2c) level of theory.

8. Hybridization and distance variation

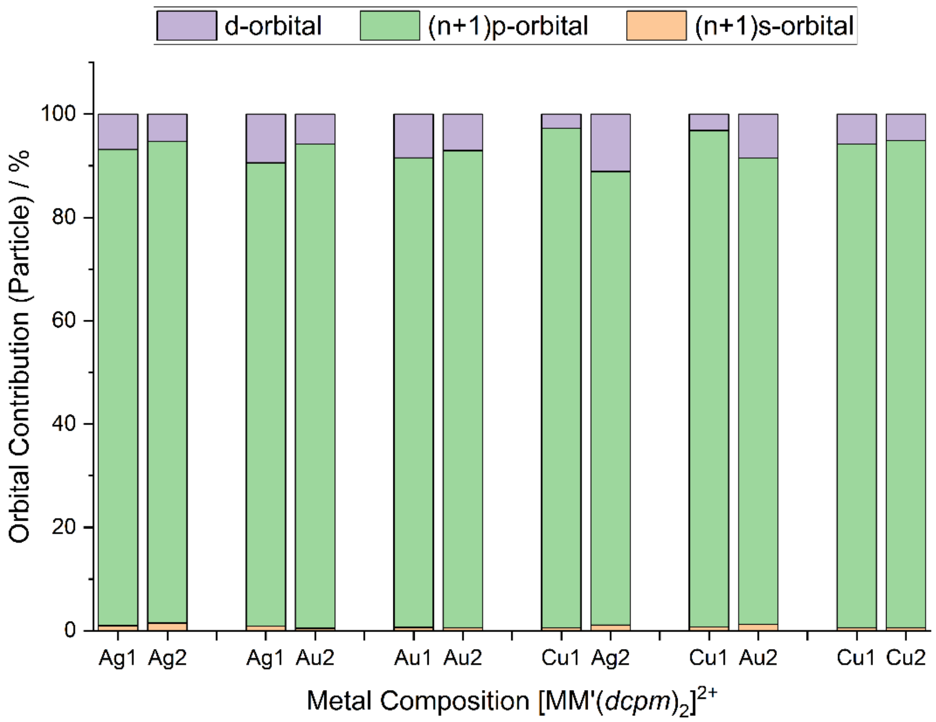

Fig. S35 Orbital contributions of $[MM'(dcpm)_2]^{2+}$ complexes of the particle unrelaxed difference densities of the bright state at *GW*-BSE (PBE0/x2c-TZVPall-2c) level of theory.

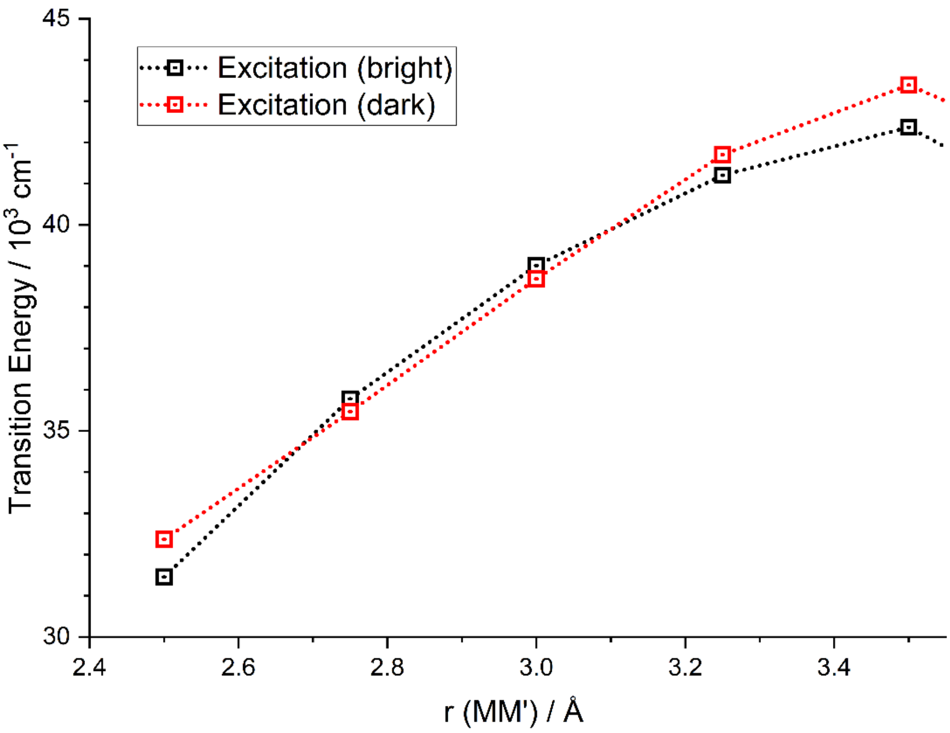

Fig. S36 Bright and dark electronic transition energies of $[Au_2(dcpm)_2]^{2+}$ complex as a function of Au-Au distance between two $[Au(dcpm)]^{+}$ monomers.

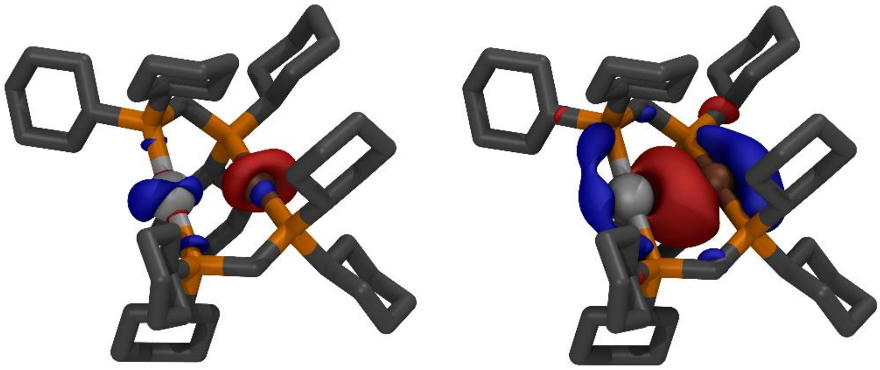

Fig. S37 Hole (left) and particle (right) natural transition orbitals of the bright electronic transition of $[CuAg(\mathit{dcpm})_2]^{2+}$ complex at M-M' distance *d* = 2.8 Å between $[Cu(\mathit{dcpm})]^{+}$ and $[Ag(\mathit{dcpm})]^{+}$ monomers.

9. Calculated transition energy properties and charge distribution

Tab. S24 Optimized metal–metal distances (*d* in pm) and natural population analysis (partial charge *q* in units of *e*) of the atoms M_1 and M_2 in $[M_1M_2(dcpm)_2]^{2+}$.

Complex	*R* (pm)	M_1	M_2	$q(M_1)$	$q(M_2)$
Ag_2	293.0	Ag	Ag	0.484	0.488
AgAu	292.2	Ag	Au	0.494	0.256
Au_2	293.4	Au	Au	0.264	0.266
CuAg	278.0	Cu	Ag	0.496	0.492
CuAu	277.9	Cu	Au	0.512	0.263
Cu_2	266.1	Cu	Cu	0.490	0.492

Tab. S25 Vertical electronic excitation energies of $[M_1M_2(dcpm)_2]^{2+}$ as obtained at the BSE level (M_1, M_2 = Cu, Ag, Au).

Complex	State	Energy (10^3 cm^{-1})	Wavelength (nm)	Oscillator Strength	Weight of Main NTO Pair
Ag_2	S_1	39.73	252	0.3489	97.7 %
	S_2	40.60	246	0.0148	98.0 %
AgAu	S_1	38.80	258	0.3373	97.8 %
	S_2	39.26	255	0.0123	98.5 %
Au_2	S_1	37.97	263	0.0088	98.7 %
	S_2	38.24	261	0.3595	97.6 %
CuAg	S_1	35.69	280	0.2694	97.6 %
	S_2	36.16	277	0.0259	98.2 %
CuAu	S_1	33.91	295	0.2628	97.9 %
	S_2	35.59	281	0.0224	98.5 %
Cu_2	S_1	32.58	307	0.2545	97.3 %
	S_2	33.61	298	0.0069	97.9 %

10. Cooperativity

We try to consider cooperativity of metal-metal-interactions in the case of electronic excitation energies. When, in general, cooperativity means *not to be able* to predict properties of a three- or two-body system from the characteristics of its components, we may establish a possibility to determine the *non-additivity* for the electronic energies of the complexes under investigation. Therefore, the transition energies of the homometallic species were compared with those of the heterometallic ones. Assuming the different homometallic nuclei would have the same "contribution" to the excitation energy, the energy of the corresponding heterometallic complexes should lie in the center of the corresponding homometallic ones. If not, there must be a cooperative effect. To quantify that influence following equation was used:[1]

$$\Delta E_{coop} = \frac{E(M_2) + E(M_2')}{2} - E(MM')$$

where $E(M_2)$ and $E(M_2')$ are the electronic transition energies of two different homo- and $E(MM')$ of the heterometallic complex. ΔE_{coop} describes the quantified cooperative effect.

Tab. S26 Experimental excitation energies of homo- and heterometallic complexes and calculated cooperative effect ΔE_{coop} in wavenumbers (10^3 cm^{-1}).

	MM	M'M'	MM'	ΔE_{coop}
E(M=Cu, M'=Ag) / 10^3 cm^{-1}	33.61	38.76	34.60	1.59
E(M=Cu, M'=Au) / 10^3 cm^{-1}	33.61	36.50	33.96	1.10
E(M=Au, M'=Ag) / 10^3 cm^{-1}	36.50	38.76	37.30	0.33

The used experimental excitation energies and resulting ΔE_{coop} are displayed in Tab. S26. The decreasing calculated deviation from the expected center value is demonstrated in the sequence: [**CuAg**]$^{2+}$ > [**CuAu**]$^{2+}$ >> [**AgAu**]$^{2+}$. The cooperative effect for [**AgAu**]$^{2+}$ is negligible, however copper seems to expose a strong effect in the mixed complexes [**CuAu**]$^{2+}$ and even larger in [**CuAg**]$^{2+}$. A peculiarity in the bonding situation of homogeneous copper complexes with different ligands (in order to modulate their metal-metal distance) was also inferred from Resonance Raman spectroscopy experiments and obtained force constants and ascribed to

[1] J. Chmela, M. E. Harding, D. Matioszek, C. E. Anson, F. Breher and W. Klopper, *ChemPhysChem*, 2016, **17**, 37–45.

solvent interaction.[2] Here, we show with our analysis above that intrinsic effects are of likewise importance.

[2] C.-M. Che and S.-W. Lai, *Coord. Chem. Rev.*, 2005, **249**, 1296–1309.

11. Geometry Optimized Structures

Tab. S27 Cartesian coordinates in Å of the optimized ground state structure of $[Ag_2(\mathit{dcpm})_2]^{2+}$ (C_2 symmetry) obtained at the PBE0/x2c-TZVPPall-2c level of theory.

148

C	0.2894371	3.3243005	0.0932339
P	-0.2969282	2.3817176	-1.3760108
Ag	0.0844771	0.0031533	-1.3460330
P	0.3112789	-2.3930810	-1.3825840
C	-0.1075676	-3.2590308	0.1928580
P	-0.7913050	-2.2519627	1.5741444
Ag	-0.2202113	0.0852367	1.5674124
P	0.6299237	2.3409806	1.6126731
H	-0.4637433	4.0914739	0.3337274
H	1.2113321	3.8596127	-0.1844975
H	-0.8035389	-4.0850004	-0.0270090
H	0.8166376	-3.7210767	0.5717051
C	-4.7198075	-2.1636677	0.1879076
C	-3.2014437	-2.0057209	0.2168840
C	-2.6022775	-2.5205012	1.5288449
C	-3.2692646	-1.8490701	2.7356465
C	-4.7883451	-2.0036241	2.6944133
C	-5.3738403	-1.4863513	1.3861581
H	-4.9719435	-3.2406590	0.1895883
H	-2.9420676	-0.9361746	0.0981355
H	-2.7677310	-3.6124445	1.5892175
H	-3.0098079	-0.7697950	2.7341067
H	-5.0457745	-3.0723258	2.8163692
H	-5.2173507	-0.3919102	1.3198722
H	-5.1159811	-1.7533513	-0.7570964
H	-2.7589082	-2.5323295	-0.6450435
H	-2.8811710	-2.2670669	3.6799551
H	-5.2341023	-1.4783281	3.5558601
H	-6.4647989	-1.6460457	1.3663670
C	1.8389427	-3.3642949	4.6039207
C	1.3335827	-2.7874469	3.2832205
C	-0.1645947	-3.0598132	3.0972868
C	-0.4832485	-4.5537488	3.2126347
C	0.0371198	-5.1217878	4.5332839
C	1.5265984	-4.8527938	4.7161352
H	1.3609188	-2.8215401	5.4412308
H	1.9038525	-3.2480462	2.4536013
H	-0.6979263	-2.5243302	3.9058712
H	-0.0094267	-5.0985664	2.3737714
H	-0.5262011	-4.6661008	5.3693336
H	2.0983553	-5.4068899	3.9469276
H	2.9242618	-3.1869286	4.6944845
H	1.5328346	-1.6995276	3.2358141
H	-1.5699395	-4.7295214	3.1340929
H	-0.1695496	-6.2045001	4.5736880
H	1.8662004	-5.2396304	5.6914200
C	4.4704992	1.1633295	0.5401207
C	-2.0477560	-2.9728155	-4.7899434

C	0.6985803	5.3331238	-4.1952690
C	2.9617008	1.3835624	0.4933729
C	-1.0255386	-2.3214622	-3.8602819
C	0.1075041	4.7261448	-2.9224506
C	2.4589457	2.2165078	1.6754949
C	-0.7776621	-3.1989283	-2.6276916
C	0.4288707	3.2309314	-2.8300543
C	2.9128103	1.6083715	3.0078037
C	-0.3611914	-4.6235064	-3.0082597
C	1.9366701	2.9730084	-2.9353846
C	4.4226915	1.3787963	3.0400770
C	-1.3942780	-5.2542910	-3.9414965
C	2.5102146	3.5847822	-4.2121965
C	4.8941718	0.5347679	1.8619060
C	-1.6337208	-4.3896890	-5.1746376
C	2.1970778	5.0744531	-4.3029697
H	4.9858057	2.1330025	0.4081200
H	-3.0310645	-3.0017445	-4.2821740
H	0.1846271	4.8992081	-5.0736889
H	2.4541177	0.3989951	0.5242662
H	-0.0806650	-2.1613880	-4.4098633
H	0.5281089	5.2489198	-2.0421951
H	2.8626122	3.2423788	1.5900759
H	-1.7436004	-3.2674413	-2.0917418
H	-0.0513335	2.7155779	-3.6839840
H	2.3932503	0.6388830	3.1569815
H	0.6177445	-4.6006577	-3.5201606
H	2.4536413	3.4233263	-2.0661754
H	4.9377200	2.3572777	3.0192699
H	-2.3462968	-5.3899584	-3.3935475
H	2.0817256	3.0614185	-5.0878088
H	4.4615105	-0.4826096	1.9398541
H	-0.7083588	-4.3501200	-5.7804448
H	2.7229518	5.6101382	-3.4893508
H	4.7776378	0.5309335	-0.3113664
H	-2.1793247	-2.3495867	-5.6907897
H	0.4887785	6.4157936	-4.2165659
H	2.6792479	1.8507499	-0.4650404
H	-1.3785036	-1.3209846	-3.5439830
H	-0.9827794	4.8949901	-2.9029541
H	2.6204701	2.2564193	3.8511356
H	-0.2325494	-5.2493591	-2.1064964
H	2.1418758	1.8861251	-2.9021222
H	4.7003960	0.9041698	3.9963093
H	-1.0573813	-6.2628958	-4.2346236
H	3.5996218	3.4138178	-4.2472909
H	5.9896877	0.4115981	1.8945328
H	-2.4037225	-4.8485875	-5.8170899
H	2.5876363	5.4881851	-5.2476537
C	-1.7981617	4.3109729	4.3737045
C	3.9792127	-2.7129317	-3.3416030
C	-4.2280066	2.2824503	-2.7439649
C	-1.3976646	3.5293447	3.1236954
C	2.5142868	-2.3674791	-3.0800174
C	-2.7116068	2.1012318	-2.7089733
C	0.1260425	3.3970896	3.0232727
C	2.0508918	-2.8803590	-1.7110940
C	-2.1030467	2.6896396	-1.4306389
C	0.8108293	4.7675530	3.0623850

C	2.9739596	-2.3528888	-0.6070526
C	-2.7877726	2.1198415	-0.1849991
C	0.3920034	5.5507728	4.3069540
C	4.4350938	-2.7080328	-0.8715742
C	-4.3010177	2.3131600	-0.2330691
C	-1.1233962	5.6778727	4.4131060
C	4.8909068	-2.1998571	-2.2340863
C	-4.8969777	1.7107913	-1.4997346
H	-1.5126825	3.7296432	5.2707324
H	4.0804987	-3.8113874	-3.4227596
H	-4.4604025	3.3608322	-2.8230665
H	-1.7837086	4.0657743	2.2357422
H	2.3823242	-1.2660269	-3.1141313
H	-2.4693159	1.0189083	-2.7575888
H	0.4620351	2.8114725	3.9005532
H	2.0798313	-3.9860413	-1.7103846
H	-2.2426738	3.7867379	-1.4387171
H	0.5323637	5.3441987	2.1595340
H	2.8733889	-1.2523908	-0.5645866
H	-2.5630293	1.0368694	-0.1195172
H	0.7833573	5.0359941	5.2046887
H	4.5578669	-3.8062556	-0.8250815
H	-4.5305276	3.3944732	-0.1934451
H	-1.5006988	6.2975147	3.5769193
H	4.8827315	-1.0919883	-2.2344435
H	-4.7627317	0.6111922	-1.4810790
H	-2.8957031	4.4181629	4.4065759
H	4.2834379	-2.3016606	-4.3189324
H	-4.6329916	1.8119135	-3.6557704
H	-1.8696951	2.5291300	3.1259191
H	1.8895859	-2.7839205	-3.8860940
H	-2.2641594	2.5654616	-3.6041255
H	1.9087427	4.6588616	3.0451858
H	2.6738361	-2.7325391	0.3850515
H	-2.3818116	2.5791649	0.7308042
H	0.8653122	6.5469436	4.2894053
H	5.0657468	-2.2902544	-0.0675344
H	-4.7594735	1.8661943	0.6661434
H	-1.3964679	6.2103338	5.3394140
H	5.9337851	-2.5023937	-2.4264703
H	-5.9844820	1.8907575	-1.5343481

Tab. S28 Cartesian coordinates in Å of the optimized ground state structure of [AgAu(*dcpm*)$_2$]$^{2+}$ (C_2 symmetry) obtained at the PBE0/x2c-TZVPPall-2c level of theory.

148

C	0.2669968	3.2699763	0.0947402
P	-0.2651739	2.3826348	-1.4325932
Ag	0.0513352	-0.0020625	-1.3990136
P	0.2468478	-2.3982394	-1.4109105
C	-0.1143995	-3.2267611	0.2012058
P	-0.7453358	-2.2015874	1.5881814
Au	-0.1439301	0.0504379	1.5155701
P	0.6309971	2.2529645	1.5820291
H	-0.5148860	3.9993058	0.3594643
H	1.1735637	3.8497762	-0.1410664
H	-0.8239332	-4.0519649	0.0269811
H	0.8209217	-3.6870362	0.5541446
C	-4.7052949	-2.0193457	0.3208413
C	-3.1841908	-1.8897648	0.3086855
C	-2.5583496	-2.4288819	1.5983528
C	-3.1776194	-1.7608386	2.8325350
C	-4.6995783	-1.8897583	2.8304873
C	-5.3117703	-1.3451805	1.5457627
H	-4.9791327	-3.0910539	0.3154005
H	-2.9083976	-0.8246992	0.1981773
H	-2.7373545	-3.5191430	1.6522490
H	-2.8976359	-0.6876628	2.8376803
H	-4.9724800	-2.9554299	2.9458528
H	-5.1360069	-0.2531781	1.4884308
H	-5.1188089	-1.5875618	-0.6071453
H	-2.7740447	-2.4128852	-0.5716824
H	-2.7709750	-2.1998536	3.7592860
H	-5.1123308	-1.3683450	3.7105126
H	-6.4056872	-1.4842048	1.5552351
C	1.9677256	-3.3104052	4.5425586
C	1.4335434	-2.7521476	3.2252646
C	-0.0788589	-2.9792022	3.1051152
C	-0.4420501	-4.4587267	3.2694769
C	0.1101622	-5.0101739	4.5842233
C	1.6130683	-4.7845943	4.7060661
H	1.5385219	-2.7304714	5.3813448
H	1.9562821	-3.2559543	2.3896484
H	-0.5630342	-2.4049380	3.9177264
H	-0.0187965	-5.0390347	2.4273390
H	-0.4076022	-4.5162248	5.4279479
H	2.1385452	-5.3765202	3.9320896
H	3.0607086	-3.1662766	4.5889506
H	1.6637391	-1.6735529	3.1382275
H	-1.5361159	-4.6000545	3.2374816
H	-0.1286117	-6.0843259	4.6598022
H	1.9755913	-5.1572102	5.6786044
C	4.5253579	1.2336931	0.5674142
C	-2.1944526	-3.0970135	-4.7329549
C	0.8904403	5.4049765	-4.1128028
C	3.0065993	1.3637572	0.5149211

C	-1.1505377	-2.4150730	-3.8506235
C	0.2362035	4.7681370	-2.8862693
C	2.4582863	2.1967645	1.6771739
C	-0.8767141	-3.2479142	-2.5927278
C	0.5409921	3.2679776	-2.8213038
C	2.9282042	1.6296080	3.0217904
C	-0.4731972	-4.6872766	-2.9292995
C	2.0496954	2.9998458	-2.8641770
C	4.4487273	1.4857451	3.0655614
C	-1.5281419	-5.3481727	-3.8161504
C	2.6863560	3.6408434	-4.0959863
C	4.9785879	0.6549468	1.9024609
C	-1.7924449	-4.5283305	-5.0745337
C	2.3900822	5.1353230	-4.1594375
H	4.9850883	2.2284487	0.4169208
H	-3.1664975	-3.1041657	-4.2032059
H	0.4138142	5.0005147	-5.0256303
H	2.5561585	0.3552094	0.5789213
H	-0.2175569	-2.2781767	-4.4260772
H	0.6194350	5.2629210	-1.9732031
H	2.8162998	3.2386486	1.5793004
H	-1.8294274	-3.2919824	-2.0304266
H	0.0971410	2.7813258	-3.7110204
H	2.4595219	0.6364883	3.1762052
H	0.4946936	-4.6869198	-3.4621496
H	2.5288885	3.4231613	-1.9604179
H	4.9071016	2.4919272	3.0359785
H	-2.4683054	-5.4604415	-3.2429715
H	2.2942465	3.1456859	-5.0043928
H	4.6099987	-0.3860020	1.9942192
H	-0.8805938	-4.5141039	-5.7015915
H	2.8826475	5.6435170	-3.3081479
H	4.8700738	0.6022936	-0.2705271
H	-2.3443071	-2.5067330	-5.6529088
H	0.6904982	6.4897229	-4.1130549
H	2.6952266	1.7867247	-0.4549060
H	-1.4932526	-1.4026882	-3.5629498
H	-0.8522554	4.9468026	-2.9126051
H	2.5955482	2.2712932	3.8548369
H	-0.3268743	-5.2803984	-2.0082414
H	2.2451282	1.9109516	-2.8510304
H	4.7458841	1.0399406	4.0297650
H	-1.2003890	-6.3679768	-4.0793970
H	3.7747627	3.4604191	-4.0859927
H	6.0793500	0.6007634	1.9437709
H	-2.5775300	-5.0079828	-5.6826562
H	2.8267475	5.5711844	-5.0734900
C	-1.9516384	3.9622086	4.3709256
C	3.8710430	-2.7715330	-3.4456637
C	-4.1276716	2.4025217	-2.9823614
C	-1.4908089	3.2654601	3.0920123
C	2.4037267	-2.4440533	-3.1730496
C	-2.6157763	2.2056384	-2.8877090
C	0.0392362	3.2088623	3.0234428
C	1.9809054	-2.8848118	-1.7664845
C	-2.0603900	2.7305456	-1.5582755

C	0.6577555	4.6065291	3.1399722
C	2.9174485	-2.2731799	-0.7183441
C	-2.8075162	2.1169117	-0.3711342
C	0.1784613	5.3059412	4.4123259
C	4.3794170	-2.6162609	-0.9914613
C	-4.3153183	2.3261033	-0.4790894
C	-1.3431682	5.3552372	4.4935778
C	4.7946413	-2.1761379	-2.3900642
C	-4.8567623	1.7831255	-1.7961038
H	-1.6566874	3.3491411	5.2434097
H	3.9963079	-3.8703225	-3.4660101
H	-4.3484789	3.4854625	-3.0236465
H	-1.8810406	3.8308133	2.2243710
H	2.2448677	-1.3500946	-3.2695626
H	-2.3797211	1.1243462	-2.9747010
H	0.3843374	2.5979715	3.8795418
H	2.0292178	-3.9879871	-1.7018897
H	-2.1827001	3.8292230	-1.5259832
H	0.3670438	5.2126303	2.2605984
H	2.7954106	-1.1741143	-0.7478912
H	-2.5928121	1.0315882	-0.3411027
H	0.5785496	4.7665523	5.2915579
H	4.5254760	-3.7075458	-0.8859190
H	-4.5399221	3.4065841	-0.4037927
H	-1.7345753	5.9989200	3.6824507
H	4.7603834	-1.0703230	-2.4510297
H	-4.7306909	0.6824365	-1.8188673
H	-3.0534195	4.0171644	4.3851125
H	4.1452060	-2.4108454	-4.4514321
H	-4.4941453	1.9764867	-3.9315653
H	-1.9146565	2.2460261	3.0295306
H	1.7731022	-2.9220610	-3.9393498
H	-2.1252875	2.7051104	-3.7403523
H	1.7598490	4.5512511	3.1390517
H	2.6433524	-2.5898539	0.3031693
H	-2.4390568	2.5306326	0.5815487
H	0.6027640	6.3232446	4.4528917
H	5.0176629	-2.1414880	-0.2258796
H	-4.8169395	1.8444098	0.3782702
H	-1.6578895	5.8259462	5.4398673
H	5.8397502	-2.4661810	-2.5894993
H	-5.9403158	1.9737135	-1.8726539

Tab. S29 Cartesian coordinates in Å of the optimized ground state structure of $[Au_2(dcpm)_2]^{2+}$ (C_2 symmetry) obtained at the PBE0/x2c-TZVPPall-2c level of theory.

148

C	0.2824370	3.2098538	0.0916168
P	-0.2718142	2.3053456	-1.4128457
Au	0.0110298	-0.0059923	-1.3536967
P	0.2291095	-2.3238516	-1.4147244
C	-0.0984776	-3.1821605	0.1848998
P	-0.7262772	-2.2125552	1.6159629
Au	-0.1544127	0.0430885	1.5753793
P	0.6079691	2.2446751	1.6255851
H	-0.4788517	3.9720780	0.3217776
H	1.2066521	3.7535703	-0.1608080
H	-0.7923708	-4.0177683	-0.0021103
H	0.8518244	-3.6314429	0.5111862
C	-4.7044718	-2.0086545	0.4201920
C	-3.1842563	-1.8746169	0.3925313
C	-2.5348605	-2.4704547	1.6449995
C	-3.1399394	-1.8672320	2.9193040
C	-4.6617373	-1.9981642	2.9314504
C	-5.2927433	-1.3922975	1.6837191
H	-4.9776993	-3.0793449	0.3694040
H	-2.9127221	-0.8050609	0.3292883
H	-2.7005966	-3.5641129	1.6499094
H	-2.8611003	-0.7953770	2.9753818
H	-4.9326472	-3.0685073	2.9979094
H	-5.1169502	-0.2985598	1.6750959
H	-5.1313591	-1.5348488	-0.4810201
H	-2.7853483	-2.3526894	-0.5181022
H	-2.7205514	-2.3520947	3.8170711
H	-5.0621267	-1.5212207	3.8418663
H	-6.3865011	-1.5316408	1.7030824
C	2.0573038	-3.3742737	4.4820206
C	1.4896991	-2.7755977	3.1967736
C	-0.0183548	-3.0353532	3.0887757
C	-0.3446862	-4.5282645	3.1992343
C	0.2402745	-5.1178510	4.4829323
C	1.7393945	-4.8618417	4.5909197
H	1.6279730	-2.8390041	5.3498803
H	2.0123177	-3.2306672	2.3333931
H	-0.5038188	-2.5049703	3.9298974
H	0.0795671	-5.0654048	2.3293582
H	-0.2751156	-4.6694588	5.3530939
H	2.2657363	-5.4097255	3.7856682
H	3.1472423	-3.2060131	4.5182169
H	1.6911504	-1.6887876	3.1519370
H	-1.4356374	-4.6939457	3.1766550
H	0.0273555	-6.1994472	4.5196102
H	2.1260613	-5.2645260	5.5419325
C	4.5338504	1.2135233	0.7577542
C	-2.2788496	-2.9524529	-4.7014887
C	1.0207096	5.1686207	-4.1875924
C	3.0142835	1.3082480	0.6692087

C	-1.2115959	-2.2860871	-3.8355242
C	0.3288956	4.6031218	-2.9468413
C	2.4326280	2.2033677	1.7673076
C	-0.9217333	-3.1345577	-2.5918023
C	0.5844912	3.0973417	-2.8209292
C	2.8757849	1.7146382	3.1513613
C	-0.5301529	-4.5720863	-2.9520921
C	2.0836835	2.7772403	-2.8282212
C	4.3970938	1.5974805	3.2373178
C	-1.6067917	-5.2177284	-3.8240074
C	2.7569344	3.3479897	-4.0748359
C	4.9686010	0.7170241	2.1317134
C	-1.8940493	-4.3825049	-5.0671859
C	2.5110158	4.8477328	-4.2013667
H	4.9771410	2.2080628	0.5625060
H	-3.2395852	-2.9584583	-4.1514344
H	0.5427696	4.7444214	-5.0906917
H	2.5810818	0.2977611	0.7914299
H	-0.2890727	-2.1530319	-4.4277027
H	0.7163067	5.1208507	-2.0483890
H	2.7881009	3.2404217	1.6198566
H	-1.8643599	-3.1798863	-2.0129410
H	0.1358876	2.5893900	-3.6959937
H	2.4167313	0.7243631	3.3463376
H	0.4263081	-4.5682652	-3.5052606
H	2.5638849	3.2200672	-1.9345753
H	4.8402764	2.6084292	3.1664689
H	-2.5348503	-5.3324938	-3.2319584
H	2.3608949	2.8299070	-4.9686047
H	4.6182124	-0.3248452	2.2711511
H	-0.9964375	-4.3672023	-5.7143971
H	3.0088135	5.3730465	-3.3636569
H	4.9090259	0.5448087	-0.0368950
H	-2.4440473	-2.3513884	-5.6117518
H	0.8575157	6.2585005	-4.2330548
H	2.7104735	1.6590804	-0.3315001
H	-1.5366407	-1.2739100	-3.5307536
H	-0.7528408	4.8154570	-2.9958066
H	2.5153458	2.3938206	3.9419705
H	-0.3671470	-5.1780213	-2.0422228
H	2.2394222	1.6837993	-2.7685894
H	4.6778039	1.2068148	4.2299386
H	-1.2891202	-6.2358247	-4.1054466
H	3.8386168	3.1331086	-4.0417613
H	6.0689676	0.6875690	2.1998124
H	-2.6954887	-4.8511604	-5.6623778
H	2.9739643	5.2324686	-5.1253460
C	-2.0438759	4.0620182	4.2790052
C	3.8104886	-2.6322310	-3.5314840
C	-4.1113074	2.4203816	-3.0112253
C	-1.5522040	3.3181859	3.0386101
C	2.3470022	-2.3165952	-3.2263221
C	-2.6046132	2.1911040	-2.9067782
C	-0.0213002	3.2576911	3.0108228
C	1.9575331	-2.7785528	-1.8166189
C	-2.0535422	2.6893140	-1.5650203

C	0.5963995	4.6582822	3.0907462
C	2.9097744	-2.1709744	-0.7796941
C	-2.8249043	2.0773930	-0.3917753
C	0.0867150	5.4046536	4.3240796
C	4.3667492	-2.5062122	-1.0861399
C	-4.3271402	2.3161595	-0.5109915
C	-1.4363560	5.4581213	4.3655392
C	4.7517789	-2.0453383	-2.4867338
C	-4.8643160	1.7998588	-1.8404832
H	-1.7720724	3.4812123	5.1805500
H	3.9418261	-3.7299031	-3.5692094
H	-4.3100934	3.5080790	-3.0398474
H	-1.9192739	3.8522780	2.1414724
H	2.1781681	-1.2234881	-3.3034220
H	-2.3880290	1.1077189	-3.0042111
H	0.3006506	2.6790517	3.8977815
H	2.0147475	-3.8822304	-1.7666379
H	-2.1478203	3.7906098	-1.5227874
H	0.3285458	5.2323201	2.1829721
H	2.7793378	-1.0730850	-0.7983424
H	-2.6299038	0.9890849	-0.3777337
H	0.4638943	4.8975949	5.2321785
H	4.5186932	-3.5983247	-0.9982653
H	-4.5345388	3.3991435	-0.4225599
H	-1.8063340	6.0718929	3.5217716
H	4.7100602	-0.9391201	-2.5319451
H	-4.7581611	0.6974744	-1.8757158
H	-3.1455749	4.1181766	4.2634085
H	4.0623007	-2.2564839	-4.5375706
H	-4.4771908	2.0146114	-3.9694696
H	-1.9759633	2.2975998	3.0030284
H	1.7040960	-2.7898910	-3.9852026
H	-2.0966996	2.6928355	-3.7477260
H	1.6980402	4.6026861	3.1191920
H	2.6566370	-2.4989030	0.2437610
H	-2.4558730	2.4710727	0.5692042
H	0.5117162	6.4223851	4.3377611
H	5.0187603	-2.0398149	-0.3272444
H	-4.8445227	1.8303749	0.3348501
H	-1.7736920	5.9636198	5.2857316
H	5.7941687	-2.3269511	-2.7109097
H	-5.9432043	2.0117105	-1.9261388

Tab. S30 Cartesian coordinates in Å of the optimized ground state structure of [CuAg(*dcpm*)$_2$]$^{2+}$ (C_2 symmetry) obtained at the PBE0/x2c-TZVPPall-2c level of theory.

148

C	0.2947626	3.2384817	0.0714068
P	-0.2918336	2.1872505	-1.3210698
Cu	0.1207142	0.0032913	-1.1390665
P	0.3451723	-2.2071825	-1.3258657
C	-0.1095146	-3.1853087	0.1719184
P	-0.8097914	-2.2492547	1.5944459
Ag	-0.2610537	0.0893086	1.6133982
P	0.6094235	2.3350200	1.6440842
H	-0.4547137	4.0244672	0.2555101
H	1.2230511	3.7461287	-0.2347062
H	-0.7990677	-3.9957194	-0.1145371
H	0.8070471	-3.6699813	0.5401702
C	-4.7729336	-2.3350159	0.2853179
C	-3.2562330	-2.1567048	0.2606801
C	-2.6150277	-2.5611178	1.5906379
C	-3.2682589	-1.8197694	2.7647238
C	-4.7834223	-2.0100311	2.7761516
C	-5.4103547	-1.5907822	1.4522824
H	-5.0071578	-3.4130388	0.3649624
H	-3.0131721	-1.0978695	0.0464138
H	-2.7545359	-3.6490080	1.7315411
H	-3.0368343	-0.7376944	2.6768381
H	-5.0138944	-3.0734050	2.9744681
H	-5.2769851	-0.5004627	1.3111599
H	-5.1991406	-1.9951603	-0.6744733
H	-2.8341390	-2.7520884	-0.5655660
H	-2.8441943	-2.1566812	3.7260268
H	-5.2187762	-1.4380269	3.6128210
H	-6.4981203	-1.7709797	1.4699155
C	1.8895937	-3.3293750	4.5777918
C	1.3466519	-2.7296073	3.2825452
C	-0.1349795	-3.0755878	3.0879594
C	-0.3712350	-4.5883148	3.1476986
C	0.1845681	-5.1765327	4.4449378
C	1.6583997	-4.8356580	4.6335691
H	1.3878364	-2.8458381	5.4372052
H	1.9371012	-3.1227014	2.4327784
H	-0.6955508	-2.6013894	3.9159957
H	0.1284960	-5.0755507	2.2886853
H	-0.3984083	-4.7834838	5.2990634
H	2.2549946	-5.3285180	3.8418683
H	2.9642789	-3.0969834	4.6713256
H	1.4853536	-1.6313585	3.2791043
H	-1.4466539	-4.8211743	3.0646792
H	0.0359090	-6.2694663	4.4446778
H	2.0230817	-5.2406821	5.5922612
C	4.4551507	1.0967076	0.6753814
C	-2.0160721	-2.4234750	-4.7738533
C	0.6929919	4.9072774	-4.3668130
C	2.9480221	1.3200452	0.5992622

C	-0.9619163	-1.8944247	-3.8033750
C	0.1071123	4.4019383	-3.0481502
C	2.4353510	2.2038950	1.7391289
C	-0.7628920	-2.8699875	-2.6374950
C	0.4274428	2.9183028	-2.8408870
C	2.8678085	1.6492373	3.1014674
C	-0.4081236	-4.2778563	-3.1251502
C	1.9343543	2.6498344	-2.9326224
C	4.3757644	1.4132605	3.1636491
C	-1.4683716	-4.7906603	-4.0996100
C	2.5023416	3.1593107	-4.2559543
C	4.8587657	0.5202879	2.0268633
C	-1.6710283	-3.8264603	-5.2637837
C	2.1905837	4.6379722	-4.4611034
H	4.9747709	2.0592310	0.5118754
H	-2.9992441	-2.4417947	-4.2651154
H	0.1739839	4.4077264	-5.2065902
H	2.4339757	0.3398149	0.6651553
H	-0.0103844	-1.7453260	-4.3438531
H	0.5323380	4.9904381	-2.2127139
H	2.8455596	3.2233516	1.6157972
H	-1.7354520	-2.9320841	-2.1137566
H	-0.0569614	2.3379970	-3.6496266
H	2.3405106	0.6898831	3.2834934
H	0.5706795	-4.2570233	-3.6378413
H	2.4566265	3.1645814	-2.1032864
H	4.8967158	2.3873967	3.1108639
H	-2.4249481	-4.9258481	-3.5595532
H	2.0685698	2.5700628	-5.0859553
H	4.4213893	-0.4918501	2.1398846
H	-0.7466997	-3.7852529	-5.8709643
H	2.7212451	5.2344586	-3.6942664
H	4.7725875	0.4307214	-0.1459951
H	-2.1175601	-1.7303470	-5.6263362
H	0.4851966	5.9854856	-4.4711853
H	2.6801802	1.7480692	-0.3813958
H	-1.2607482	-0.9024961	-3.4152687
H	-0.9828965	4.5733100	-3.0362217
H	2.5680657	2.3335437	3.9129664
H	-0.3055781	-4.9765016	-2.2750137
H	2.1380665	1.5681640	-2.8166145
H	4.6376387	0.9759197	4.1418504
H	-1.1765470	-5.7879449	-4.4696439
H	3.5914171	2.9846108	-4.2831669
H	5.9532523	0.3948976	2.0788428
H	-2.4634983	-4.2003090	-5.9334690
H	2.5772824	4.9760963	-5.4369414
C	-1.8501361	4.4335981	4.2808275
C	3.9943289	-2.4820712	-3.3247937
C	-4.2337194	2.0763239	-2.6785098
C	-1.4364542	3.5908017	3.0756007
C	2.5503571	-2.0932478	-3.0133604
C	-2.7190343	1.8812004	-2.6460596
C	0.0880922	3.4524727	2.9990593
C	2.0664367	-2.7284438	-1.7036615
C	-2.0983280	2.4998953	-1.3887195

C	0.7754083	4.8223627	2.9810217
C	3.0176199	-2.3717722	-0.5565079
C	-2.7828968	1.9727223	-0.1241802
C	0.3427272	5.6655410	4.1808787
C	4.4593005	-2.7634754	-0.8727920
C	-4.2946997	2.1762772	-0.1697910
C	-1.1735541	5.7999495	4.2615129
C	4.9351243	-2.1365376	-2.1777791
C	-4.9016662	1.5439561	-1.4164219
H	-1.5763995	3.8965881	5.2085745
H	4.0386084	-3.5693654	-3.5233133
H	-4.4564837	3.1544440	-2.7849357
H	-1.8121554	4.0822601	2.1576250
H	2.4749793	-0.9894815	-2.9263715
H	-2.4891276	0.7969599	-2.6645867
H	0.4134871	2.9076681	3.9061188
H	2.0444814	-3.8277060	-1.8237761
H	-2.2287602	3.5976156	-1.4289561
H	0.5095824	5.3553137	2.0479763
H	2.9692671	-1.2812264	-0.3847284
H	-2.5653363	0.8900983	-0.0297562
H	0.7218052	5.1944625	5.1073851
H	4.5301624	-3.8649590	-0.9440614
H	-4.5156378	3.2600738	-0.1589452
H	-1.5391582	6.3784783	3.3913649
H	4.9844249	-1.0360018	-2.0616128
H	-4.7760628	0.4441198	-1.3684010
H	-2.9478100	4.5433161	4.2952147
H	4.3150219	-1.9847805	-4.2558380
H	-4.6476192	1.5856857	-3.5756202
H	-1.9093063	2.5922383	3.1236981
H	1.9025664	-2.3884270	-3.8538306
H	-2.2719561	2.3147040	-3.5564885
H	1.8731880	4.7111334	2.9831264
H	2.7063087	-2.8512642	0.3872364
H	-2.3688023	2.4547500	0.7760441
H	0.8184806	6.6588749	4.1206872
H	5.1122343	-2.4635067	-0.0347339
H	-4.7516274	1.7581746	0.7439657
H	-1.4570982	6.3774097	5.1571895
H	5.9604347	-2.4693937	-2.4102826
H	-5.9878697	1.7315594	-1.4509379

Tab. S31 Cartesian coordinates in Å of the optimized ground state structure of $[CuAu(\textit{dcpm})_2]^{2+}$ (C_2 symmetry) obtained at the PBE0/x2c-TZVPPall-2c level of theory.

148

C	0.3822661	3.2149880	0.1050736
P	-0.0867140	2.2299834	-1.3798318
Cu	0.0738520	0.0335669	-1.1195248
P	0.2655813	-2.1696181	-1.2922651
C	0.3137163	-3.0144633	0.3356583
P	-0.6269815	-2.2010760	1.6793126
Au	-0.1653972	0.0843415	1.6487811
P	0.6141607	2.2832734	1.6709367
H	-0.3917192	3.9805554	0.2716701
H	1.3198313	3.7516806	-0.1096880
H	0.0028316	-4.0667982	0.2294354
H	1.3609126	-3.0098799	0.6769817
C	-4.5004804	-1.9166524	0.2004481
C	-3.0432691	-1.5760301	0.4923057
C	-2.3991056	-2.6050364	1.4303105
C	-3.1914340	-2.6685516	2.7428997
C	-4.6609539	-2.9920615	2.4711537
C	-5.3015571	-2.0122000	1.4943213
H	-4.5515684	-2.8776191	-0.3466971
H	-2.9932129	-0.5895015	0.9901209
H	-2.4263921	-3.6048137	0.9566943
H	-3.1136506	-1.6934563	3.2629352
H	-4.7298504	-4.0177376	2.0621104
H	-5.3566388	-1.0098991	1.9609288
H	-4.9323967	-1.1527625	-0.4695161
H	-2.4745748	-1.4710971	-0.4478569
H	-2.7727147	-3.4283982	3.4221075
H	-5.2141118	-3.0030123	3.4252733
H	-6.3410121	-2.3129068	1.2816941
C	1.8207585	-3.1344453	4.9102178
C	1.3732913	-2.5265263	3.5818917
C	-0.0329027	-3.0118165	3.2059437
C	-0.1001220	-4.5428983	3.1659182
C	0.3424930	-5.1353019	4.5034865
C	1.7383453	-4.6574110	4.8892642
H	1.1776353	-2.7403062	5.7194758
H	2.0943166	-2.8145644	2.7921557
H	-0.7297285	-2.6444718	3.9827902
H	0.5718629	-4.9176696	2.3712754
H	-0.3816424	-4.8436558	5.2874190
H	2.4749976	-5.0553145	4.1651278
H	2.8486285	-2.8049631	5.1393867
H	1.3913558	-1.4223012	3.6388377
H	-1.1175805	-4.8894174	2.9134728
H	0.3121533	-6.2363526	4.4458582
H	2.0218224	-5.0654444	5.8737418
C	4.5361670	1.0652451	1.0579840
C	-2.9612230	-2.9422253	-3.8410261
C	1.4775255	4.8891812	-4.2269607
C	3.0286953	1.2166263	0.8814354
C	-1.7619843	-2.2071244	-3.2466062
C	0.6972552	4.4255740	-2.9964532

C	2.4271453	2.1836839	1.9082016
C	-1.0750413	-3.0653734	-2.1791168
C	0.8844273	2.9223469	-2.7695964
C	2.7818754	1.7503139	3.3354413
C	-0.6698646	-4.4406274	-2.7203552
C	2.3680939	2.5523386	-2.6673113
C	4.2907867	1.5797160	3.5052205
C	-1.8828336	-5.1589273	-3.3112219
C	3.1335984	3.0174671	-3.9044217
C	4.8778950	0.6212930	2.4755465
C	-2.5675589	-4.3137707	-4.3804341
C	2.9528749	4.5139672	-4.1373686
H	5.0306618	2.0304790	0.8399727
H	-3.7343835	-3.0617619	-3.0571265
H	1.0329851	4.4284772	-5.1293434
H	2.5483128	0.2270051	1.0150806
H	-1.0448906	-1.9589980	-4.0500121
H	1.0567635	4.9806535	-2.1087787
H	2.8298532	3.1984299	1.7301032
H	-1.8183555	-3.2403708	-1.3788983
H	0.4729798	2.3823157	-3.6440571
H	2.2751581	0.7894999	3.5568046
H	0.0969590	-4.3227493	-3.5067237
H	2.8119925	3.0355267	-1.7757824
H	4.7782538	2.5677441	3.4070008
H	-2.6023420	-5.3856643	-2.5011136
H	2.7689342	2.4572475	-4.7862781
H	4.4747219	-0.3962845	2.6472463
H	-1.8832055	-4.1865728	-5.2407606
H	3.4249766	5.0730265	-3.3066924
H	4.9234277	0.3429726	0.3178960
H	-3.4163804	-2.3289373	-4.6373002
H	1.3617685	5.9795418	-4.3465037
H	2.7951706	1.5410986	-0.1463418
H	-2.0832333	-1.2442172	-2.8070508
H	-0.3711456	4.6748684	-3.1152683
H	2.4104115	2.4832865	4.0708443
H	-0.2145579	-5.0586866	-1.9252948
H	2.4829925	1.4606827	-2.5307972
H	4.5059646	1.2303738	4.5291225
H	-1.5680997	-6.1303122	-3.7283698
H	4.2027859	2.7671712	-3.7946710
H	5.9709915	0.5489931	2.6024324
H	-3.4562655	-4.8389320	-4.7685569
H	3.4800630	4.8225036	-5.0555166
C	-2.1574090	4.2072448	4.1091561
C	3.2407699	-2.1517114	-4.1909963
C	-3.7847695	2.4122019	-3.2866907
C	-1.5999960	3.4128469	2.9292842
C	1.8805825	-1.9820788	-3.5179314
C	-2.2883263	2.1923680	-3.0721009
C	-0.0707054	3.3322015	2.9997807
C	1.8796611	-2.5357744	-2.0852960
C	-1.8447168	2.6562411	-1.6794958
C	0.5643893	4.7253286	3.0774392
C	3.0171612	-1.9056653	-1.2705915
C	-2.7040699	2.0079762	-0.5885410
C	-0.0103800	5.5166766	4.2525310
C	4.3719116	-2.0814385	-1.9524421

C	-4.1955160	2.2351020	-0.8151105
C	-1.5316872	5.5956248	4.1905904
C	4.3586385	-1.5219702	-3.3697359
C	-4.6200056	1.7512835	-2.1967146
H	-1.9555052	3.6531508	5.0451923
H	3.4454027	-3.2301113	-4.3267298
H	-3.9914949	3.4987083	-3.2987117
H	-1.9038495	3.9148139	1.9906996
H	1.6200062	-0.9037880	-3.4834695
H	-2.0552113	1.1140205	-3.1853927
H	0.1889453	2.7732435	3.9190023
H	2.0124839	-3.6325881	-2.1163253
H	-1.9410808	3.7562862	-1.6179128
H	0.3642722	5.2753202	2.1380338
H	2.8087105	-0.8230624	-1.1536445
H	-2.5018985	0.9199659	-0.5947946
H	0.2970891	5.0316104	5.1981430
H	4.6285337	-3.1567959	-1.9812450
H	-4.4235198	3.3126486	-0.7129258
H	-1.8338358	6.1869864	3.3048850
H	4.2144539	-0.4238528	-3.3312739
H	-4.4965154	0.6513161	-2.2543410
H	-3.2545436	4.2802178	4.0194807
H	3.2050192	-1.7139113	-5.2029793
H	-4.0715747	2.0325102	-4.2818708
H	-2.0350601	2.3965150	2.9059322
H	1.1032671	-2.4720448	-4.1260257
H	-1.7231629	2.7220690	-3.8569772
H	1.6611513	4.6529437	3.1766348
H	3.0613208	-2.3279384	-0.2510539
H	-2.4113024	2.3712281	0.4114159
H	0.4310458	6.5274023	4.2641182
H	5.1541316	-1.5921341	-1.3463290
H	-4.7708596	1.7196699	-0.0260220
H	-1.9201026	6.1364153	5.0696348
H	5.3335099	-1.6905919	-3.8568175
H	-5.6915623	1.9532470	-2.3617238

Tab. S32 Cartesian coordinates in Å of the optimized ground state structure of $[Cu_2(dcpm)_2]^{2+}$ (C_2 symmetry) obtained at the PBE0/x2c-TZVPPall-2c level of theory.

148

C	0.2968895	3.1623748	0.1028965
P	-0.2012464	2.1966558	-1.3804321
Cu	0.0808428	-0.0041606	-1.2294508
P	0.2307080	-2.2145914	-1.4220958
C	-0.0986017	-3.1299841	0.1445535
P	-0.6914549	-2.1042237	1.5524439
Cu	-0.2199899	0.0655052	1.4139073
P	0.5165705	2.1574332	1.6282801
H	-0.4621532	3.9384765	0.2881222
H	1.2428618	3.6829162	-0.1132079
H	-0.8085341	-3.9502647	-0.0474736
H	0.8448662	-3.5967422	0.4650649
C	-4.7527904	-2.2085310	0.5992570
C	-3.2418825	-2.0567700	0.4372955
C	-2.4887080	-2.4176060	1.7205840
C	-3.0313408	-1.6299534	2.9213193
C	-4.5422799	-1.7957195	3.0675649
C	-5.2754755	-1.4119176	1.7884691
H	-4.9954216	-3.2785972	0.7388633
H	-3.0060732	-1.0112503	0.1609819
H	-2.6164215	-3.4988575	1.9125770
H	-2.7939284	-0.5542929	2.7817018
H	-4.7681550	-2.8483451	3.3210604
H	-5.1388621	-0.3295602	1.5963236
H	-5.2549401	-1.8948543	-0.3324508
H	-2.9000510	-2.6900038	-0.3981636
H	-2.5318300	-1.9455398	3.8531440
H	-4.8972346	-1.1899600	3.9183764
H	-6.3601151	-1.5718078	1.9066921
C	2.2757660	-3.0211872	4.3244636
C	1.6174582	-2.5350364	3.0356287
C	0.1116673	-2.8228558	3.0387523
C	-0.1715095	-4.3097947	3.2729571
C	0.5035793	-4.7958259	4.5562862
C	1.9999578	-4.5027275	4.5590047
H	1.8859891	-2.4310045	5.1754366
H	2.0951590	-3.0513274	2.1812227
H	-0.3322372	-2.2461410	3.8725005
H	0.2097586	-4.8978414	2.4160846
H	0.0283624	-4.2991316	5.4231363
H	2.4934204	-5.0968014	3.7658743
H	3.3619648	-2.8294800	4.2807265
H	1.8000969	-1.4540221	2.8908855
H	-1.2569052	-4.4987101	3.3313219
H	0.3205238	-5.8764507	4.6799426
H	2.4491134	-4.8274115	5.5123949
C	4.4352968	0.9702916	0.9650837
C	-2.3706632	-2.5813205	-4.6770755
C	1.1571192	4.9831909	-4.2081454
C	2.9276639	1.1374271	0.8056628
C	-1.2487054	-2.0116041	-3.8112910
C	0.4323434	4.4521031	-2.9712137

C	2.3352160	2.0777396	1.8603569
C	-0.9758474	-2.9259891	-2.6115356
C	0.6780494	2.9498557	-2.7985723
C	2.7044791	1.6133870	3.2737869
C	-0.6679420	-4.3637246	-3.0424646
C	2.1757921	2.6223709	-2.7625381
C	4.2134747	1.4258607	3.4254524
C	-1.7956204	-4.9149594	-3.9149180
C	2.8844551	3.1610949	-4.0038733
C	4.7852928	0.4884235	2.3680602
C	-2.0689767	-4.0117896	-5.1130828
C	2.6463301	4.6579265	-4.1737946
H	4.9333108	1.9382061	0.7684915
H	-3.3167385	-2.5626519	-4.1022996
H	0.7018018	4.5369198	-5.1123606
H	2.4418177	0.1472414	0.9180705
H	-0.3362799	-1.9008142	-4.4230243
H	0.7993006	4.9911881	-2.0768975
H	2.7327933	3.0977407	1.7033319
H	-1.9084301	-2.9475997	-2.0165047
H	0.2469351	2.4206022	-3.6700457
H	2.1912628	0.6545786	3.4881736
H	0.2756296	-4.3854626	-3.6170477
H	2.6364424	3.0795189	-1.8655890
H	4.7079099	2.4120306	3.3457772
H	-2.7146865	-5.0101041	-3.3055976
H	2.5104218	2.6226453	-4.8951562
H	4.3778620	-0.5311216	2.5181048
H	-1.1873839	-4.0127606	-5.7820707
H	3.1231654	5.2026025	-3.3362675
H	4.8134426	0.2661835	0.2032994
H	-2.5258907	-1.9336064	-5.5567166
H	0.9995452	6.0720305	-4.2865815
H	2.6885351	1.4889839	-0.2133167
H	-1.5142343	-0.9978829	-3.4574197
H	-0.6475887	4.6653377	-3.0502798
H	2.3484812	2.3361858	4.0263098
H	-0.5170601	-5.0157327	-2.1630610
H	2.3263941	1.5292295	-2.6766697
H	4.4352379	1.0509462	4.4388665
H	-1.5373949	-5.9339158	-4.2491479
H	3.9643173	2.9446144	-3.9371374
H	5.8789478	0.4065216	2.4839811
H	-2.9073140	-4.4123081	-5.7072261
H	3.1356048	5.0180979	-5.0941064
C	-2.2117904	3.9678052	4.2154099
C	3.7214952	-2.5676824	-3.6857262
C	-4.0097830	2.2456401	-3.0732947
C	-1.6823051	3.2315115	2.9858796
C	2.2823140	-2.2159743	-3.3117153
C	-2.4990055	2.0627051	-2.9411775
C	-0.1517464	3.1567371	3.0097374
C	1.9286054	-2.7179235	-1.9060889
C	-1.9865676	2.5572496	-1.5841296
C	0.4740429	4.5506640	3.1300607
C	2.9406396	-2.1813888	-0.8872594
C	-2.7662872	1.9122971	-0.4339138
C	-0.0709394	5.2874778	4.3537622
C	4.3721742	-2.5563000	-1.2610374

C	-4.2723649	2.1057564	-0.5801363
C	-1.5938797	5.3564526	4.3401787
C	4.7218445	-2.0552957	-2.6570580
C	-4.7662454	1.5874084	-1.9254354
H	-1.9787521	3.3747911	5.1199121
H	3.8114330	-3.6668834	-3.7701470
H	-4.2418053	3.3269170	-3.0923927
H	-2.0138210	3.7753534	2.0806499
H	2.1501574	-1.1147605	-3.3447090
H	-2.2499030	0.9878542	-3.0503719
H	0.1335453	2.5651319	3.9007588
H	1.9531217	-3.8237847	-1.8997962
H	-2.1085317	3.6553221	-1.5315266
H	0.2423148	5.1375897	2.2207106
H	2.8539437	-1.0782491	-0.8626779
H	-2.5403440	0.8270251	-0.4262181
H	0.2677986	4.7658059	5.2687798
H	4.4854728	-3.6557735	-1.2200093
H	-4.5124836	3.1813519	-0.4858110
H	-1.9263455	5.9834733	3.4905761
H	4.7195509	-0.9473207	-2.6592065
H	-4.6252001	0.4890117	-1.9702423
H	-3.3116004	4.0357584	4.1605320
H	3.9484576	-2.1617246	-4.6860192
H	-4.3440891	1.8412626	-4.0436026
H	-2.1158650	2.2155440	2.9282025
H	1.5966500	-2.6386935	-4.0624652
H	-1.9900968	2.5905905	-3.7650838
H	1.5737057	4.4846860	3.1932801
H	2.7138813	-2.5365118	0.1329316
H	-2.4279253	2.3069814	0.5380706
H	0.3632090	6.3005930	4.3953877
H	5.0698528	-2.1442562	-0.5115029
H	-4.7924382	1.5973365	0.2505051
H	-1.9602490	5.8548627	5.2531118
H	5.7441988	-2.3643386	-2.9316048
H	-5.8493737	1.7661061	-2.0306806